MEVTV WORKSHOP ON TECTONIC FEATURES ON MARS

Edited by
Thomas R. Watters and Matthew P. Golombek

April 20–22, 1989

Held at
Richland, Washington

Sponsored by
Lunar and Planetary Institute
NASA/MEVTV Study Project

Lunar and Planetary Institute 3303 NASA Road 1 Houston, Texas 77058-4399

LPI Technical Report Number 89-06

Compiled in 1989 by the
LUNAR AND PLANETARY INSTITUTE

The Institute is operated by Universities Space Research Association under Contract NASW-4066 with the National Aeronautics and Space Administration.

This report may be cited as:
Watters T. R. and Golombek M. P., eds. (1989) *MEVTV Workshop on Tectonic Features on Mars*. LPI Tech. Rpt. 89-06. Lunar and Planetary Institute, Houston. 126 pp.

Papers in this report may be cited as:
Author A. A. (1989) Title of paper. In *MEVTV Workshop on Tectonic Features on Mars* (T. R. Watters and M. P. Golombek, eds.), pp. xx–yy. LPI Tech. Rpt. 89-06. Lunar and Planetary Institute, Houston.

This report is distributed by:

ORDER DEPARTMENT
Lunar and Planetary Institute
3303 NASA Road 1
Houston, TX 77058-4399

Mail order requestors will be invoiced for the cost of shipping and handling.

Cover photo: Portion of the Yakima fold belt in the Columbia River flood-basalt province. The anticlinal ridges trend roughly east-west and are bounded by the Cascade Range to the west. The Columbia River dissects the Saddle Mountains anticline (top of image) and flanks the Columbia Hills anticline (bottom of image) (Landsat 4, band 7, scene ID # 4009518173).

Contents

Introduction

The MEVTV (Mars: Evolution of Volcanism, Tectonics and Volatiles) Workshop on "Tectonic Features on Mars" was held at the Hanford Science Center in Richland, Washington, April 20–22, 1989. The objectives of the workshop were to determine the state of our knowledge of tectonic features on Mars and assess kinematic and mechanical models for their origin. The Columbia Plateau in eastern Washington was chosen for the location of the workshop because many of the structures that occur in the area may serve as potential analogs to martian tectonic features.

The workshop was composed of three sessions: (I) Wrinkle Ridges and Compressional Structures, (II) Strike-slip Faults, and (III) Extensional Structures. Each session began with an overview of the features under discussion. In the case of wrinkle ridges and extensional structures, the overview was followed by keynote addresses by specialists working on similar structures on the Earth. The format of the workshop was designed to stimulate questions and the free exchange of ideas.

The first session of the workshop focused on the controversy over the relative importance of folding, faulting, and intrusive volcanism in the origin of wrinkle ridges. By the end of the various exchanges it was clear that none of the mechanisms proposed completely explained all aspects of these landforms. The session ended with discussions of the origin of compressional flank structures associated with martian volcanoes and the relationship between the volcanic complexes and the inferred regional stress field.

The second day of the workshop began with the presentation and discussion of evidence for strike-slip faults on Mars at various scales. Evidence included rhombohedral plateaus analogous to terrestrial push-up ranges and prominent lineaments associated with the Gordii Dorsum escarpment and with some wrinkle ridges. In the last session of the workshop, the discussion of extensional structures ranged from the origin of grabens, tension cracks, and pit-crater chains to the origin of Valles Marineris canyons. Shear and tensile modes of brittle failure in the formation of extensional features and the role of these failure modes in the formation of pit-crater chains and the canyons of Valles Marineris were debated. The relationship of extensional features to other surface processes, such as carbonate dissolution (karst) were also discussed.

The final day of the workshop was devoted to a field trip through the Yakima fold belt. The emphasis of the field trip was on the

geometry and mechanical response of the basalts to folding and faulting. A second informal field trip, which focused on strike-slip faults associated with the anticlines in the southern portion of the fold belt, was held following the workshop.

It became clear to those who attended the workshop that our knowledge about the origin of familiar structural landforms such as wrinkle ridges and grabens on Mars is far from complete. After more than a decade of analysis of the Viking images, it is particularly intriguing that strike-slip faults are now being recognized on Mars. The excursions into the Yakima Fold Belt highlighted many of the similarities and differences between the anticlines and planetary wrinkle ridges. The vigorous discussions and exchange of ideas during the talks and the field trips contributed enormously to the success of the workshop. The morphologic, kinematic, and mechanical analyses of tectonic features reported on in the session summaries and abstracts contained in this volume are a synopsis of our present understanding of these structures and their significance to the tectonic history of Mars.

Thomas R. Watters and Matthew P. Golombek

Program

Thursday Morning, April 20, 1989

8:00 a.m. Registration

8:30 a.m. Opening Remarks:
M. Golombek and T. Watters, Conveners

SESSION I — WRINKLE RIDGES AND COMPRESSIONAL STRUCTURES
Chairman: Sean Solomon

Origin of Planetary Wrinkle Ridges—An Overview
T. A. Maxwell

Folding in Layered Media (Overview)
A. Johnson

Fault-Related Folding on the Earth with Applications to Wrinkle Ridges on Mars and the Moon (Overview)
J. Suppe and W. Narr

New Evidence—Old Problem: Wrinkle Ridge Origin
D. H. Scott (presented by M. Chapman)

Morphologic Components of Wrinkle Ridges on Mars: Comparison with Lunar Mare Ridges and Implications
J. Aubele

Thursday Afternoon, April 20, 1989

SESSION I CONTINUED
Chairman: George McGill

Structural Geometry, Strain Distribution and Fold Mechanics within the Eastern Untanum Fold Ridge
A. J. Watkinson and E. H. Price

Crosscutting Periodically Spaced First-Order Ridges in the Ridged Plains of Hesperia Planum: Another Case for a Buckling Model
T. R. Watters and D. J. Chadwick

Involvement of the Lithosphere in the Formation of Wrinkle Ridges on Mars
M. Golombek, J. Suppe, W. Narr, J. Plescia, and B. Banerdt

The Olympus Mons Scarp: A Fault-Propagation Fold Generated by Gravity Failure of the Volcano?
A. Borgia, J. Burr, W. Montero, L. D. Morales, and G. I. Alvarado

Flank Tectonics of Martian Volcanoes
P. J. Thomas, S. W. Squyres, and M. H. Carr

Volcanic Flank Structure and the Evolution of Mars Volcanic Edifices
L. S. Crumpler and J. C. Aubele

Friday Morning, April 21, 1989

SESSION II — STRIKE SLIP FAULTING
Chairman: Matt Golombek

Ubiquity and Diversity of Strike-Slip Faulting on Earth; a Generality or an Exception for Comparative Planetology? (Overview)
R. D. Forsythe

Origin and Characteristics of Dextral Strike-Slip Faults Within the Yakima Fold Belt, Columbia River Flood-Basalt Province, U.S.A.
T. L. Tolan, J. L. Anderson, and M. H. Beeson

Strike-Slip Faulting Associated with the Folded Columbia River Basalts: Implications for the Deformed Ridged Plains of Mars
T. R. Watters and M. J. Tuttle

Strike-Slip Faulting in the Ridged Plains of Mars
R. A. Schultz

The Transcurrent Fault Hypothesis for Mars' Gordii Dorsum Escarpment
R. D. Forsythe and J. R. Zimbelman

Friday Afternoon, April 21, 1989

SESSION III — EXTENSIONAL STRUCTURES
Chairman: Tom Watters

A Review of Extensional Tectonic Features on Mars (Overview)
M. Golombek

Terrestrial Analogues for Planetary Extensional Structures (Overview)
G. E. McGill

Development of Grabens, Tension Cracks and Pits Southeast of Alba Patera, Mars
K. L. Tanaka, P. A. Davis, and M. P. Golombek

Do Pit-Crater Chains Grow Up to be Valles Marineris Canyons?
R. A. Schultz

Geology of the Hebes-Juventhae-Gangis Area: Implications for Canyon Formation
S. K. Croft

Normal Faulting Associated with the Daedalia Impact Basin, Mars
R. A. Craddock, J. R. Zimbelman, and T. R. Watters

Overview of Yakima Fold Belt
S. P. Reidel

ADJOURN WORKSHOP

Saturday Morning, April 22, 1989

FIELD TRIP TO THE YAKIMA FOLD BELT
Leaders: S. P. Reidel, K. R. Fecht, and T. L. Tolan

Summary of Technical Sessions

SESSION I
WRINKLE RIDGES AND COMPRESSIONAL STRUCTURES: OVERVIEW PAPERS

Summarized by Thomas R. Watters

The workshop began with a session, co-chaired by Sean Solomon (Massachusetts Institute of Technology) and George McGill (University of Massachusetts), that focused on the characterization and origin of wrinkle ridges and other compressional structures on Mars. The first half of the session was devoted to overviews relevant to discussions of the origin of wrinkle ridges. Wrinkle ridges are complex landforms consisting of a number of morphologic elements that include long, narrow, relatively high relief ridges and broad, low relief arches. The objective of the overviews was to provide a background on the nature of wrinkle ridges and explore kinematic and mechanical models for terrestrial structures that might be applicable to these landforms.

The first of the overviews was delivered by Ted Maxwell (Smithsonian Institution) who presented the progression of discovery and characterization of wrinkle ridges from the lunar mare to the smooth plains of Mercury to Mars. Lunar ridges have been studied with Earth-based telescopic observations through the time of the Apollo missions, yet very little is known about these features. There is only limited subsurface data available and only one ridge was visited in the field. Evidence of upwarping of subsurface reflectors (regolith interbeds) in the area of a mare ridge, detected by the Apollo lunar sounder experiment (ALSE) flown on Apollo 17, formed a basis for a structural interpretation. The correlation between concentric ridge systems in mare basins and the location of suspected subsurface basin peaks suggest that these prebasalt structures strongly influenced the formation of the wrinkle ridges.

Investigations of the wrinkle ridges associated with the Tharsis region of Mars have shown the ridge system to be concentric to the topographic high. In contrast to ridge systems in lunar basins, the Tharsis ridge system has no apparent relationship to basement structure. Unresolved problems identified were (1) whether or not there is a single origin, (2) that subsurface influences are unconstrained, and (3) that ridges that cannot be attributed to a local or regional control have no clear tectonic implications.

During the discussion it was pointed out that there is good evidence of embayment of lava flows by wrinkle ridges suggesting that the growth of the ridges was syntectonic with the emplacement of the mare basalts. This is a characteristic shared by the anticlinal ridges of the Columbia Plateau. Arvid Johnson (Purdue University) noted that kink folds observed in landslides he has been studying developed first as a low-amplitude, symmetric buckle or "pucker," followed by reverse faulting.

Johnson began the second overview with the observation that "words are the problem." When a structure is called a "fold," for example, the mode of origin is dictated by the terminology. Often there is little evidence that structures given the same name formed the same way. The use of experiments is important in the study of the folding process, and such experiments show many fold forms that are composites of a number of waveforms. In attempting to match the field expression of a fold, it is important to incorporate the contribution of the first-, second-, and third-order waveforms in the model. These various waveforms often result from the boundary conditions. The models produce identical results for the viscous and elastic rheology, and whether the layers in the multilayer have free-slip or are bonded. A change in the properties of the contacts (i.e., frictional effects) between the layers, particularly if they are nonlinear (i.e., power-law), strongly influences the fold form. In general, folds are highly localized. The power-law effects of slip at contacts has the localizing effect that generates the perturbation that results in a fold. The "seed" waveforms spontaneously generate higher order waveforms when the effects of power-law slip are included. The first- and third-order waveforms, together with localized or power-law slip, begin to produce folds that are kink-like in form (i.e., sharp anticlines and subdued synclines). Thus, the buckling wavelength can be determined considering only the first-order waveforms; however, to model the fold shape, the higher order waveforms must be incorporated.

A question raised during the discussion concerned whether surface topography alone could be used to invert the problem and obtain the mechanical properties. Johnson's response was he "wouldn't dare do it"; the subsurface information is very important. He also stated that analogs are important for identifying the fundamental mechanism, but that is not the same as explaining the fold forms. We need to have a better fundamental knowledge of these processes.

The final overview, dedicated to fault-related folding on Earth, was given by John Suppe (Princeton University). Suppe noted that after examining the topographic profiles across lunar and martian wrinkle ridges prepared by Matt Golombek (Jet Propulsion Laboratory), linear morphologic segments similar to those of oil field anticlines could be recognized. Regional elevation changes from one side of the structure to the other are also commonly associated with oil field anticlines. Many of the folds observed on

the Earth are composed of angular segments and are fault-related. The fault-related folds identified are (1) fault-bend folds, (2) fault-propagation folds, (3) lift-off folds, and (4) box folds. Of these, the most important mechanisms are fault-bend folding and fault-propagation folding. Fault-bend folds are the result of bending of a thrust sheet as it is translated over a nonplanar surface. Fault-propagation folds develop at the tip of a propagating thrust fault and tend to be more complex than fault-bend folds. Geometric and kinematic relationships between the fault and the fold shape formulated for both these mechanisms have proven very successful when tested against very well constrained fold and thrust structures (i.e., western foothill belt of southcentral Taiwan). Active deposition during deformation significantly modifies the fold shape.

As the discussion evolved, it was noted that there is no mechanical basis for the geometric and kinematic relationships developed for fault-bend or fault-propagation folding. Suppe argued that the geometric relationships are known to work well in spite of any strong mechanical basis in fold or fault mechanics. It was asked if the fault-bend fold mechanism requires the existence of two planar, mutually parallel surfaces connected by a fault before any folding occurs. Suppe responded that such an assumption was necessary to the mechanism.

SESSION I
WRINKLE RIDGES AND COMPRESSIONAL STRUCTURES: CONTRIBUTED PAPERS

Summarized by Ted A. Maxwell

Following the overviews of planetary and terrestrial compressional structures, several contributed papers presented evidence for folding of the martian plains surface, as well as new models for the deformation surrounding martian volcanoes. In keeping with the workshop mode, questioning and critical comments were incorporated into the presentations, and several suggestions for the evolution of martian landforms received instantaneous reviews. The first alternative suggestions for the origin of wrinkle ridges were put forward by Dave Scott (U.S.G.S., Flagstaff), who pointed out the correspondence of ridges with extensional structures and their continuation as aligned pit craters, promoting an extensional origin for certain ridges. Although ably presented by Mary Chapman (also of U.S.G.S., Flagstaff), such an origin was not highly favored except, possibly, for certain individual ridges. Jayne Aubele (Brown University) provided an extensive morphologic classification of the various attributes of ridge systems on the Moon and Mars, noting that common features include arches, parabolic segments, and predictable patterns of small ridges either flanking or atop the crests of major structures. All of these features were attributed to the reaction of surface layers to a major structural disturbance at depth within a compressional stress regime (though the geometry of the particular feature at depth remains unconstrained).

Structural reconstruction and field investigations of the Umtanum fold ridge by John Watkinson (Washington State University, Pullman) and Ed Price (CER Corp., Las Vegas) indicate that both faulting and folding were involved in the deformation that produced this terrestrial analog to planetary ridges. Because no subsurface information is available, the extent of faulting at depth is not known. Two faults observed in the ridge consist of an upper thrust fault that dies out along strike, and a lower thrust whose dip angle is based on the dip of the fold at the surface. According to Tom Watters and John Chadwick (Smithsonian Institution), ridged plains in the Hesperia Planum region of Mars exhibit cross-cutting relations that may locally be used to determine the time sequence of folding. Using a buckling model for ridge formation, they proposed that such structures could form from two periods of compressional stress at orientations of 90° to each other, although the necessary strength contrasts for such a model were questioned. Matt Golombek (Jet Propulsion Laboratory) and others proposed that the primary structural feature of ridges is the offset in topography that, when combined with the spacing of ridge systems and assumed dips of thrust faults, could form by thrusts that extend well into the crust. Although it was pointed out that not all ridges have this topographic offset, and such a model may not fit lunar basin ridge systems, this mode of formation might provide the missing link between lithospheric stress and surface response.

The tectonic deformation of martian volcanoes is evident in Viking images that show scarps, subtle concentric hills on the flanks, and regional systems of ridges and grabens that surround the structures. By analogy with faults on the flanks of volcanoes in Costa Rica, Andrea Borgia (Jet Propulsion Laboratory) and others proposed that the Olympus Mons scarp resulted from faulting generated by the collapse of the volcano. Paul Thomas (Cornell University) and others investigated the upper scarps of Olympus Mons by means of a finite element model, concluding that such scarps are the result of thrust faulting. The possibility of strike-slip faulting could not be excluded, however, since the calculations of hoop stress have not yet been considered.

In the final talk of the day, Larry Crumpler (Brown University) and Aubele considered the regional tectonic "signature" of martian volcanic complexes, finding that the oldest volcanoes have the least apparent relationships to the regional stress field. They further suggested that self-generated stresses were not the primary cause of the regional systems of faults and possible folds surrounding martian volcanoes.

SESSION II
STRIKE-SLIP FAULTING
Summarized by K. Tanaka

This session was chaired by Matthew Golombek (Jet Propulsion Laboratory) and included review talks by Randall Forsythe (University of North Carolina) and Terry Tolan (Portland State University). These talks showed the relations of strike-slip faults and related structures in plate-tectonic and local settings, including the Yakima fold belt. Other presentations and discussions centered on features that may result from strike-slip deformation on Mars.

Diverse structural features associated with strike-slip faulting on Earth may be identifiable on images of the martian surface. Although strike-slip offsets of geologic features (e.g., offset craters) are rarely seen on Mars, secondary deformational features such as shear fractures and folds in relatively soft material may be more readily discerned. A terrestrial example is the absence of features having large amounts of displacement along the San Andreas strike-slip fault system; however, many of the secondary structures confirm the strike-slip deformation. Such features included splayed faults at the surface of the fault zone in which small fault blocks may have been uplifted or downdropped ("flower structures"). Also, *en echelon* normal faults and anticlinal ridges commonly form along the fault zone, and primary and secondary Reidel shears may form (the primary ones trend at a low angle to the main fault). Where the main fault steps over, zones of compression (transpression) or extension (transtension) may occur between the fault steps, causing secondary faulting and folding structures and either uplift or downdrop. These features commonly have rhombic or sigmoidal forms.

Strike-slip faults on Earth may be categorized according to their size and depth of penetration. Transform faults like the San Andreas penetrate through the entire lithosphere and have relatively steady movement and abundant secondary structures. Transcurrent faults are commonly associated with subduction zones that are at oblique angles to the direction of relative plate motions and probably do not cut entirely through the crust.

The Yakima fold belt in southeastern Washington State, which may be analogous to planetary wrinkle ridges, formed in a sequence of late Tertiary flood basalts whose stratigraphy is well documented. Three categories of primarily dextral, northwest-trending strike-slip structures have been studied: (1) Tear faults bound anticlinal ridge segments and occur only near areas of ridge uplift; (2) Other tear faults have very little displacement (tens of meters or less), and although associated with development of the fold belt, these faults do not control fold geometry and may be related to a broad "distributed shear" system in the basement of western North America; and (3) Regional wrench faults may bound anticlinal ridges, as in the first category, but they also continue into, and commonly through, adjacent basins and may have hundreds of meters of displacement. In transpressive zones along these faults, *en echelon*, faulted, asymmetric, doubly plunging anticlines have formed, whereas in transtensional areas, horsts and grabens are found. This last category was produced by strike-slip faulting that originated prior to fold-belt development. Crumpler showed that gentle anticlines and small grabens also occur in association with strike-slip faults in the Springerville volcanic field in Arizona.

Tom Watters (Smithsonian Institution) noted that orientations of regional strike-slip and fold structures in the Yakima fold belt are consistent with compressional structural deformation models; therefore, if similar compressional models describe the formation of wrinkle ridges on Mars, strike-slip faults and their associated secondary structures as described above may be common as well. Some scarps associated with wrinkle ridges on Lunae Planum south of Kasei Valles and north of Hebes Chasma may be martian candidates for similar-style tear faults.

Another style of strike-slip deformation may explain the morphology of offset wrinkle ridges southeast of Valles Marineris, according to Richard Schultz (NASA Goddard Space Flight Center). Here, *en echelon* linear structures connect wrinkle-ridge segments; where the linear structures overlap, rhombohedral plateaus have developed between them. The plateaus are morphologically distinct from wrinkle ridges and appear more likely to result from contractional uplift in stepover zones between the *en echelon* strike-slip faults.

The north-northwest-trending Gordii Dorsum escarpment in the highland/lowland transition zone southwest of Olympus Mons may be a transcurrent fault, as discussed by Forsythe. The fault zone juxtaposes surfaces of distinct morphology, age, and elevation. On the higher side, conjugate fracture systems and possible fold ridges suggest left-lateral strike-slip movement. Questions remain regarding the timing of the faulting and the extension of the hypothesis to similar ridges to the west.

Overall, an unexpected amount of interest in strike-slip faulting on Mars, given the paucity of previously offered evidence, was shown at the workshop. This interest was stimulated by demonstrations of terrestrial associations of strike-slip structures with both extensional and compressional structures. Such associations provide tools and insights that previously have not been applied to a significant extent on Mars. Although evidence for plate-boundary transform faulting on Mars appears to be lacking, several local martian structures may indicate the occurrence of strike-slip deformation in special structural and tectonic settings.

SESSION III
EXTENSIONAL STRUCTURES

Summarized by Randall D. Forsythe

The third session was primarily dedicated to the presentation of papers on extensional structures, but ended with an overview of the Yakima fold belt by Steve Reidel and co-workers in preparation for the following day's field excursion.

The session started with an invited overview by Matthew Golombek on the extensional structures of Mars. Setting the stage for some of the contributed papers to follow, he divided extensional phenomena into a series of classes ranging from simple grabens and tensional fissures, to more complex phenomena such as aligned pit craters and fault-bounded major chasms (e.g., Valles Marineris). Simple graben systems, although quite common on the Moon and Mars, appear to be rare on Earth. He discussed elevation and slope data that have previously been used to infer dips for the fault planes of around 60°, which, together with the spatial relations observed between inward dipping fault pairs, have formed the basis of the argument for shallow (0.5 to 5 km) fault nucleation under relatively low (perhaps tens of MPa) stress. Richard Schultz (NASA Goddard Space Flight Center) raised questions regarding some geometric and mechanical assumptions underlying the depth of faulting estimates, and expressed concern regarding their applicability to prefractured rock. As Sean Solomon (Massachusetts Institute of Technology) pointed out, however, regardless of the likely variations in failure angles (e.g., 45°–75°), the structures are undoubtedly shallow, and reveal an upper regolith of relatively low strength. Further comment was made by Randy Forsythe (University of North Carolina) on the appropriateness of a two-dimensional (dip section) model for explaining the three-dimensional (map) character of graben systems on Mars. This appears especially problematic where, in map view, fault scarps bounding grabens converge into a narrow tip without systematic shallowing of the graben floors. Golombek also briefly presented arguments for deeper fissuring in association with some of the normal faults. The overview raised many important issues to be addressed by some of the ensuing speakers, namely, the extrinsic and intrinsic parameters controlling the mode of extensional failure, the relation of "basement" and "cover" in extensional provinces, the underlying mechanisms inducing extensional failure, and the contribution of surface processes in the modification of tectonic features.

The general discussion of martian extensional features was followed with an overview by George McGill (University of Massachusetts) of the Earth's variable tectonic regimes for extensional faulting. The presentation focused on the uniqueness of terrestrial tectonic settings. This was, in turn, used to argue for caution in drawing any direct analogies between the Earth's tectonic features and those on our neighboring planets. This raised some debate between James Head (Brown University) and McGill over the analogy that has been drawn between the Earth's accreting (extensional) plate boundaries and topographic ridges on Venus. Head emphasized that there were a number of lines of evidence from a variety of locations to support the spreading ridge interpretation.

The presentation then turned to consider in a more positive light what insight could be gathered for either martian simple graben or tension "crack" phenomena through an examination of two cases of graben or fissure formation on Earth (one example from the Colorado Plateau, the other from Iceland). Before moving into this discussion, the first-order differences in martian morphologies of extensional features alluded to by McGill (i.e., tension crack or normal fault) were questioned by Ted Maxwell (Smithsonian Institution) who raised the issue of whether or not these features could have been significantly modified by surface processes. A debate ensued concerning the intrinsic or extrinsic conditions determining a shear or tensile mode of failure in the martian regolith. John Suppe (Princeton University) pointed out that the mode of failure was determined by a trade-off between fluid pressure and cohesion. Because, intuitively, one would not expect strengths in unconsolidated materials to support tensional failure, the compositional and mechanical nature of the martian "megaregolith" was central to these discussions. McGill suggested that some healing or cementing agent (e.g., calcium carbonate) may be at work. The discussion of horst and grabens occurring in the region of Canyonlands (western U.S.) provided the format for a lively discussion of the relation of basement movements to the shallow system of normal faults. This brought participants' attention to a consideration of the fundamental mechanism for extension. Arvid Johnson (Purdue University) pointed out that distributed extension in the underlying Paradox Formation could account for the even spacing seen between the normal fault traces, but Suppe countered that the faults in question did not appear to be developed regionally to support such a model. McGill concluded this debate by saying that a gravitational sliding model seemed most appropriate. The talk ended with a brief presentation of a spectacular example of collapse "grabens" with aligned pit craters on Iceland. Most participants agreed that in this case there seems little doubt that the pit crater formation was linked to fissuring and the subsequent draining of surficial materials into the deeper parts of the fissure.

The third presentation was given by Kenneth Tanaka (U.S.G.S., Flagstaff) on the graben and pit crater relationships (under current investigation) in the Alba

Patera region. The presentation again focused attention and discussion on the mechanical nature of the materials composing the martian surface. While the case for tensional fissuring at depth under many of the aligned pit craters was supported by their co-occurrence and alignments with the grabens, their specific origins remain clouded by other uncertainties. Specifically, debate on this issue indicated a lack of consensus on the contribution of dissolution phenomena, eolian erosion, and to a lesser extent, redeposition in their formation. At present, therefore, conclusions arising from quantitative structural models appear nonunique. The obvious progressive enhancement of pit crater development along successively closer lines to Valles Marineris was pointed out by Suppe, and in response, Tanaka suggested that this could be the result of pronounced extension as one approaches the valley. The discussion of pit craters again led to open speculation on the possible presence and composition of soluble materials (e.g., calcium carbonate) within the martian regolith.

The extensional tectonics session continued with a presentation by Schultz that focused on the negation of the generalization that pit crater chains are an early stage in the formation of canyons. There was some discussion and debate over the various examples cited that reflected some persisting confusion over the various morphologic classes of valley and canyon walls. Despite these differences, most agreed that relations indeed negate a simple evolutionary tie between these two morphologic phenomena, no matter how they happen to be individually viewed or defined. The underlying interpretation that pit craters are more likely reflective of tensional mode failures (as a possible response to diking at depth) was somewhat in accord with the tensional model discussed previously by Tanaka and Golombek. Nevertheless, there remained major uncertainties as to the contribution of other surface and near surface processes in the formation of pit craters.

Following up on the problems of pit crater formation, Steve Croft (University of Arizona) then presented a brief discussion of possible karst phenomena in the Hebes-Juventhae-Gangis area. Debate arose concerning these features, as well as, again, what soluble materials might exist within the martian regolith. It was clear from his presentation, however, that not all pit craters are aligned or, for that matter, found in obvious association with fault scarps or tensional fissures.

Finally, Robert Craddock (Smithsonian Institution) presented evidence for a system of ancient normal fault scarps in the Memnonia area. These were postulated, based on a regional analysis of their trends, to form a set of radial faults to a previously postulated Daedalia Basin (Daedalia Planum). The principal criticism voiced by Golombek and others is that the features were not conclusively demonstrated to be normal faults. While a tectonic origin appears clear, further work is needed to clarify their kinematic significance.

ABSTRACTS

MORPHOLOGIC COMPONENTS AND PATTERNS IN WRINKLE RIDGES: KINEMATIC IMPLICATIONS;

J.C. Aubele, Dept. Geological Sciences, Brown University, Providence, R.I. 02912

INTRODUCTION The origin and mechanism of formation of planetary wrinkle-ridges has been in question since the initial discovery of these features on the moon. Subsequently, ridges similar in form and appearance to lunar mare ridges have been identified on Mercury, Mars and Venus and, in a few instances, on Earth. Theories of the origin of wrinkle-ridges can be classified into tectonic, volcanic, or combined processes. Sharpton and Head [1] have summarized and evaluated the evidence for lunar mare wrinkle-ridge origins proposed by other workers and have concluded that mare ridges and their characteristic morphology are the surface expressions of tectonic deformation. Previously proposed structural models have described thrust faults [1,2,3,4], stike-slip faults [5], vertical faulting [6], keystone-style splay faults [1], anticlinal folding [7,8] and upwarp due to underlying topography [9]. Many workers have compared the morphology of mare-type ridges on the other planets with similar features on Earth formed by known mechanisms, such as thrust fault deformation associated with recent earthquakes, anticlinal folding in the Columbia Plateau flood basalts, deformation on the surface of a collapsed lava lake, and small-scale pavement folds due to landslide movement [4,7,10]. All of the structural models and terrestrial analogues involve compression.

Mare type wrinkle-ridges were originally described [11,12] as composed of three morphologic parts or, as they will be referred to here, components; 1) a broad linear rise, which may not always be present or may be visible only under low illumination angles; 2) an arch, which may be up to 200m high and 7 km wide; and 3) a crenulated ridge which may be up to 100 m high and 1.5 km wide and may be central or marginal to the position of the arch. In cross section, the arch may appear symmetrical or asymmetrical with alternating scarp directions [13].

Wrinkle-ridges on all planets exhibit this characteristic morphology. In fact, it is by this morphology alone that they are identified. Understanding this morphology, then, is necessary to understanding the ridges themselves. Furthermore, any regular pattern in the morphology should be indicative of the kinematics of wrinkle-ridge formation. For this reason, the morphological components of a large number of lunar and Mars ridges have been mapped in detail and these components and their patterns have been characterized.

OBSERVATIONS A wrinkle ridge can be treated as a system of related individual components, as previously described by Aubele [14], or as an "assemblage", as described concurrently by Watters [15]. All of the morphologic components, rise, arch and crenulated ridges occur as segmented features along the general trend of the wrinkle ridge, with individual component segment lengths that are shorter than the overall length of the wrinkle ridge. Each component segment tends to be arcuate to sinuous in map view, with sinuosity increasing with decreasing size. In map view, the entire wrinkle ridge can be modeled as a series of individual parabolic curves of different sizes and alternating orientations. All component segments overlap, so that minor (small) crenulated ridges can be thought of as being superimposed on major (large) crenulated ridges which are superimposed on arches which, in turn, occur on rises. The only exceptions to this generalization are minor crenulated ridges (less than 200 m wide) which sometimes occur off the arch, either parallel to or at some angle to the main trend of the wrinkle ridge.

The crenulated ridge component segments of a typical wrinkle-ridge occur in a range of sizes that can be divided into general categories: major ridges ($\geq$ 0.2 km in width); and minor ridges ($\leq$ 0.2 km in width), as named by Aubele [14] or 1st, 2nd and 3rd order ridges, as named by Watters [15]. As illustrated in Figure 1, the major crenulated ridges tend to occur along the outer margins of the arch, frequently crossing from one side to the other in a sinuous or en echelon pattern. Where a crenulated ridge is superimposed at one margin of an arch and then crosses to the other margin, it gives the entire wrinkle ridge a general appearance of asymmetrical and alternating scarps. In cross-section, however, each component of a wrinkle ridge can be individually modeled as a symmetrical curve, or an anticlinal fold, while the overlap of individual components presents a somewhat misleading appearance of assymetry in the wrinkle ridge when viewed as a whole. In general, there is a direct relationship between widths of arch and major crenulated ridge segments within a wrinkle ridge.

The orientation of the major crenulated ridge segments and the arch segments of a wrinkle ridge form a distinct and regular pattern (Fig.1, close-up A and B). The crenulated ridge segments occur either: 1) generally parallel to the arch in a sinuous map pattern, first along one margin and then along the other margin of the arch (Fig. 1A); or 2) at some angle to the main trend of the arch in an en echelon pattern (Fig. 1B). In fact, when tangents are drawn along the major crenulated ridge segments of an entire wrinkle-ridge, they are all oriented in the same general direction, regardless of the orientation of the main trend of the arch. The arch tends to follow pre-existing structure; for example, the circumference of basins or the rims of buried craters. The crenulated ridge segments tend to occur oriented in a dominant direction along the entire length of the wrinkle-ridge. When the strike of both arch and crenulated ridge segments coincide, then the crenulated ridges occur in their sinuous pattern moving from margin to margin of the arch (Fig. 1A). When the strike of the arch and crenulated ridge segments diverge, then the crenulated ridges continue to follow their original strike and occur in a series of en

echelon segments crossing the strike of the arch (Fig. 1B).

ANALYSIS The regular pattern in crenulated ridge and arch orientation, is an indication of the kinematics of wrinkle ridge formation. The orientation of the crenulated ridge component appears to be related to a dominant direction of regional compression. For example, the crenulated ridge segments of the wrinkle-ridges in southern Serenitatis are predominantly oriented in a N-S direction, while the arch, and the general wrinkle-ridge system itself, is apparently aligned with the circumferential basin margin or buried basin ring. This supports previous work [16] that identified the N-S trending wrinkle ridges in the center of several lunar basins as indicating a dominant E-W compressive stress regime which existed during the formation of the wrinkle-ridges. The major crenulated ridge component segments, therefore, apparently exist perpendicular to the dominant direction of compression; the arch component segments can be affected by local stress, and can exist either perpendicular to the direction of compression or at some oblique angle to the direction of compression. In ordinary circumstances, strike-slip movement might be expected along the oblique angle segments. Experiments in clay [17,18] have shown that en echelon folds can occur as initial conjugate features along a zone which is oblique to a dominant direction of compression and undergoing shear. These are known as "pre-peak" structures, referring to the fact that they occur just before the shear strength is exceeded. No strike slip fault forms when the total strain is very small and the shear strength of the material is not exceeded. This implies that minimal strain is associated with the formation of the en echelon segments of lunar wrinkle-ridge morphology, which agrees with previous estimates of small percentages of surface shortening and horizontal deformation of craters [13,1].

Any mechanism of formation for wrinkle ridges must take into account the existence and observed characteristics of the morphologic components that make up wrinkle ridges; the change in wrinkle ridge morphology with change in terrain or geologic unit; the primary occurrence of wrinkle ridges on planetary plains units, basins, and volcanic calderas; and the fact that recognizable wrinkle ridges are infrequently observed on Earth. In addition, the relationship in width of the crenulated ridge and arch components, and their regular and predictable patterns implies that the components are related during formation but are capable of reacting in different ways to the mechanism of formation. The pre-peak en echelon folds imply minimal strain associated with formation. This evidence indicates that wrinkle ridges are not the direct result of a major thrust fault breaking the surface, but rather the indirect result of some subsurface fault that is manifested as associated minor ruptures and slip close to the surface and folds at the surface (Fig. 2). This type of structural movement has been observed in terrestrial anticlines formed in layered material and as a precursor surface manifestation of thrust faults that have not yet propagated to the surface [A. Johnson, pers. comm., 1989]. Three conditions are necessary for this type of structure: (1) layered stratigraphic sequence with intercalated incompetent beds that can act as slip planes; (2) no pre-defined major fractures of joints in the stratigraphic sequence; and (3) a subsurface disturbance, either a compressional fault or subsidence over pre-existing topography, that causes folding of the stratigraphic sequence above it. In response to the subsurface disturbance, the layered sequence experiences minor converging or diverging ruptures, called symmetrical overthrusting, along slip planes. These faults are detached from, but related to, the major subsurface fault or disturbance and may alternate in orientation to produce surface anticlinal folds of sizes related both to the growth of the wrinkle ridge structure and the thickness of the layers experiencing folding. This model would predict the existence of layered plains units and subsurface discontinuities wherever planetary wrinkle ridges are observed; and explains the morpologic components, their patterns, the change in morphology with change in terrain, and the lack of recognition of these features on Earth with its active erosional regime.

CONCLUSIONS Wrinkle-ridges consist, not of random combinations of scarps and "wrinkles", but of consistent patterns of (1) morphology, (2) trends of morphologic components, and (3) trends between morphologic components. The typical wrinkle-ridge morphology can be produced by small compressive strains. The entire wrinkle-ridge structure appears to be the result of "pre-preak" compression of the surface. The amplitude of the stress field at the surface, generated by faulting or displacement along pre-existing structures at depth, does not exceed the shear strength of the surface material. As a consequence, the surface warps, "wrinkles" and experiences minor ruptures and multiple sytles of deformation at the surface. Any major rupture at depth need not break the surface. It appears that a dominant direction of regional compression generates the consistently oriented major crenulated ridge components, while local compressive influences affect the arch components. Where the crenulated ridge and arch component segments are at an angle to each other, then they represent a general zone of incipient transpression and the crenulated ridge components form en echelon conjugate compressive features perpendicular to the dominant direction of compression. Based on this study, the major crenulated ridge components, not the entire wrinkle-ridge, should be used to indicate the direction of regional compression.

References [1] Sharpton, V.L. and Head, J.W., 1987, Proc. LPSC, 18th [2] Conel, J. E., 1969, Jet Propulsion Laboratory Space Program Summary 37-56, v.111, p.56-63. [3] Howard, K.A. and Muehlberger, W. R., 1973, Apollo 17 Prelim. Science Report, NASA SP-330, p. 31/22-31/25. [4] Pieccia J.B. and Golombek, M.P., 1986, G.S.A. Bull, v. 97, p. 1289-1299. [5] Tjia, H.D., 1970, G.S.A. Bull., v. 81, p. 3095-3100. [6] Luchitta, B.K., 1976, Proc. Lunar Science Conference, 7th, p. 2761-2782. [7] Watters, T.R. and Maxwell, T.A., 1985. Reports Planetary Geology and Geophysics Programs, 1984, NASA T.M.87563, p. 479-481. [8] Watters, T.R., 1987, G.S.A. Abst.w/programs, v.19, p. 883. [9] Solomon, S.C. and Head, J.W., 1979, J. Geophys. Res., 84, p. 1667-1682. [10] Greeley, R. and Spudis, P.D., 1978, Lunar Science Conference, 9th (Abst.), p.411-412. [11] Strom, R.G., 1972, *in* Runcorn,

S.K. and Urey, H.C., (eds.), The Moon, IAU Symposium no. 47, p.187-215. [12] Hodges, C.A.,1973, Apollo 17 Prelim. Sci. Report, NASA SP-330, p. 31-12 to 31-21. [13] Lucchita, B.K., 1977, Proc. Lunar Science Conference, 8th, p. 2961-2703. [14] Aubele, J.C., 1988, LPSC 19 (abst), p. 19-20. [15] Watters, T., 1988, LPSC 19 (abst), p. 1245-1246. [16] Fagin, S.W., et al., 1978, Proc. LPSC, 9th, p. 3473-3479. [17] Tchalenko, J.S., 1970, G.S.A. Bull., v.81, p.1625-1640. [18] Wilcox, R.E., et al., 1973, AAPG Bull. v.57, no 1, p. 74-96.

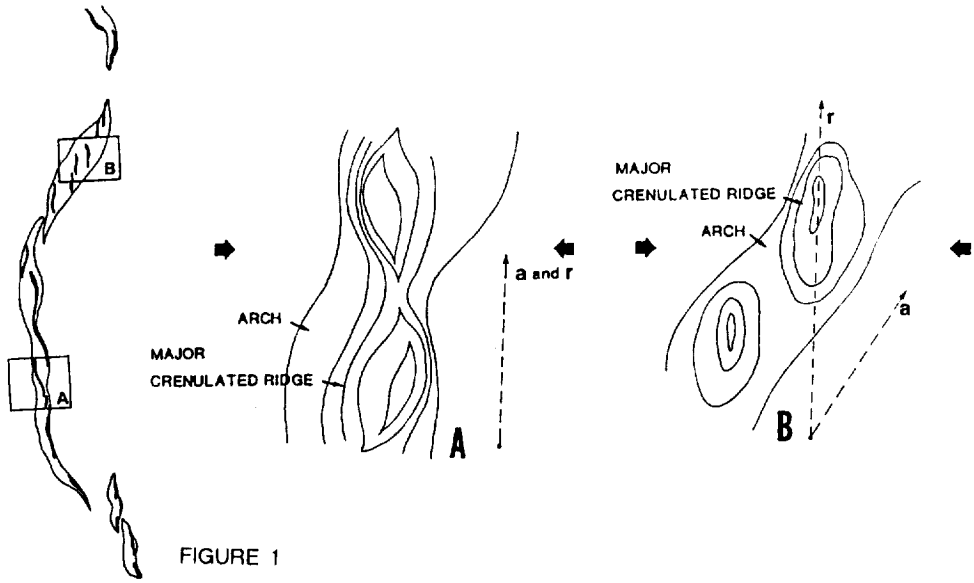

FIGURE 1

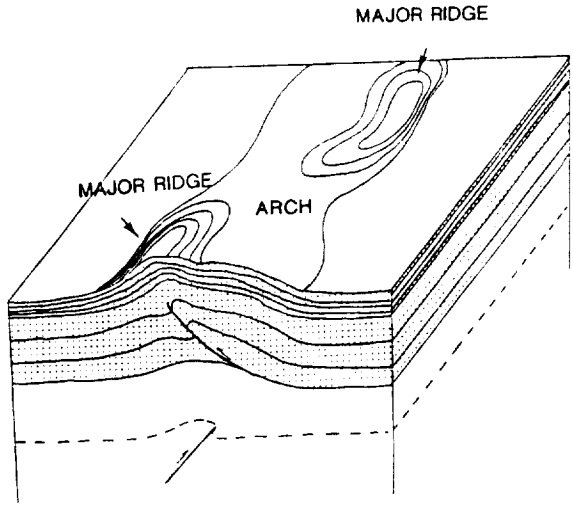

FIGURE 2

FIGURE 1. Schematic morphologic map of a typical lunar wrinkle-ridge showing the arch and crenulated ridge components. Narrow black lines outline arch component segments. Thick black lines represent major (large) crenulated ridge component segments.
CLOSE-UP A and B. Crenulated ridge superimposed on arch is indicated by generalized contour lines. Dashed arrows indicate strike of arch component (a) and crenulated ridge component (r). Large arrows indicate direction of regional compression.

FIGURE 2. Block diagram of proposed model. Only one of many related minor ruptures is shown. A converging overthrust in a direction opposite to the one shown, and occurring behind the plane of the paper, would account for the major ridge component at far right. Minor ridge components, not shown , would be produced by slip and ruptures between layers closer to the surface.

THE OLYMPUS MONS SCARP: A FAULT-PROPAGATION FOLD GENERATED BY GRAVITY FAILURE OF THE VOLCANO?;

Andrea Borgia, Jet Propulsion Laboratory, California Institute of Technology, 4800 Oak Grove Drive, Pasadena, CA 91109, USA; Jeremia Burr, Department of Geological Sciences, MacAllister College, 1600 Grand Avenue, St. Paul, MN 55145, USA; Walter Montero and Luis Diego Morales, Escuela Centroamericana de Geologia, Universidad de Costa Rica, Ciudad Universitaria "Rodrigo Facio", Costa Rica; Guillermo Induni Alvarado, Departamento de Geologia, Instituto Costarricense de Electricidad, Apt. 10032, San Jose, Costa Rica.

The prominent scarp that surrounds Olympus Mons on Mars has been interpreted to be a result of: 1) differential erosion between outer more erodible tuff deposits and inner less erodible lava flows (Carr et al., 1973; King and Riehle,1974; Williams, 1988); 2) landsliding of the outer flanks of the volcano (Head et al., 1976; Lopes et al., 1980; Francis and Wadge, 1983); and 3) subglacial birth of Olympus Mons (Hodges and Moore, 1979). None of these interpretations fully accounts for the available topographic data (for instance: the ridges and the gentle counter slope uphill from the scarp, the secondary scarps downhill from the scarp, and the mirror symmetry of the scarp around the volcano). We suggest that the scarp is the surface expression of a fault-propagation fold that has formed by gravitational failure and spreading of the volcano.

This thesis is based on a terrestrial analog found in the Central Costa Rica Volcanic Range. This west-northwest trending volcanic range is bordered by 10-20 km long and 100-200 m high scarps, which are symmetrically located 20 km to the north and to the south of the range, parallel the range axis, and face away from it. A ridge and secondary scarps exist at the summit and at the base of the scarp respectively. The southern scarp (the Alajuela Scarp) was interpreted as: 1) a lake or alluvial terrace; 2) a normal fault of an intra-arc basin; or 3) lava flow fronts. The northern scarps (the San Miguel and the Guappiles Scarps) were interpreted as the normal faults delimiting a back-arc basin (the Nicaragua Graben).

Detailed geological and geophysical work was conducted on the Alajuela Scarp and preliminary work on the other two scarps (Borgia et al., 1987). The stratigraphic sequence consists of the Pliocene, clay-rich, volcano sedimentary Aguacate Formation overlyain by Pleistocene, massive, >10 m thick, basaltic andesite lava flows and ignimbrites interbedded with weathered, partially consolidated ash beds. Recent fluvial and lake deposits crop out uphill and downhill from the scarp; lahars and talus slope deposits exist only downhill from the scarp. The structure shows that the scarps are the steeply dipping frontal limbs of asymmetric angular anticlines that verge away from the Volcanic Range (Fig. 1). The ridges correspond to the hinge zone of the anticlines whose back limbs gently dip towards the range. The geometry of these anticlines and associated faults suggest that they are fault-propagation folds (Suppe, 1985) formed in front of low-angle thrust faults at the base of the volcanic range. The thrust faults step up from depths of about 500 m over distances of approximately 2 km and terminate in the axial surfaces of the frontal synclines. Frequently, syncline breakthrough and high-angle breakthrough are observed. Tear faults separate blocks with different fault-propagation fold geometries. The hanging wall of each fault has been thrusted about 200 m away from the volcanic edifice. The presence of secondary scarps in front of the main one suggests that thrusting might occur also along secondary thrust faults. Thrusting on the lower flanks of the range is compensated by extention on the range axis with the formation of summit grabens. Gravity and magnetic surveys of the Alajuela Scarp are consistent with this interpretation. Shallow seismicity in the volcanic range indicates that tear faulting and thrusting are still active. We suggest that the thrust faults are located at the Pliocene-Pleistocene boundary and formed by gravitational failure and consequent spreading of the Volcanic Range possibly triggered by the intrusion of magma over the last 50 ka.

The morphologies of the Olympus Mons scarp and related structures, such as tear faults and secondary scarps, are very similar to those of the Central Costa Rica Volcanic Range and to the geometry of fault-propagation folds. Thus, we envision a similar process for the formation of the

scarps at Olimpus Mons. In this senario, the structure of Olympus Mons (and perhaps part of the lithosphere) failed under its own weight. The consequent spreading along low-angle thrust faults produced the scarps according to the fault-propagation fold mechanism. The presence of low-angle thrust faults on Olympus Mons and its aureole has also been suggested by Harris (1977). Spreading of the lower flanks of the volcano was predominantly towards the northwest and the southeast, and induced rifting and volcanic activity along a northeast-southwest trend (Francis and Wadge, 1983). The increase in topographic gradient at the scarp during uplift of the anticline produced the large landslides found in the aureole. This model suggests that Olympus Mons has been fairly symmetric and that no ancestral Olympus Mons (Harris, 1977; Lopes et al., 1980) nor rotation in the stress field (Francis and Wadge, 1983) are necessary to account for the presence of the scarp and for the orientation of the latest northeast-southwest volcanic activity.

References

Borgia A., Burr J., Montero W., Morales L.D., and Alvarado G.I., 1987. Trans. Am. Geoph. Union, v. 68, n. 16, p. 406.
Carr M.H., Masursky H., and Saunders R.S., 1973. J. Geoph. R., v. 78, p. 4031-4036.
Francis P.W. and Wadge G., 1983. J. Geoph. R., v. 88, n. B10, p. 8333-8344.
Harris S.A., 1977. J. Geoph. R., v. 82, p. 3099-3107.
Head J.W., Settle M., and Wood C., 1976. Nature, v. 263, n. 5579, p. 667-668.
Hodges C.A. and Moore H.J., 1979. J. Geoph. R., v. 84, p. 8061-8074.
King J.S. and Riehle J.R., 1974. Icarus, v. 23, p.300-317.
Lopes R. M.C., Guest J.I., and Wilson C.J., 1980. The Moon and the Planets, v. 22, p. 221-234.
Suppe J., 1985. Prentice-Hall, Inc., pp. 537.
Williams S.H., 1988. Lunar and Planetary Science XIX, p. 1279-1280.

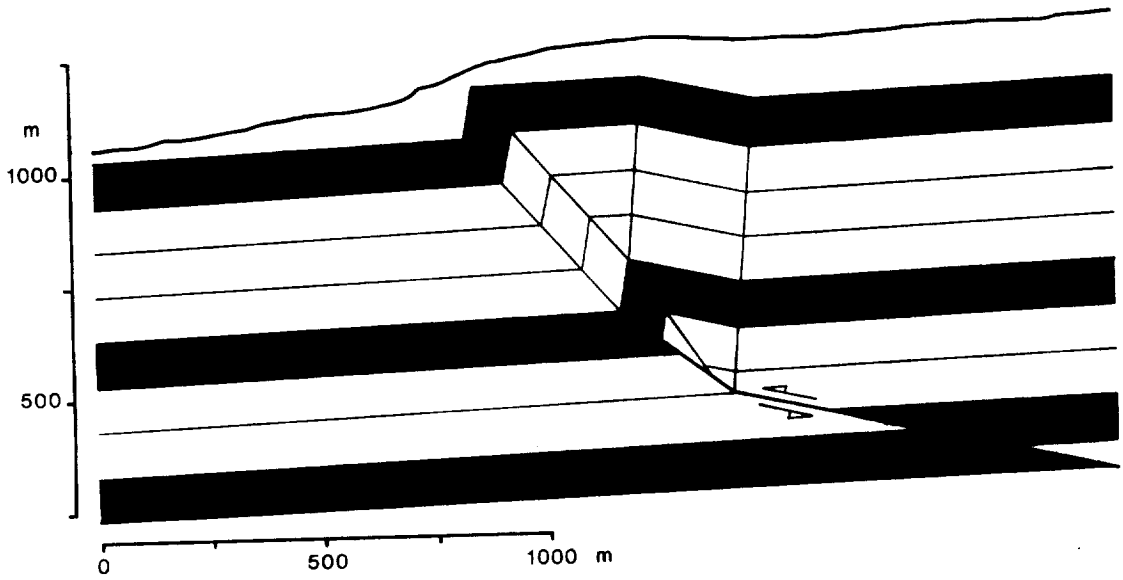

Fig. 1. Retrodeformable geologic cross-section of the Alajuela Scarp along Rio Itiquis. Geometry of surficial beds is measured, dip structure is based on fault-propagation fold theory (Suppe, 1985). Upper continuos line is topography. North is to the right. A similar model may be applicable to Olympus Mons scarp.

NORMAL FAULTING ASSOCIATED WITH THE DAEDALIA IMPACT BASIN, MARS; Robert A. Craddock, James R. Zimbelman, and Thomas R. Watters; Center for Earth and Planetary Studies, National Air and Space Museum, Smithsonian Institution, Washington, D.C. 20560

Identification of impact basins on Mars is important for several reasons: accurate knowledge of the number of basins is necessary for determining cratering flux and the role of resurfacing processes, large and/or numerous impacts may have played an important role in establishing the present crustal dichotomy (1,2), and basins influence a wide variety of surface processes due to the intense energy released during formation and the associated large-scale modification of the crust. Geomorphic evidence based upon Viking photographic and earth-based radar data suggest that an additional 1100- to 1500-km-diameter basin exists in the Daedalia Planum region of the western hemisphere of Mars (3,4). This large semi-circular region contains Hesperian to Amazonian age volcanic materials (5) and is bounded by numerous features which may be related to possible ring structures.

The first suggestion of a Daedalia Planum basin was made by Plescia et al. (1980; 6) using earth-based radar observations (Fig. 1). These observations showed fault blocks tilted symmetrically towards 120.0° longitude. This corresponds closely to the Daedalia basin center (-26.0°, 125.0°) determined by the structural analysis of highland features which morphologically resemble lunar Imbrium Sculpture (3,4,7,8). More recently, correlation of results from photogeologic mapping (9,10) with the earth-based radar observations has identified several north-south oriented normal faults within the ancient materials near Mangala Valles (11,12; Fig. 2). The vertical relief along the faults ranges from 500 to 2500 meters, and the N5E orientation for the faults indicates that they probably are not related to stresses associated with the Tharsis uplift as exemplified by the N65E trend for graben of Memnonia Fossae. The oldest unit of the Mangala Valles materials superposed on the eastern margin of the faulted highland materials is lower Hesperian in age, supporting a Noachian age for the large faults (12). The faults are approximately concentric to the proposed Noachian age impact basin in Daedalia Planum and may be related to an extended ring system for that basin (4). Compressional features such as wrinkle ridges are frequently associated with the faults (Fig. 3), suggesting that zones of weakness caused by the impact were reactivated during isostatic rebound following basin formation or crustal loading due to mare style volcanism.

REFERENCES: (1) Wilhelms, D.E. and S.W. Squyres, Nature, 309, 138-140, 1984. (2) Frey, H. and R.A. Schultz, Geophys. Res. Lett., 15, 229-232, 1988. (3) Craddock, R.A. et al., Lunar and Planet. Sci., 20, 195-196, 1989. (4) Craddock, R.A. et al., Evidence for an Ancient Impact Basin in Daedalia Planum, Mars.

NORMAL FAULTING ASSOCIATED WITH THE DAEDALIA BASIN
R.A. Craddock, J.R. Zimbelman, and T.R. Watters

Submitted to Jour. Geophys. Res. (5) Scott, D.H. and K.L. Tanaka, U.S. Geol. Surv. Misc. Invest. Series Map I-1802-A, U.S. Geol. Surv., Denver, CO, 1986. (6) Plescia, J.B. et al., Lunar and Planet. Sci., 11, 891-893, 1980. (7) Craddock R.A. et al., Lunar and Planet. Sci., 19, 213-214, 1988a. (8) Craddock, R.A. et al., Abstracts for the MEVTV-LPI Workshop: Early Tectonic and Volcanic Evolution of Mars, 12-14, 1988b. (9) Greeley, R. and R.A. Craddock, Geologic Map of the Southern Mangala Valles Region of Mars (MTM -20147), submitted for review. (10) Zimbelman, J.R. et al., Geologic Map of the Southern Mangala Valles Region of Mars (MTM -15147), submitted for review. (11) Zimbelman, J.R., Trans. AGU 69 (16), 390, 1980. (12) Zimbelman, J.R., Lunar and Planet Sci., 20, 1239-1240, 1989. (13) Zimbelman, J.R., Abstracts for the MEVTV-LPI Workshop: Early Tectonic and Volcanic Evolution of Mars, 72-74, 1988. (14) U.S. Geological Survey, Map I-1187 (MC-16 SE), U.S. Geol. Surv., Denver, CO, 1979.

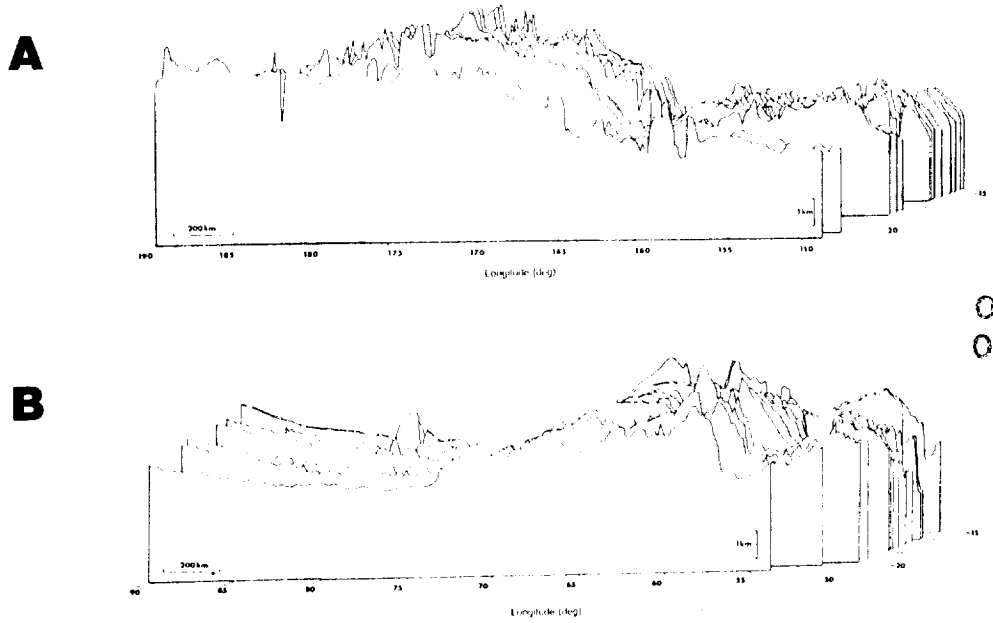

Figure 1. Topographic profiles obtained from earth-based radar measurements (from 6). (A) Data from the Memnonia region (190° to 150° long.) and (B) data from the Syria Planum region (90° to 50° long.). Note the slope of materials tilted towards each other and symmetric to the 120° longitude line, or roughly the center of Daedalia Planum. Plescia et al. (1980; 6) interpreted these tilted blocks as being the result of Tharsis tectonics or representing the rim of an ancient impact basin centered in Tharsis. Photogeologic and structural analysis of the surrounding region suggests that the latter interpretation is correct (3,4,7,8).

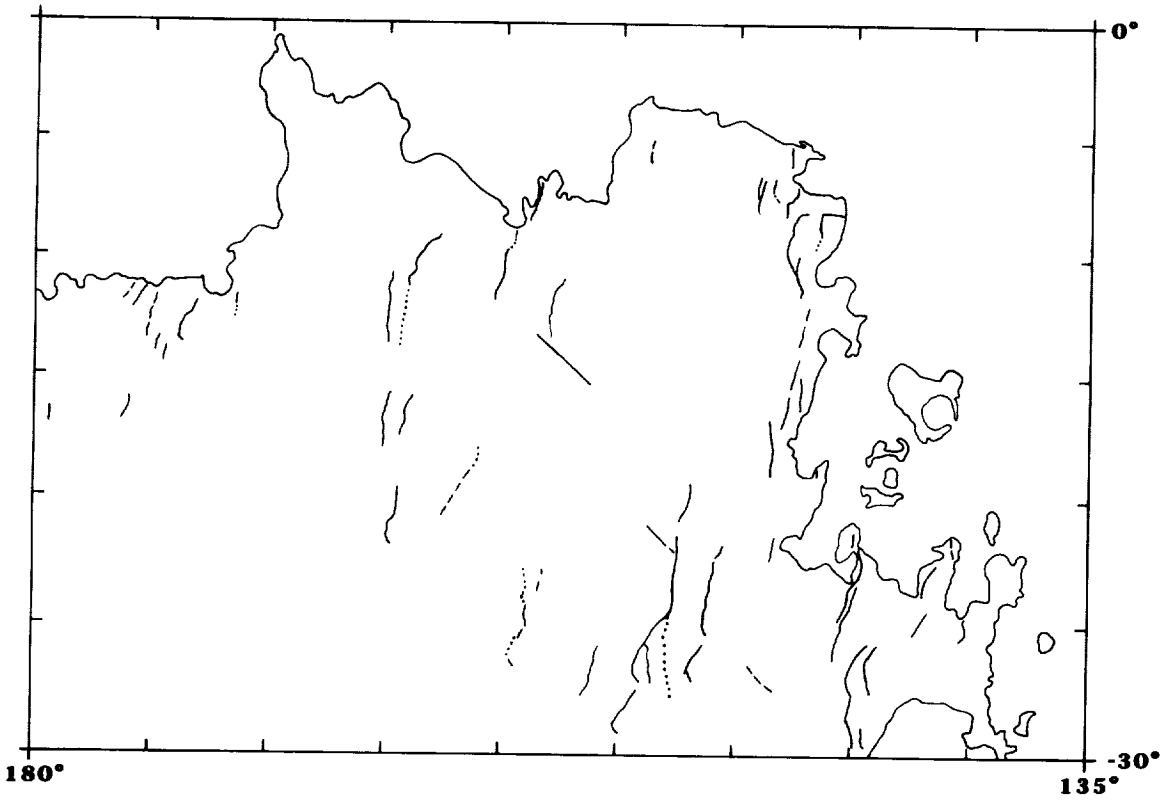

Figure 2 (above). Location of the major faults within the Memnonia quadrangle. Heavy lines show normal faults, dashed lines show presummed normal faults, and dotted lines show compressional features. Trend is to the northeast, indicating that the faults are concentric to the Daedalia basin. Modified from (13).

Figure 3 (right). Photomosaic (14) of a Memnonia normal fault with some strike-slip (arrow). Inset shows location of normal faults and their relationship with compressional features. Area shown is from about 15°S to 30°S and from 146°W to about 157°W.

SPELUNKING ON MARS: THE CARBONATE-TECTONIC HYPOTHESIS FOR THE ORIGIN OF VALLES MARINERIS. Steven K. Croft, Lunar & Planetary Laboratory, University of Arizona, Tucson, AZ 85721.

Introduction. The canyon complex associated with Valles Marineris is one of the more spectacular and tectonically important features on the surface of Mars. Several hypotheses have been proposed for the origin of the canyons invoking erosion and tectonism in various combinations (1,2,3). A particular problem has been explaining the numerous closed depressions (e.g., Ganges Catena and Hebes Chasma, see figure 1 for locations) and their relationships to the larger open canyons. These depressions are generally rimless pits occurring singly or in chains that often merge directly into the larger linear canyons, as in Tithonium Chasma or at either end of Candor Chasma. The depressions and areas of 'chaos' also associated with the canyon system bear striking resemblance to the sinkholes, box canyons, and cockpit clusters found in terrestrial karst terrains (cf. 4). Three models have been proposed to account for the morphology and occurrence of these features.

1) Thermokarst: This model assumes the uppermost layers of Mars' surface to consist of ice-filled soils. Canyon formation begins by local melting of the ice followed by evaporation of the water and eolian dispersal of the remaining cohesionless dust (e.g.,5). The main problem with this model is physical: ice-saturated materials cannot support the observed topography. This is because the multi-kilometer high walls generate shear stresses of hundreds of bars which would drive viscous collapse on time scales of hours to days (6) and immediate shear failure in permafrost materials, even at the prevailing surface temperature near 225 K. Both the viscosity and shear strength (some 40-80 bars at 225 K, 7) of ice/soil mixtures decrease rapidly with depth in the warm interior, exacerbating the support problem. Theoretical calculations (8) indicate that only solid rocks are strong enough to support the canyon walls. Further, observed failure surfaces of large debris slides and block slumps cut several kilometers down and back into the pre-existing wall. If wall cohesion and strength were provided by interstitial ice, then the failure surfaces extend several kilometers into the thawed zone where subsurface temperatures reach 273 K, free water exists, and shear strengths and viscosities drop effectively to zero. Such failure surfaces are mechanically unlikely. Assuming such slip surfaces could form, new scarp faces should show some form of collapse or seepage (which are not evident) at the level in the scarp (about one km down) of the top of the thawed zone.

2) 'Real' Karst: Spencer & Croft(6) proposed that the canyons formed at least in part as collapse structures in massive deposits of carbonate rock - "real" karst as opposed to "thermokarst". The competent carbonate rock could support the observed topography and produce the collapse structures. This model requires an extensive active hydrosphere and early seas in which the carbonates could precipitate. The suggestion of even thick sequences of carbonate rock is reasonable from both an atmospheric (9) and geochemical (10) point of view. The original difficulties with this model were the lack of any direct evidence for carbonate rocks on Mars and the extremely large volumes of water that must be circulated to remove the observed volume of the canyons (e.g., 10^{10} km^3 to remove just the material in Hebes Chasma). However, the recent spectroscopic detection of a carbonate derived rock (scapolite, 11) on Mars and evidence for carbonate materials in the SNC meteorites (12), which apparently come from Mars, ameliorate the first difficulty. Two possible solutions to the second difficulty have been proposed. First (13), the ground waters on Mars may contain significant concentrations of sulfuric acid which would dissolve carbonates more efficiently (e.g., only 10^8 km^3 needed for Hebes). Second (14), much of the volume for the canyons may be due to tectonic subsidence (see below). In addition, both 13 and 14 noted that the amount of water required may be reduced further still if part of the material is removed as suspended sediment. This would require large contiguous caverns (as opposed to merely porous rock layers) connecting closed depressions to open outflow channels.

3) Extensional Tectonics: The most recent version of this model (15) invokes the formation of extensional cracks into which the material of the closed depressions can drain. The main problem here is simply the enormous depths (far into the martian mantle) the cracks must extend for any reasonable crack width to provide enough volume to account for the observed surface depressions.

The Carbonate-tectonic Model: The model currently preferred here is a combination of the karst and tectonic models based on a re-analysis of canyon structure and the mechanism(s) of canyon formation in and around Valles Marineris using local high-resolution geologic mapping (primarily in Hebes and Juventae Chasmata), regional geologic analysis, topography and stability analyses, and regional spectral

analysis. The following geologic observations are relevant to the model: 1) Karst terrain morphologies. As noted above, individual closed pits, pit strings, and chaos areas are typical karst forms. Several different types of canyon-related depressions exist on Mars: closed, rough-floored canyons (e.g., Hebes), flat-floored canyons opening into outflow channels (Echus, Gangis), closed sinkhole-like depressions (Ganges Catena), and rugged, closed depressions in and around pre-existing impact craters (Coprates Lx and Ku). Geometric relationships tie these multiple canyon types together into long (order 1000 km) "strings" related to the E-W regional tectonic structure (e.g., Echus-Hebes-Ganges Catena-Coprates Lx-Juventae, see figure 1). At least three major "strings" parallel each other through the entire Coprates quadrangle: Echus-Juventae, Candor-Gangis, and Ius-Coprates, with several smaller parallel branches. Each of the strings includes an obvious outflow channel, generally at the topographically low east end. Evidence for large amounts of water flowing into the main canyons (including the closed depression of Hebes) is provided by the blunt,coarsely dendritic side canyons that have been interpreted as sapping channels (16). Note that sapping can account for the open side channels but not for the closed depressions, which are more characteristic of karst. 2) Tectonic Subsidence: The strings are obviously tectonically controlled and run along the crest of a topographic ridge extending eastward from the sub-circular Tharsis uplift (and which may be a distinct structure). A few large N-S faults apparently cut through the area, e.g., the east wall of the box-like Ophir Chasma aligns with the west wall of Juventae. Tectonic subsidence (in addition to tectonic control) is indicated by post-wall formation fault movement in Melas-Coprates (1) and differential erosion patterns on the floor of eastern Ophir Chasma (17). Detailed mapping in Hebes Chasma has shown, in addition to the surficial debris slides (tens of km^3) off the rugged 'spur-and-gully'-type walls that line most of the canyons and the large debris slides (100's of km^3) that form sheer arcuate wall segments tens of km long in some sections, that coherent subsidence blocks (100's of km^3) with horizontal dimensions up to several tens of km occur. The floor of Hebes also has two patches of chaotic terrain at distinct topographic levels 4 and 5 km below the surrounding plateau. Other occurrences of chaotic terrain are associated with surface layers that have been disrupted by near-surface subsidence. The implication is that the chaotic areas in Hebes have been tectonically dropped as separate blocks by several kilometers. Similarly, a 20 by 20 km block of plateau material sits at the bottom of Gangis Chasma, again possibly due to tectonic subsidence. 3) Long-range underground water transport: There are several examples of outflow channels issuing abruptly from large surface cracks, e.g., Mangala Vallis emerging from one of the Memnonia Fossae and the channels at the NE end of Tempe Fossae. Similarly, smaller channels descending into Echus, Hebes, Tithonium and Melas Chasmata follow pre-existing fractures, indicating localization of underground water flow over large areas. The inferred watersheds for these channels extend uphill for many hundreds of kilometers, indicating movement of water along subsurface fractures for at least comparable distances. Thus it is not unreasonable that underground watercourses could physically link the various collapse features of the tectonic strings. 4) Not all runoff slopes have karst features: The karst structures of Valles Marineris are fairly localized. Minor collapse features are found near Alba Patera, scattered thinly to the SE of Tharsis, and near Elysium Mons. Yet channels occur rather widely. In particular, the inferred water discharge in Mangala Vallis is comparable to that of Juventae Chasma or Shalbatana Vallis, yet there are no local collapse features at Mangala as there are at the Valles Marineris locations. This implies that the 'erodable stratum' is not everywhere present on Mars (additional evidence against the thermokarst model). In the carbonate interpretation, these observations imply that thick (several km) beds of carbonate material are located under Lunae and Sinai Plana, thin beds under Alba, parts of Tharsis, and Elysium,and very little anywhere else (except perhaps in the putative deposition areas in the Northern plains).

Together, these observations imply that both tectonic subsidence and karst processes have operated in Valles Marineris, motivating the combined carbonate-tectonic model. The question then becomes one of the relative importance of the two processes. Volumes of identifiable depressions in the Valles Marineris complex range from 10^2 to 10^3 km^3 for the simple pits and pit chains, jumping to 10^5 to 10^6 km^3 for Hebes and the larger canyons, with almost no intermediate volume structures. All of the larger canyons have tectonically controlled straight sides, whereas the sides of the pits and chains all consist of collapse segments, with Hebes being a transitional case. The volumes of enlargement features in the main canyons due to sapping, karst processes, and landslides (presumably due to undermining of cliff walls by solution processes) are also in the 100 to 1000 km^3 range. This implies that karst processes

can account for individual features up to on the order of 1000 km^3 in volume, but that larger features are primarily due to tectonic subsidence. This interpretation is shown in the cross sections of various features in the Valles Marineris area in figure 2: pits and catenae form as collapse structures over caverns formed by ground water along major faults through soluble rocks whereas the major canyons form initially as subsidence structures (like grabens) that are subsequently enlarged somewhat by solution-driven mass wasting.

The inferred structure and history of Valles Marineris based on the cited geologic features and the carbonate-tectonic model are as follows: Mars originally had a fairly thick ($\approx$ 5 bar) CO_2 atmosphere allowing the presence of a (shallow?) ocean in the vicinity of the present Valles Marineris and smaller seas elsewhere. Carbonates were deposited in the seas depleting the atmosphere and allowing the surface to cool. Regional uplift (related to Tharsis?) generated regional fractures and high topography. Tharsis-related volcanism then covered the fractured carbonates with basaltic lavas to depths of 1 - 2 km (based on thicknesses of layered sequences in the canyon walls and the widths of grabens in the Tithonium-Echus area). Continued uplift formed the present ridge and generated rift-like subsidence to form the major canyons. The aquifers were charged by snow/rainfall (from a sea on the northern plains?), driving subsurface circulation through the fractures in the carbonate materials. Lakes apparently formed in Hebes, Ophir, Candor, Gangis, and Juventae Chasmata (assuming a lacustrine origin of the layered deposits) which discharged through subsurface rivers to the outwash channels. Roof collapse over the subsurface rivers generated the closed depressions in the open plains (Ganges Catena) and in the fracture systems associated with some craters (Cop. Lx). Solution processes in near-surface carbonate deposits produced the chaos regions. Fluvial erosion flattened the floors of the outwash channels (Echus, Coprates-Capri). Lateral canyon enlargement continued by sapping, continued groundwater solution, landslides, and minor tectonic subsidence. While the bulk of the canyons' volume was produced by tectonic subsidence, most smaller features were produced by solution processes and/or fluvial removal of sediments. If terrestrial analogs are any guide, Mars' spectacular collapse features indicates the presence of equally spectacular caverns that may ultimately be some of the most interesting (and useful) geologic structures on Mars.

REFERENCES. 1. Sharp R.P. (1973) J. Geophys. Res. 78:4063. 2. Blasius K.R. et.al.(1977),JGR 82,4067. 3. Carr M. (1984) Mars, in NASA SP-469,p.207. 4. Jennings J.N. (1985) Karst Geomorphology, Blackwell. 5. McCauley J.F. (1972) Icarus 17:289. 6. Spencer J.R.& S.K. Croft(1985) MECA Workshop on Evol. of Mars Atm.,p.40. 7. Phukan A. (1985) Frozen ground engineering. 8. Clow G.D. & H.J. Moore (1988) Lunar Planet. Sci. XIX, 201. 9. Kahn R. (1985) Icarus 62: 175. 10. Warren P.H. (1987) LPI Tech. Rpt. #87-01, p. 120. 11. Clark, R.,G. Swayze, & R. Singer (1988)EOS Dec. 13,p.1634. 12. Gooding J.L. (1989) 4th Int. Conf. on Mars, p. 115. 13. Spencer J.R., F.P. Fanale and J.E. Tribble (1989)4th Int. Conf. on Mars, p. 193. 14. Croft S.K. (1989) 4th Int. Conf. on Mars, p. 88. 15. Tanaka K.L. & M.P. Golombek (1989) Proc. Lunar Planet. Sci Conf. 19th, p. 383. 16. Papers in: Howard A.D., R.C. Kochel & H.E. Holt, editors (1988) Sapping features of the Colorado Plateau. NASA SP-491. 17. Lucchitta B.K. (1989) Geologic map of Valles Marineris, in prep.

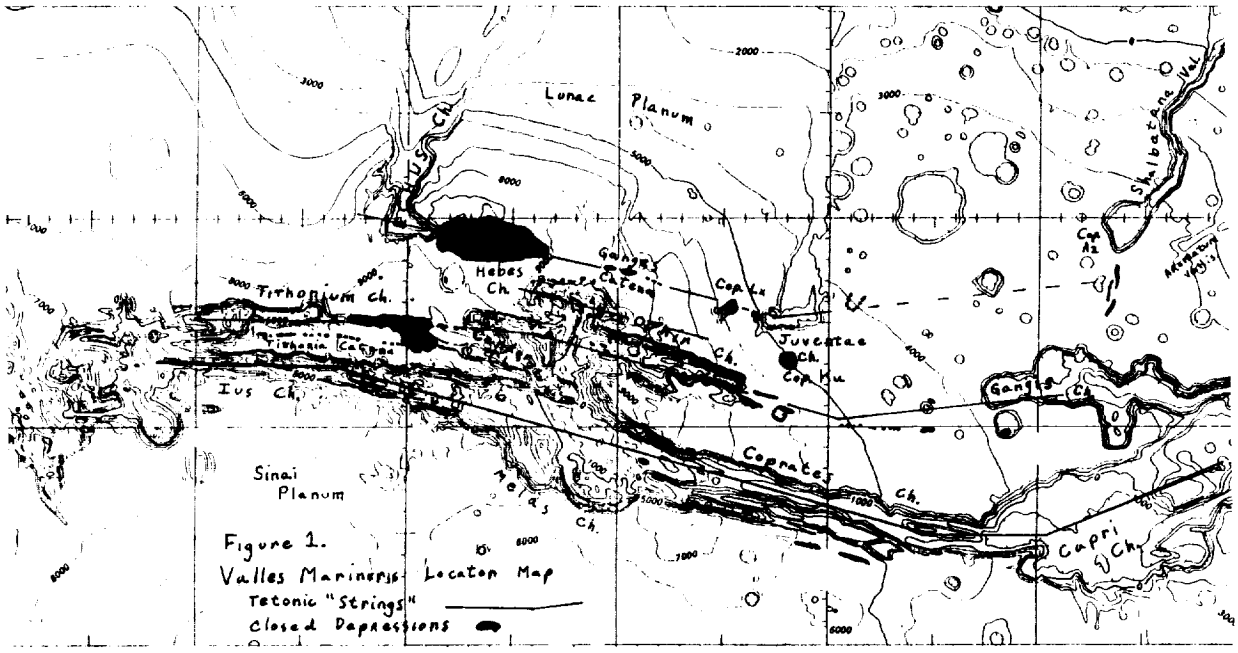

Figure 1.
Valles Marineris Locator Map
Tetonic "Strings"
Closed Depressions

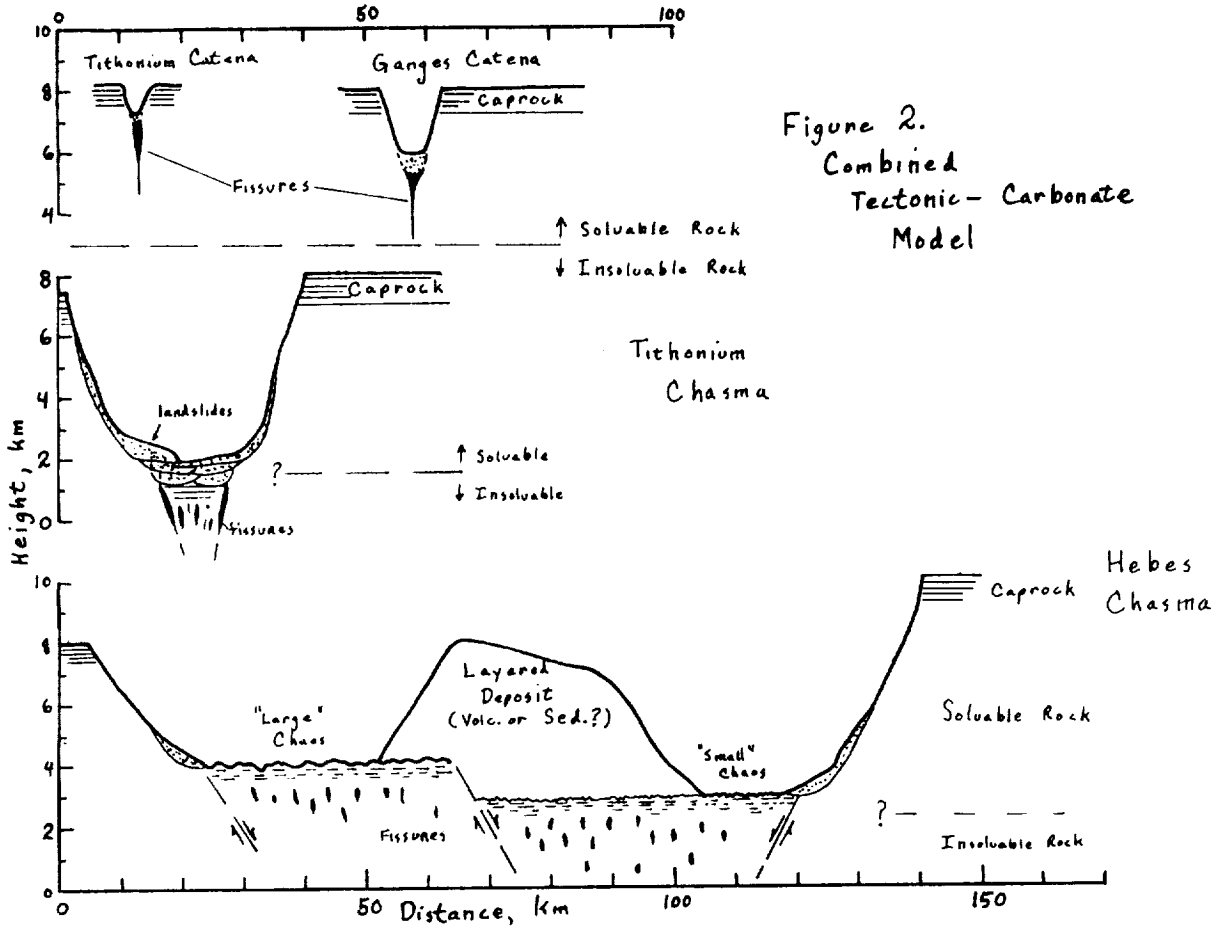

Figure 2.
Combined Tectonic-Carbonate Model

Influence of Tectonic and Volcanic Stresses on the Flank Structure of Martian Volcanoes.

L.S.Crumpler and Jayne C. Aubele, *Department of Geological Sciences, Brown University, Providence, RI 02912*

Introduction. A range of characteristics structural features are known to occur in association with volcanism on Earth and frequently reflect a relationship between the overall magmatic type of volcanism and the tectonic environment. In addition to this influence on the fundamental type of volcanism, on Earth the influence of the orientation and magnitude of the regional tectonic stresses is also reflected in the orientation and magnitude of detailed structural characteristics on the flanks of volcanoes [1,2]. The association of magmatic type with regional tectonic style reflects the complex chemical as well as thermal evolution of each planet, and no two planets are likely to have similar correlations between these two characteristics. However, the fundamental influence of tectonic stresses on the geometry, orientation, location, evolution, scale, length, and width of magmatic feeding dikes and vents [3] may be predicted for most of the terrestrial planets, together with the influence of tectonic stresses on flank structure. In the following we examine the relative importance of teconic stresses in terrestrial volcanoes, define several catagories of their occurrence, identify the presence of similar range of structural features in Martian volcanoes, and assess the significance of these features in characterizing the magnitude and history of tectonic stresses contemporaneous with active growth of Martian volcanoes.

Influence of Regional Stress Field on Flank Structure. The influence of regional tensile stress on the presence and orientation of fissure trends [4] and the local and regional orientaion of individual dikes and dike plexi [5,6] are fundamental. On the basis of an examination of the type of regional and flank features and its correlation with regional tectonic stresses on terrestrial volcanoes, we identify four simple catagories of flank structure. These are characterized by the degree of influence and interaction with regional stress fields as: (i) strong, (ii) moderate, (iii) weak, and (iv) none.

Type (i), strong influence of regional stress, is characterized by regional linear patterns in the vent arrangements and alignments wherein a significant linear pattern occurs both on a regional and local scale both in the presence of central volcanoes and in isolated areal volcanic fields consisting of multiple, relatively short-lived vents. If a pre-existing structural fabric consisting of several orientations is present, only one orientation is well-developed in this type. Where developed in association with a central volcano, a single fissure trend usually dominates and whose trend bisects the central vent, caldera, or nested caldera (Fig.1A). Although not entirely understood, there is often a concentric arrangement of the faulting and eruptive fissures near the summit and local less dominant radial fissures [7]. A few examples of this type on Earth include the Galapagos central volcanoes, West African Rift volcanoes such as Niyragongo, and Hekla volcano, Iceland.

Type (ii), moderate influence of regional stress, is characterized by structures influenced by both regional and local tectonic stress sources. In this type, there may be some tendency for vents, rifts, and faulting to follow regional stress orientations, but there is also a tendency for vents, fissures, and rifts to follow pre-existing structural fabric orientations [8] and local tectonic or gravitational stresses [9]. The resulting volcanic patterns of fissures and vents reflects the sum of tectonic and body stresses, and local structural fabrics oriented in differing directions and varying in local intensity, often with time, as the volcano or its nearest neighbors grow and interact (Fig. 1B). The latter effects are largely a consequence of the so-called "edifice effects" and are a result of the gravitational body stresses in the flanks in response to shape of the volcano [9] , magmatic inflation and deflation, the presence of a weak substrate, and the presence or absence of a buttressing effect by adjacent volcanoes [8,10]. On Earth the young Hawaiian volcanoes are the best known example of this type of complex interaction between tectonic and local stress fields. Other volcanoes known to exhibit some of these characteristics include many oceanic islands, such as Reunion [10].

Type (iii), weak interaction with a regional stress field, are characterized by little apparent regional tectonic influence on the orientation of eruptive fissures and vents, and gravitational or body stresses may even dominate (Fig.1C). In addition to a few oceanic volcanoes, many continental central (composite) volcanoes are noted frequently to be dominated by potential gravitational stress influences on the orientation of flanking structures [10,11]. Examples of this type of independent development in the absence of a strong regional stress pattern are the Geisha seamounts [12].

Type (iv), no interaction with a regional stress field, is not identified on Earth in large volcanoes, although it may occur in small vents, including minor plains-type shield volcanoes and cinder cones. In the absence of any regional gradients in the stress field or local gravitational body stresses, the stresses in association with the inflation and deflation of the magma chamber, if present, are likely to dominate (Figure 1D), and simple radial and concentric patterns may occur.

Tectonic Stresses on Martian Volcanoes

Crumpler, L.S. and Aubele, J.C.

Flank Structure of MartianVolcanoes. The pattern of flank structures on large volcanoes of Mars which developed during their constructive phases, including the location, orientation, and shape of individual vents, graben, and central calderas, are analogous to a variety of the patterns discusssed above. On the basis of detailed mapping of the location and evolution of structural features on their flanks, together with the detailed characterizations above, variable degrees of influence of both regional and tectonic stresses on Martian volcanoes are identified. In terms of the dominance of a single structural orientation, Arsia Mons, Pavonis Mons, Ascreus Mons, and Apollinaris Patera are most similar to type (i), Hecates Tholus, Olympus Mons, and Elysium Mons are most similar to type (ii), Tharsis Tholus, Alba Patera, and Uranius Patera are similar to type (iii), and Biblis Patera in particular, plus Uranius Tholus, Ceranius Tholus, Jovus Tholus, Ulysses Patera, and Albor Thjolus may be similar to type (iv).

These catagorizations of Martian shield volcanoes are tentative, particularly for types (iii) and (iv), and require more detailed analysis to be confirmed, but is is clear that regional tectonic stresses are expressed in the evolution and structure of these volcanoes. The influence of gravitational body stresses on flank structures are not strongly expressed, at least in a geologically recognizable form, on any of the large shields, although some aspects of the flank morphology of Olympus Mons have been interpreted as reflecting body stresses in the edifice and/or their influence on eruptive vents [13]. Aside from the presence of distinct linear trends in association with those volcanoes classified as type (i) above, there are few unequivocable vents or eruption sources on the flanks of many Martian volcanoes.

In summary we note that in addition to the influence of regional and local stresses on the structure and evolution of volcanoes, there is evidence that volcanoes on Mars are large enough and massive enough that they may exert an influence on the tectonic history of the adjacent lithosphere[14]. And finally, this prelimary study suggest that, in general, the earlier volcanoes within each volcanic province may be less influenced by a regional stress orientation than are the later volcanoes.

Conclusions. Dominant geologic structure, including vent patterns, on Martian volcanoes document and reflect the dominance, presence, orientation, and influence of regional tectonic stress fields existing during the time of their eruption and development. This is in contrast to the Earth where a variety of gravitational and local magmatic stresses may influence the pattern of structures and vents on the flanks of both continental and oceanic composite and shield volcanoes. Whereas gravitational stresses are prominent in many terrestrial shield volcanoes, gravitational, or self-generated, stresses are not as dominant as regional tectonic stresses on structural development of Martian volcanoes. Based on regional patterns in these associations, tectonic stress orientations may have been more influential in the younger volcanoes, reflecting secular trends in either the mechanical characteristics of the lithosphere or in the thermal and mechanical characteristics associated with regional Martian tectonism.

References. [1] Nakamura, K., 1977, Volcanoes as possible indicators of tectonic stress orientation. *J. Volc. Geoth. Res.*, **2**, 1-16; [2] Nakamura, K., 1984, Distribution of flank craters of Miyake-jima volcano and the nature of the ambient crustal stress field. *Bull. Earthq. Res. Inst.*, **29**, S17-S23; [3] Wilson, l. and J.W.Head, 1981, Ascent and eruption of magma on Earth and Moon. *J. Geophys. Res.*, **86**, 2971-3001; [4] Anderson, E.M., The dynamics of faulting and dyke formation with application to Britain, Oliver&Boyd, London, 2nd edition, 206pp.; [5] Ode, H., 1957, Mechanical analysis of the dike pattern of the Spanish Peaks, Colorado. *Geol. Soc. Am. Bull.*, **68**, 567-576; [6] Muller, O., and D.D. Pollard, 1977, The stress state near Spoanish Peaks, Colorado determined from a dike pattern. *Pure Appl. Geophys.*, **115**, 69-86; [7] McBirney, A.R., and H. Williams, 1969, Geology and petrology of the Galapagos Islands. Geol. Soc. Am. Mem.118, 21-100; [8] Fiske, R.S., and E.D.Jackson, 1972, Orientation and growth of Hawaiian volcanic rifts: the effects of regional structure and graviational stresses. *Proc. R. Soc. London, Ser. A*, **329**, 299-326; [9] McTigue, D.F., and C.C. Mei, 1981, Gravity-induced stresses near topography of small slope. *J.Geophys. Res.*, **86**, 9268-9278; [10] Duffield, W.A., L.Stieltjes, and J. Varet, 1982, Huge landslide blocks in the growth of Piton de la Fournaise, La Reunion, and Kilauea volcano, Hawaii. *J. Volc. Geoth. Res.*, **12**, 147-160; [11] Francis, P., and Abbott, 1973, Sizes of conical volcanoes. *Nature;* [12] Smoot and Vogt, 19 , J. Geophys. Res.; [13] Thomas, P.J., S.W.Squyres, and M.H.Carr, 1989, Flank tectonics of Martian volcanoes, this volume; [14] Comer, R.P., S.C.Solomon, and J.W.Head, 1985, Thickness of the lithosphere from the tectonic response to volcanic loads.*Rev. Geophys.*, **23**, 61-92.

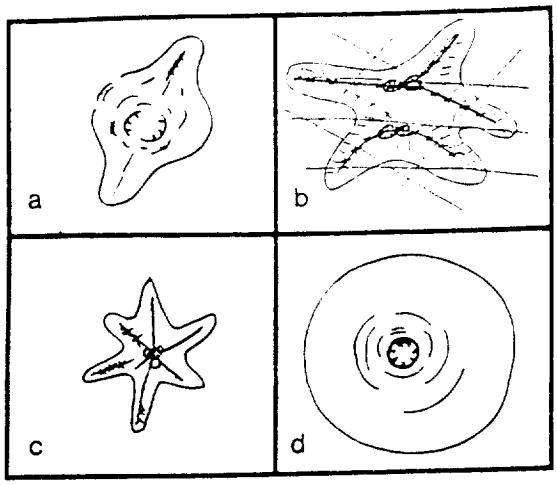

Figure 1. Four catagories of of tectonic stress field interaction with volcanoes defined in this paper. See text for discussion of each type.

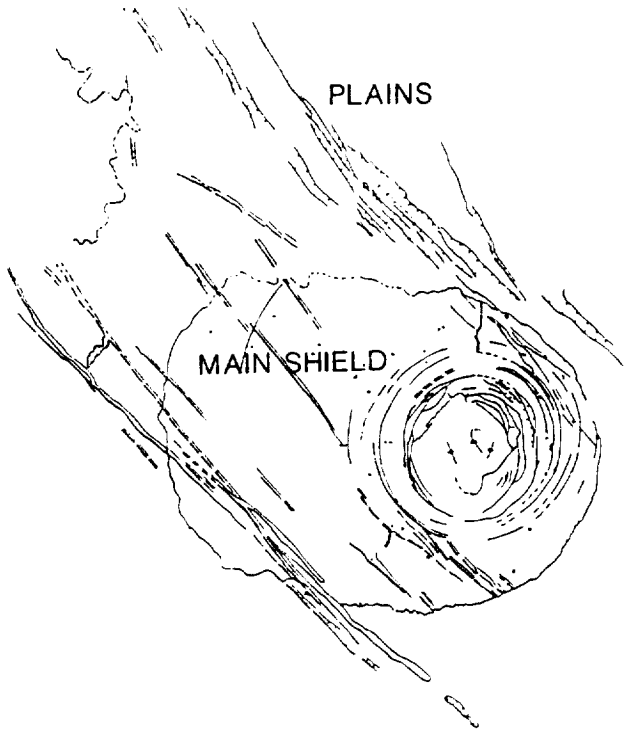

Figure 2. Tectonic sketch map of Biblis Patera, Tharsis region. The circularity of faulting patterns associated with the central caldera illustrate either the absence of a strong regional stress gradient during its formation or the local dominance of the caldera collapse-related stresses over regional stresses. Parallel and linear grabens and faults post-date volcanism.

The ubiquity and diversity of strike-slip faulting on Earth;
a generality or exception for comparative planetology?

Randall D. Forsythe, Dept. Geography and Earth Science, UNC at Charlotte; Charlotte, NC 28223

The great diversity of character and settings of occurrence for strike-slip faults on Earth should be kept in mind when seeking to interpret structural features on other planetary surfaces. Because planetary studies in structural geology and tectonics are reliant on comparative analysis with structures of the Earth's crust the state of knowledge of Earth's structures remains a critical limiting factor in such inquiries. On one hand there are areas of our knowledge over the Earth's strike-slip faults and shear zones, such as for oceanic transforms, which are still in a very primitive stage. Remote sensing of the ocean floor while having been greatly improved with new sonar imaging systems (1) is still in its first generation technology and the coverage of transforms remains limited with only moderate 100 m or poorer resolution. On the other hand geoscientists working in continental regions within the last decade have come to more fully appreciate the complexities, if not dichotomies, of structures which co-exist within continental regions of diverse plate tectonic settings (2,3,4). The global kinematic paradigm of plate tectonics does little at present to explain this complexity, and many structural geologists are awakening to the reality that large extents of the Earth's continental 'lithosphere' remains viscid, seismogenic, and continue to be subjected to patterns of complex deformation. The culling of examples of strike-slip faulting out of this complexity documents their diverse geometric and kinematic characteristics, and initiates a reference frame for comparative planetary studies.

Strike-slip faults and shear zones, are merely those discontinuities of shear in the Earth's crust and lithosphere which have displacement vectors oriented parallel to the strike of the discontinuity (3,5). They can be viewed or classed in many different ways and take many faces depending on: extrinsic factors such as temperature, pressure, state of stress, and the amounts and rates of displacement; intrinsic factors such as rock composition, fabric, large-scale layering or pre-existing structures. They can also control, or be influenced by, the presence of fluids or magmas in the crust or lithosphere.

Independent of extrinsic and intrinsic conditions, they are found to play a diverse kinematic role (6,2). The longest of the strike-slip faults, e.g. those most easily imaged from space and likely to be most directly comparable with that capable of being imaged on another planet's surface, tend to be singular faults or fault zones that are, by their singularity, zones of large-scale simple shear. Some of these, such as the Earth's transform faults, are major features affecting the entire oceanic or continental lithosphere. They have rapid (cms/yr) rates of slip, and can have large cumulative amounts (100s km) of displacement. Other lithosphere-scale singular strike-slip fault or shear zones, e.g. Atacama or Sumatra fault zones, have rates and amounts of cumulative displacements of marginal plate kinematic significance. Of a more complex character are the zones of transcurrent faults that accommodate large continent-scale deformation with pure and simple shear components (7,8). These distributed, and often conjugate, zones of strike-slip deformation are still poorly studied but are found associated with zones of both intraplate continental extension and contraction. On a much more reduced level of global significance, are those strike-slip features which are limited to the upper crust and

underplated at depth by low-angle extentional or contractional faults or shear zones. These while also not adequately understood can be singular features, or arrays of parallel or conjugate shear zones that have accommodated additional simple and/or pure shear displacements with the detached upper crust (9,10). These include strike-slip faults that transfer or relay extensional or contractional deformation from one region or crustal level to another within an otherwise grossly uniform or homogeneous zone of deformation; simple shear accommodation zones that, through the developments of singular or arrays of subparallel shear zones, permit differential contraction or extension with 'oroclinal' provinces; and pure shear accommodation zones that permit general strains to be obtained in zones dominated mechanically by fold and thrust development the latter of which inherently favors plane strains.

Finally, on the smallest scale, individual fault blocks and folds on the Earth eventually tend to be reactivated under non-ideal 'nonAndersonian' conditions. Such non-ideal reactivation typically produces within-structure small-scale secondary, or 'nested' accommodation structures(11).

Just, as not all strike-slip faults visible in the upper crust are found to penetrate down into the lower crust or mantle, some deep vertical shear zones do not appear to have produced upper crustal strike-slip faults of the same orientation. On the ocean floor these are perhaps indicated by the overlapping spreading centers, and by the replacement of a well a defined fracture zone with a more diffuse zone of block faulting. In continental regions, these appear to be represented by diffuse zones of block faulting in association with large rotations (12,13).

Is the role of strike-slip faulting on the Earth a general guide, or exception thereof, for what is to be expected on other planets such as Mars or Venus? The Earth's major transforms and transcurrent faults, that basically form lithosphere-scale zones of simple shear, are linked mechanically and kinematically in rather unique ways to the Earth's global kinematic pattern of shifting plates. On Mars such a mobilistic history may have been present in its ancient past (14), but resurfacing processes have largely destroyed this early record. On Venus, on the other hand, evidence is accruing for accreting plate boundaries(15), and with this one should expect to find evidence for transforms of some kind or another. The ubiquity and diversity of moderate to small scale strike-slip accommodation features within the Earth's contractional and extensional provinces should however continue to stand as a lesson for what in general one should expect in association with extensional or contractional provinces.

(1) Searle, R. C., 1979, J. Geol. Soc. Lon. 136, 283-292, (2) Harding, T. P. and Lowell, J. D., 1979, AAPG 63, 1016-1058, (3) Sylvester, A. G., 1988, Geol. Soc. Am. 100, 1666-1703, (4) Dewey, J. F., 1988, Tectonics, 7, 1123-1140, (5) Bates, R. L., Jackson, J. A., 1987, Glossary of Geology, AGI, Alexandria, VA, 788 p. (6) Woodcock, N. H., 1986, Roy. Soc. Lon. Phil. Tran. A., 317, 13-29, (7) Peltzer, G. and others, 1988, JGR 93, 7793-7812, (8) Gates, A. E., Simpson, C., and Glover, L.,III, 1986, Tectonics, 5, 119-180, (9) Sengor, A.M.C. and others, 1985, SEPM Spec. Pub. 37, 227-264, (10) Royden, L.H., 1985, SEPM Spec. Pub. 37, 319-338, (11) Philip, H., and Meghraoui, M., 1983, Tectonics, 17-50, (12) Luyendyk and others, 1985, Geol. Soc. Am. Bull. 91, 211-217, (13) Ron and others, 1984, JGR 89, 6256-6270, (14) Forsythe, R. D., and Zimmbelman, J. R., 1988, Nature, 336, 143-146, (15) Head, J. W. III, and Crumpler, L. S., 1987, Science, 238, 1380-1385.

The transcurrent fault hypothesis for Mars' Gordii Dorsum Escarpment

Randall D. Forsythe, Dept. Geography and Earth Science, UNC at Charlotte; Charlotte, NC 28223
James R. Zimbelman, Center for Earth and Planetary Studies, National Air and Space Museum, Smithsonian Inst., Washington D.C. 20560

The Gordii Dorsum Escarpment has been hypothesized to represent an exhumed ancient (Noachian - early Hesperian) left-lateral transcurrent fault zone within the equatorial transitional region to the west of Tharsis Montes (see fig. 1, ref. 1,2). Within this province, which has been argued to be intermediate in age between the Amazonian age surfaces to the north, and the intensely cratered, Noachian, surfaces to the south, the Gordii Dorsum is merely one of a number of NNW trending ridges that appears to be a distinctive or characteristic feature of this province (3-5). It is thus reasonable to argue that what is true for the Gordii Dorsum is likely to be also true for these other NNW trending ridges.

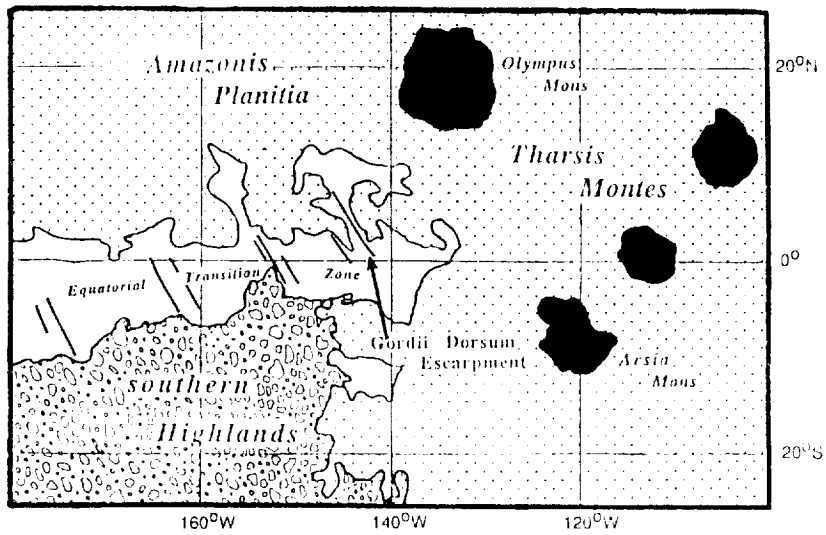

Figure 1. Location and terrain map for the equatorial region to the west of Tharsis Montes. The Gordii Dorsum Escarpment is merely one of a series of sub-parallel NNW trending ridges or escarpments in this 'transitional' province between the highlands of the southern hemisphere and the plains of the northern hemisphere.

The Gordii Dorsum Escarpment was originally interpreted as a fault zone that vertically displaced the surface a couple hundred meters, as well as juxtaposed surfaces of variable morphologies and age (3).

The later arguements for left-lateral strike-slip movement were based on the comparative analysis of surface features along the escarpment with other faults on Mars, Earth, or in laboratory analogs. First, it was readily apparent that the morphology of the escarpment was distinct from that typical of either 'wrinkle ridges' or horst and graben-bounding faults developed in Martian plain materials (fig. 2). Secondly, as illustrated in figure 3 (and documented in ref. 1,2) the Gordii Dorsum Escarpment is bordered by a narrow zone of oblique trending lineaments. The lineaments' orientation, distribution, and relation to the staggered or en echelon fault scarps that compose the main

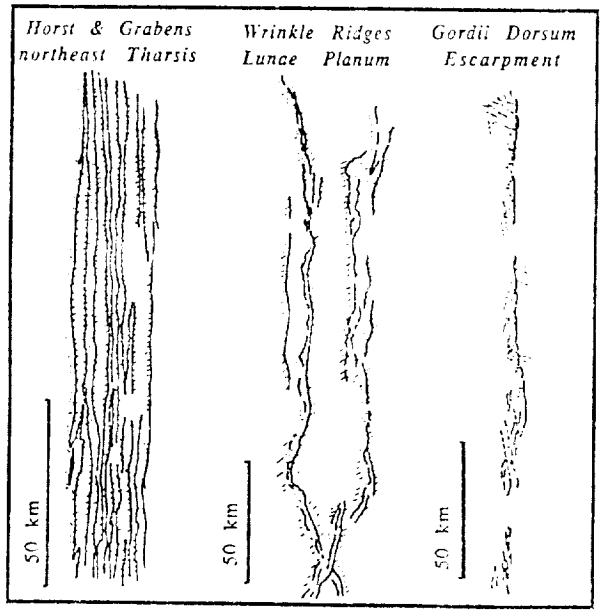

Fig. 2. Comparative tectonic surface morphologies (1,6,7).

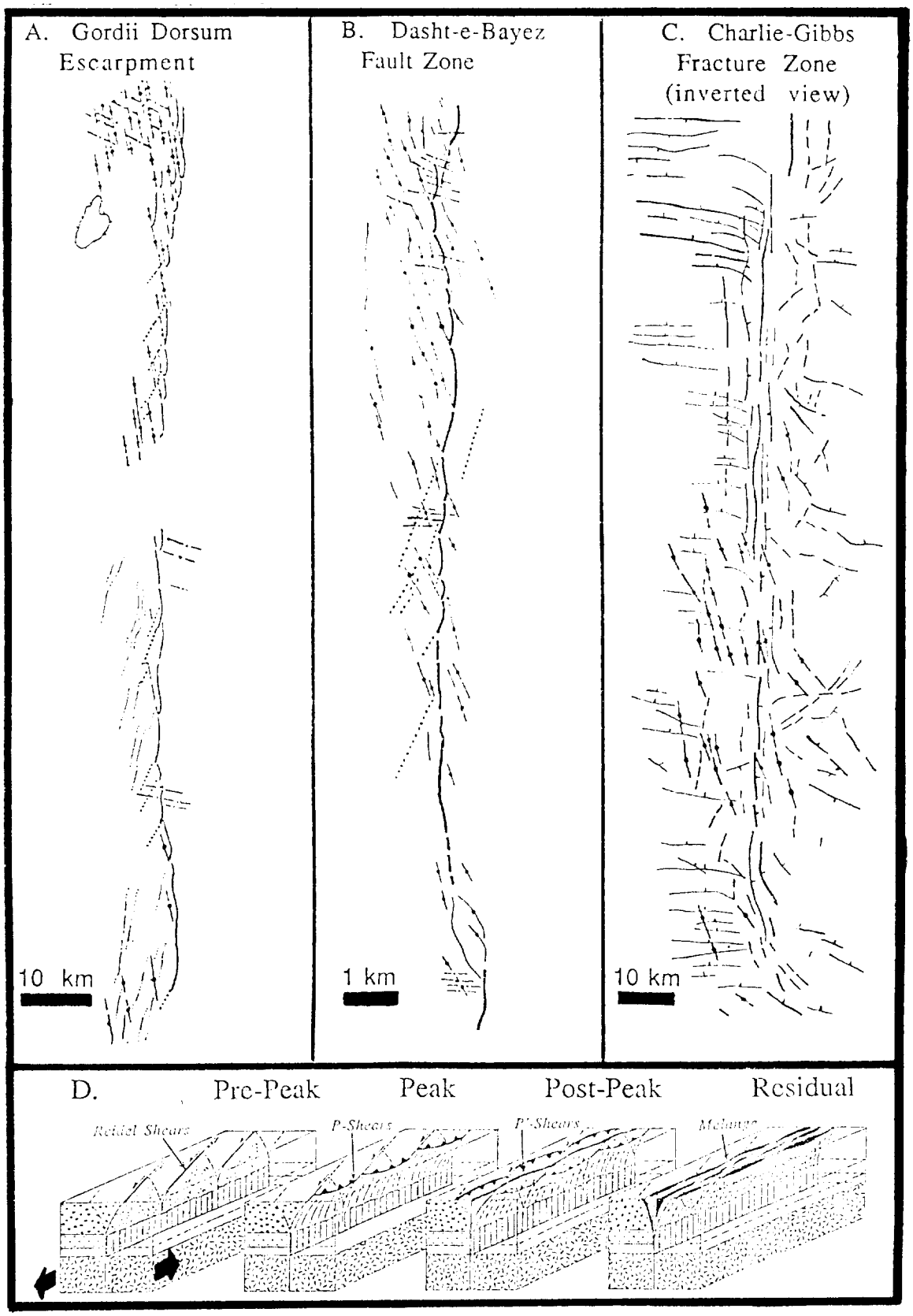

Figure 3. A. Fault and lineament tracings for the Gordii Dorsum Escarpment (1,2), B. Fault and surface fracture tracings for the active Dasht-e-Bayaz left-lateral fault of northern Iran. (8) C. Fault and scarp traces for the active transform portion of the Charlie Gibbs Fracture Zone, inverted view to provide sinistral perspective (9) D. Block diagrams illustrating the stages of evolution for a strike-slip fault (10,11).

escarpment are believed directly comparable to the array of oblique trending features seen along some of the strike-slip faults on Earth or in laboratory models. In these situations a discrete strike-slip fault at depth is believed to propagate upwards through unconsolidated or semi-consolidated strata that cover the basement (Wilcox et al., 1973; Tchalenko, 1970) in a progression of stages during which oblique trending features are formed and the resistance to shearing in the cover first rises and then falls (Fig. 3d). On the Earth the marginal fringe of oblique-trending secondary faults is found to be a trait common for transcurrent faults in both continental and oceanic crust (fig. 3a-c). Experiments in the laboratory have demonstrated the unique way in which the early-formed oblique-trending 'Reidel shears' influence the eventual geometry of a mature strike-slip fault zone (fig. 3d).

On the basis of the comparative structural analysis we argue for the presence of a deep lithospheric fault zone of left-lateral character under the general trace of the escarpment that has propagated upwards into less competent cover and evolved through stages similar to that of Earth or laboratory analogs. The cover is probably a semi-consolidated composite of impact ejecta, volcanic units, and eolian and mass wasting deposits. The nature of the basement is unknown. The pattern of repeating NNW trending ridges see in fig. 1 is somewhat comparable to that of oceanic transforms on Earth. However, in what high resolution sensing (side-scan sonar) has been done of Earths' oceanic transforms, there has appeared the dominance of a cross-striking series of normal fault scarps (fig. 3c). Continental transcurrent faults, while having limited zones of extensional tectonism ('pull-aparts') are not commonly found to have a pervasive or systematic array of such extensional features. To the contrary, in the latter the 'Reidel shears' tend to dominate. Thus, at first glance, there is little other than the spatial pattern of the NNW ridges in the western equatorial region of Mars to suggest an oceanic transform analog. The finer details of the Gordii Dorsum are found most analogous to that of the continental Dast-e-Bayaz left-lateral fault in Iran (fig. 3a&b).

Despite the number and internal consistency of arguements for the Gordii Dorsum Escarpment representing a left-lateral fault zone, the hypothesis raises a number of perplexing issues concerning the age and interrelation of faulting to other processes that have shaped the Martian landscape in the transitional regions. The apparent ages (from crater densities) of surfaces adjacent the escarpment are not in agreement with the structural analysis. While undeformed flat lying strata at the base of the escarpment are sparsely cratered (51 craters/9,000 km^2); consistent with their origin as part of the northern Amazonian plains materials, the uplifted and deformed side of the escarpment does not have a single visible crater in an area of 16,000 km^2. Further complicating the relations are ablated, but previously intensely cratered, surfaces that appear to onlap and bury the escarpment's southern extension towards the southern Highlands. Acceptance of the hypothesis that the Gordii Dorsum escarpment is ancient fault zone that remains buried in its southern extension along the boundary between the 'transitional zone' and the ancient cratered surfaces of the southern Highlands necessitates rethinking of the ages of surface materials and surface processes of the equatorial transitional regions.

REFERENCES (1) Forsythe, R. D., Zimbelman, J.R., 1988, LPSC XIX, 344-345, (2) Forsythe, R. D., Zimbelman, J.R., 1988, Nature, 336, 143-146, (3) Scott, D. H., Tanaka, K. L., J. Geophy. Res., 1982, 87, 1179-1190, (4) Scott, D. H., Carr, M. H., 1978, U.S. Geol. Surv. Map I-1083, (5) Schaber, G. E., and others, 1982, U.S. Geol. Surv. Map I-893, (6) Plescia, J. B., Golombek, M. P., 1986, G. S. A. Bull., 97, 1289-1299, (7) Carr, D. H., 1981, The Surface of Mars, Yale Univ. Press, 232, (8) Tchalenko, J. S., Abraseys, N. N., 1970, G. S. A. Bull., 81, 41-61, (9) Searle, R. C., 1979, J. Geol. Soc. Lon., 136, 283-292, (10) Wilcox, R. E., Harding, T. P., Seely, D. R., 1973, Bull. A. A. P. G., 57, 74-96, (11) Tchalenko, J. S., 1970, G. S. A. Bull., 81, 1625-1640.

A REVIEW OF EXTENSIONAL TECTONIC FEATURES ON MARS; Matthew Golombek, Jet Propulsion Laboratory, California Institute of Technology, M. S. 183-501, 4800 Oak Grove Dr., Pasadena, CA 91109.

The most common type of extensional tectonic feature on Mars is the simple graben. These grabens define the enormous radial fracture system around Tharsis (Wise et al., 1979). This observation and their interpretation resulted from analogous structures having already been identified on the moon (e.g., Quaide, 1965; McGill, 1971; Baldwin, 1971) and studied on the earth (Smith, 1966; McGill and Stromquist, 1979). Similar structures also exist on three of the four Galilean satellites (Schaber, 1980; McKinnon and Melosh, 1980; Golombek, 1982) and on some of the Saturnian and Uranian satellites (Smith et al., 1981; 1982; 1986). Nevertheless, in addition to the simple grabens, a variety of other extensional tectonic features have been identified on Mars: complex grabens (Plescia and Saunders, 1982); tension cracks (Schumm, 1974; Tanaka and Golombek, 1989), downdropped blocks within Valles Marineris (e.g., Frey, 1979; Lucchitta et al, 1989), and giant polygon structures that have been interpreted to be small grabens (Pechmann, 1980), but don't resemble any structures known to be tectonic in origin (McGill, 1986). In this review, I will briefly discuss all but the latter extensional tectonic features on Mars and their probable origin, as well as what can be inferred from them about shallow crustal and lithospheric structure.

Simple grabens are found in a variety of forms and settings within the Tharsis and Elysium regions of Mars. At their simplest, they are long (many hundreds of kilometers) narrow (a few kilometers wide) troughs with large spacings (tens of kilometers) between them (e.g., Memnonia, Sirenum, and Icaria Fossae). In other places the individual grabens are also generally narrow, although shorter in length (tens of kilometers), and spaced immediately adjacent to each other. These terrains (e.g., Claritas and Ceraunius Fossae) have a highly disrupted appearance with ridge-groove topography and less well defined individual grabens. In other places such as Alba Patera, grabens appear in swarms. Individual structures are wider (up to ten kilometers) with well defined flat floors. The grabens typically intersect each other at small angles, with younger grabens utilizing older graben faults for short distances. In many places (e.g., Noctis Labyrinthus and Valles Marineris) graben structures are highly eroded by mass wasting or other processes, so that individual fault bounded structures are either highly modified or difficult to define.

Simple grabens are a special class of grabens that are very common on the surfaces of the planets and satellites, yet rare on the earth. They are named for their simple surface morphology, which in turn requires a simple geometry and subsurface structure (McGill and Stromquist, 1979; Golombek, 1979; Golombek and McGill, 1983). The grabens are bounded by two inward dipping normal faults, whose surface scarps have equal heights and whose shoulders are at the same elevation. The floor of the graben is flat (not tilted) and unbroken by subsidiary or antithetic faults. The equal scarp heights of the bounding faults and the flat graben floor indicate that both faults have experienced equal displacements (on the order of tens to hundreds of meters). This suggests that both faults are of equal importance,

and extend to their mutual point of intersection at depth and terminate, indicating that both faults initiate at a common point at depth and propagate to the surface. Analysis of a variety of simple grabens indicates that the depth at which the faults initiate is typically controlled by a subsurface mechanical discontinuity where extensional stresses are concentrated; this provides a convenient and straightforward explanation for the consistent graben widths and equal spacings between members of a set.

A number of arguments and data indicate that faults bounding simple grabens typically dip at about 60°. Fault dips of about 60° are supported by observations of fault dip on the moon, mechanical scale model studies, fault angle information from experimental work (Golombek, 1979 and discussion and references therein), and likely failure criteria based on the frictional resistance to sliding on preexisting faults applicable to the shallow crust of Mars (Tanaka and Golombek, 1989 and discussion and references therein). Contrary to previous interpretations suggesting near vertical dips for faults bounding grabens on Mars (Carr, 1981), unambiguous surface expressions of faults in the walls of troughs and valleys provide direct measurements of fault dips of about 60° (Davis and Golombek, 1989). For this fault dip, faults bounding grabens intersect at depths of 0.5 to 5 km beneath the surface (Runyon and Golombek, 1983; Tanaka and Davis, 1988; Davis and Golombek, 1989), with a distinct peak in frequency of intersections at about 1 km depth. This indicates failure of only the uppermost crust (not failure of the entire lithosphere), which effectively limits the maximum stress differences required for shear failure associated with simple grabens to on the order of tens of MPa. The only type of fracture possible beneath the intersection of faults bounding grabens that does not violate their simple geometry is a tension crack, for which there is support for a small subset of Martian grabens (Tanaka and Golombek, 1989).

In many intensely faulted regions surrounding Tharsis, larger more complex grabens can be found. These complex grabens range in width from about 5 km to 100 km and typically have multiple border faults and deeper, multiply faulted floors. The largest of this type of structure is 100 km wide, a few kilometers deep, and more than a thousand kilometers long (in Claritas Fossae) and resembles large rifts on the earth (Plescia and Saunders, 1982). The border faults are reactivated older faults with greater slip and the floor is intensely fractured, with many tilted blocks. Many other complex grabens share many of these characteristics except that they are narrower and shallower than this, yet wider and deeper than simple grabens; obvious volcanism is absent. The inherited border faults probably propagate deeper into the crust as they become involved in deformation associated with larger more complex structures. As a result, these large complex grabens probably mark the site of failure deeper into the lithosphere than simple grabens (depth of failure is most likely proportional to the width of the structure). It seems likely that the largest of these structures involves failure of the entire lithosphere, as is the case for rifts on the earth.

Enlarged tension cracks and joints have also been identified in near surface rocks and deep within the crust of Mars (Schumm, 1974; Tanaka and Golombek, 1989). Tension cracks are morphologically distinct from simple grabens in that they are typically narrow deep structures without identifiable flat floors. Examples

include grooves within near surface rock units, ice-wedge polygons, some channels, volcanic fissures and subsurface tension cracks. Near Valles Marineris, the association of collapse pits and pit chains with simple grabens, implies deep tension cracks beneath the grabens that may accommodate some subsurface drainage of material. Pit chains within grabens in Tantalus Fossae (east side of Alba Patera) suggest that these grabens are also underlain by tension cracks. Depending on the mechanical properties of the rocks and subsurface conditions such as possible pore-water pressure, these tension cracks could extend to substantial depths (tens of kilometers). Failure criteria suggest yield stresses in the hundreds of MPa at these depths and implies much if not all of the lithosphere has failed.

The identification of structural blocks defined by scarps and apparent downdropped surfaces has suggested for some time that many, if not most of the troughs making up Valles Marineris are block-faulted structures analogous to rifts on the earth (e.g., Frey, 1979; Lucchitta et al., 1989 and references therein). Although there has clearly been severe subsequent mass wasting and collapse, triangular facets along trough edges provide strong evidence for fault control of many of the troughs. There has been little detailed work on what these scarps imply for the subsurface structure of the troughs, but it seems likely that at least some of the troughs are modified fault bounded valleys. If so, their width (tens to hundreds of kilometers wide) and size (individually hundreds of kilometers long, together thousands of kilometers long and many kilometers deep; Frey, 1979) suggest faulting of the entire lithosphere, analogous to rifts on earth.

In summary, the most common extensional tectonic structure on Mars is the simple graben, which provides direct evidence for failure of only the upper few kilometers of the crust. Wider and more complex grabens are present (although fewer in number) that imply deeper failure and involvement of the lithosphere. The largest complex graben on Mars resembles rifts on earth, indicating the likely extensional failure of the entire lithosphere. Tension cracks are also present in surface materials on Mars, and collapse features associated with grabens suggest deep underlying tension cracks (tens of kilometers deep) that could allow the observed subsurface drainage of material. Some troughs within Valles Marineris are probably highly modified fault bounded valleys, whose size and loose analogy with rifts on earth, suggest extensional failure of the entire lithosphere

References:

Baldwin, 1971, JGR 76, 8459. Carr, 1981, The Surface of Mars. Davis and Golombek, 1989, LPS XX, and JGR, in press. Frey, 1979, Icarus 37,142. Golombek, 1979, JGR 84, 4657. Golombek, 1982, PLPSC 13, JGR 87, A77. Golombek and McGill, 1983, JGR 88, 3563. Lucchitta et al., 1989, 4th Int. Conf. Mars abs., 36. McGill, 1971, Icarus 14, 53. McGill, 1986, GRL 13, 705. McGill and Stromquist, 1979, JGR 84, 4547. McKinnon and Melosh, 1980, Icarus 44, 454. Pechmann, 1980, Icarus 42, 185. Plescia and Saunders, 1982, JGR 87, 9775. Quaide, 1965, Icarus 4, 374. Runyon and Golombek, 1983, LPS XIV, 660. Schaber, 1980, Icarus 43, 302. Schumm, 1974, Icarus 22, 371. Smith, 1966, USGS Ann. Prog. Rep., 65. Smith et al., 1981, Science 212, 163, 1982, Science 215, 504, 1986, Science 233, 43. Tanaka and Davis, 1988, JGR 91, 14,893. Tanaka and Golombek, 1989, PLPSC 19th, in press. Wise, Golombek & McGill, 1979, Icarus 38, 456.

INVOLVEMENT OF THE LITHOSPHERE IN THE FORMATION OF WRINKLE RIDGES ON MARS; M. Golombek[1], J. Suppe[2,3], W. Narr[3], J. Plescia[1], and B. Banerdt[1]; [1]Jet Propulsion Laboratory, Caltech, Pasadena, CA 91109, [2]Seismological Laboratory, Caltech, Pasadena, CA 91125, [3]Dept. Geological and Geophysical Sciences, Princeton University, Princeton, NJ 08544.

Recent work on the origin of wrinkle ridges suggests that they are compressional structures, but the subsurface structure and the possible involvement of the lithosphere in their formation are not understood. In this abstract, we briefly review important characteristics of Martian wrinkle ridges, including their subsurface structure and amount of shortening, both of which suggest that they are the surface expression of thrust faults that extend through much of the lithosphere.

Photoclinometric topographic profiles across wrinkle ridges in Lunae Planum and Amazonis Planitia show an average regional elevation offset across the ridges (plains on one side of the ridge are at a distinctly different elevation than plains on the other) of about 100 m. The offset in regional elevation extends for many kilometers on either side of the ridge and requires a fault beneath the structure; simple fold structures or faults that flatten into a decollement cannot readily explain the elevation offset. Vertical faulting at depth does not provide an obvious mechanism for producing the broad low positive relief structure characteristic of wrinkle ridges. A combination of folding and low-angle faulting, however, can produce both the observed ridge morphology and the offset in regional elevation. The lateral extent of the regional elevation change requires a planar fault that does not shallow with depth, because the regional elevation change would decrease to zero above the point where the fault flattens to a decollement (Golombek et al., 1989).

We have calculated the amount of shortening due to folding for Martian wrinkle ridges (5-25 m) by simply unfolding the surface profile along the ridge . The shortening due to faulting was obtained by dividing the regional elevation change, which is produced by slip on the fault, by the tangent of the fault dip. Although the dip of the fault is not known, measurements of the dip of normal faults on Mars (Davis and Golombek, 1989) and lab experiments of prefractured rock suggest a dip of about 25° for thrust faults (Brace and Kohlstedt, 1980; Byerlee, 1978). Shortening due to faulting averages between 100 and 300 m. Total shortening across Martian wrinkle ridges is therefore on the order of hundreds of meters, similar to values for lunar wrinkle ridges (Golombek et al., 1988); strain is on the order of a few percent. The ratio of shortening due to faulting to that due to folding is in the range of 5 to 20, indicating that faulting is the dominant mechanism for accommodating shortening in Martian wrinkle ridges and that folding is subsidiary.

A number of attempts have been made to identify kinematic models capable of explaining the salient characteristics of wrinkle ridges. In particular, fault-bend and fault-propagation folding have been suggested as possible models for the development of wrinkle ridges (Plescia and Golombek, 1986; Watters, 1988). Fault-bend folding (Suppe, 1983) can produce an anticlinal fold when surficial rocks are translated over a surface-flattening bend in a thrust fault. Fault-propagation folding (Reidel, 1984; Suppe, 1985; Suppe and Medwedeff, 1984; Woodward et al., 1985; Jamison, 1987) occurs when displacement along a reverse fault at depth is accommodated by folding of overlying layers. Both types of structures are capable of producing surface folds with complex near surface faulting, similar to wrinkle ridges. More detailed considerations suggest, however, that the gross structure of wrinkle ridges is different from typical fault-bend and fault-propagation folds. In particular, faults responsible for both fault-bend and fault-propagation folds most commonly shallow out into horizontal decollements at bedding-plane contacts between rocks with distinct mechanical properties. In addition, where observed on the earth, the step-up ramps associated with these types of structures are sharp, rather than gradual, so that a gradually changing fault dip (for example a thrust fault gradually shallowing with depth) beneath wrinkle ridges is not supported by observations on earth. If the fault dip shallowed or completely flattened with depth, the offset in regional elevation would also

decrease or disappear and abrupt changes in fault dip would produce correspondingly abrupt changes in surface elevation away from wrinkle ridges. In addition, the slip across wrinkle ridges is small, much less than that likely by formation of these structures by fault-bend or fault-propagation folding. For these types of folds, the long rear limb of the fold is produced by translation of rocks above the thrust ramp. This in turn requires that the slip across the structure be roughly equal to the width of the rear limb. The rear limb of most wrinkle ridges is many kilometers wide, which is an order of magnitude greater than the shortening that can be reasonably accommodated across them. Thus, the lack of evidence for horizontal decollements beneath wrinkle ridges and the excessive strains suggested for fault-bend and fault-propagation folds indicate that a different deep subsurface structure might be more applicable for the overall geometry of planetary wrinkle ridges. Fault-bend and fault-propagation folding could still be responsible for the complex near-surface folding and faulting implied by wrinkle ridges.

In northwestern Lunae Planum wrinkle ridges are spaced about 50 km apart and consistently have an uplifted eastern side. Within the accuracy of the photoclinometric method the regional elevation change appears to persist laterally for many kilometers away from the ridges. There is no evidence for tilted blocks between the ridges (dips of 1° or greater would have been detected), and no evidence for any folding or warping of the surface between the ridges. To first approximation, the faults beneath these ridges must dip to the east, to produce the uplifted eastern side, and continue at least 50 km to the next ridge. If the fault dips at roughly 25°, then the fault is roughly 25 km beneath the surface at this distance. Steeper dips would result in greater depths of penetration; a 45° dipping fault would be at 50 km depth beneath the adjacent ridge. Note that even if the surface between adjacent wrinkle ridges was tilted at less than a degree, the underlying fault must still continue laterally to the next ridge, at which point it would probably be tens of kilometers below the surface (e.g., Erslev, 1986). This indicates that the faults responsible for wrinkle ridges clearly involve a significant thickness of the Martian lithosphere and are not simply surface folds affecting the upper few kilometers of the crust.

There is strong evidence that faults beneath foreland basement uplifts, such as the Rocky Mountains, are underlain by planar faults that root in the weak ductile lower crust near the Moho. Best known of these basement thrusts is the Wind River thrust (Smithson et al., 1979), which dips about 40°, has slipped about 5-7 km, and is clearly imaged on seismic profiles to about 20 km depth. Geometric considerations indicate the fault zone flattens near the Moho at about 35 km depth. Numerous other basement thrusts have been documented in the Rocky Mountain foreland and elsewhere worldwide in the course of petroleum exploration (for example Gries, 1983; Gries and Dyer, 1985). Many of these basement thrusts have small offsets on the order of hundreds of meters and have a change in elevation across the structure, similar to wrinkle ridges. Some of the best documented examples are in the Wind River basin (Gries and Dyer, 1985). The deformation is entirely by fault slip in the basement, but as the fault enters the 1-3 km thick sedimentary cover, fault-bend folding, wedging and fault-propagation folding produce structures that are quantitatively similar to the kilometer-scale aspects of wrinkle ridges.

On Mars, a number of supporting arguments and models also permit the rooting of faults responsible for wrinkle ridges in a weak ductile lower crust or lithosphere. The flexure of volcanic loads on the Martian surface (Comer et al., 1985) and the magma source region required beneath the giant Tharsis volcanoes (Carr, 1973; Blasius and Cutts, 1976) both suggest a lithosphere on the order of 50 km thick at the period in Tharsis history when wrinkle ridges formed. Assuming a 50 km thick lithosphere, with a basaltic crust 30 km (Bills and Ferrari, 1978) to 100 km thick (Sjogren and Wimberly, 1981; Sjogren and Ritke, 1982; Janle and Ropers, 1983) and an olivine mantle (Wood and Ashwal, 1981; Francis and Wood, 1982), requires thermal gradients of 9°/km to 16°/km from ductile creep properties of basalt and olivine. Thermal evolution models of Mars (Toksoz et al., 1978) also predict a present average crustal thermal gradient of 9°/km, which is a likely minimum as thermal gradients were undoubtably greater during Tharsis volcanic and tectonic activity. Given these constraints, we have assumed 9°/km, 15°/km, and 20°/km and various crustal thicknesses for the construction of lithospheric strength envelopes (brittle and ductile yield stress versus depth curves) to gain a better understanding of likely lithospheric strong and weak zones at depth.

Results show that even under the coolest conditions a lower crustal weak zone is present below 40 km, assuming a minimum 50 km thick crust. Under the warmer conditions more likely for Tharsis, lower crustal weak zones begin at about 20 km depth, with all strength in the upper mantle gone at 40-60 km depth. These calculations indicate that under conditions likely during Tharsis deformation, weak zones at fairly shallow depths existed within the crust and mantle in which thrust faults could root, analogous to faults beneath foreland basement uplifts on the earth.

In conclusion, the observation that some regularly spaced wrinkle ridges accommodate regional elevation changes with a consistent uplifted side suggests that planar thrust faults extend to depths of tens of kilometers. Consideration of earth analogs most compatible with this subsurface structure and the low strains measured across wrinkle ridges (a few percent) suggest foreland basement uplifts are more appropriate earth analogs for the overall structure of wrinkle ridges; fault-bend and fault-propagation folding are probably responsible for the near-surface folding and faulting associated with wrinkle ridges. Foreland basement uplifts on earth are typically underlain by moderately dipping thrust faults that root in a weak ductile zone at the base of the crust. Evaluation of likely conditions around Tharsis indicates that faults beneath wrinkle ridges also could have rooted in a ductile zone of the lower crust at depths of a few tens of kilometers. These results suggest that deformation associated with wrinkle ridges involves much of the lithosphere.

REFERENCES

Bills and Ferrari, 1978, J. Geophys. Res.,v. 83, p. 3497. Blasius, K., and J. Cutts, 1976, Proc. Lunar Sci. Conf. 7th, p. 3561. Brace, W. and D. Kohlstedt, 1980, J. Geophys. Res., v. 85, p. 6248. Byerlee, J., 1978, Pageoph., v. 116, p. 615. Carr, M., 1973, J. Geophys. Res., v. 78, p. 4049. Comer, R., S. Solomon, J. Head, 1985, Rev. Geophys., v. 23, p. 61. Davis, P., and M. Golombek, 1989, Lunar Plan. Sci. Abs. XX. Erslev, E., 1986, Geology, v. 14, p. 259. Francis and Wood, 1982, J. Geophys. Res., v. 87, p. 9881. Golombek, M., J. Plescia, and B. Franklin, 1988, Lunar Plan. Sci. XIX, 395. Gries, R., 1983, Amer. Assoc. Petrol. Geol. Bull., v. 67, p. 1. Gries, R., and R. Dyer, 1985, Seismic Exploration of the Rocky Mtn. Region, Rocky Mtn. Assoc. Geol., 299p. Jamison, W., 1987, J. Struct. Geol., v. 9, p. 207. Janle and Ropers, 1983, Phys. Earth Planet. Int., v. 32, p. 132. Plescia, J., and M. Golombek, 1986, Geol. Soc. Amer., v. 97, p. 1289. Reidel, S., 1984, Amer. J. Sci., v. 284, p. 942. Sjogren and Ritke, 1982, Geophys. Rer. Lett., v. 9, p. 739. Sjogren and Wimberly, 1981, Icarus, v. 45, p. 331. Smithson, S., J. Brewer, S. Kaufman, J. Oliver, and C. Hurich, 1979, J. Geophys. Res., v. 94, p. 5955. Suppe, J., 1983, Amer. J. Sci., v. 283, p. 684. Suppe, J., 1985, Principles of Structural Geology, Prentice-Hall, 537p. Suppe, J., and D. Medwedeff, 1984, Geol. Soc. Amer. Abst. Prog., v. 16, p. 670. Toksoz et al., 1978, Moon and Planets, v. 18, p. 281. Watters, T., 1989, J. Geophys. Res., v. 93, p. 10,236. Wood and Ashwal, 1981, Proc. Lunar Planet. Sci. Conf. 12B, p. 1359. Woodward, N., S. Boyer, and J. Suppe, 1985, An Outline of Balanced Cross Sections, Univ. Tenn. Dept. Geol. Sci., Studies Geol. 11, 170p.

FOLDING IN LAYERED MEDIA

Arvid M. Johnson, Earth and Atmospheric Sciences, Purdue University, West Lafayette, Indiana 47907; Virginia J. Pfaff, Geology Department, Portland State University, Portland, Oregon 97207

Theoretical analysis of folding of layered viscous media indicates that forms of folds are controlled by the behavior of layer contacts, the relative stiffnesses of the multilayer and confining media, and the scale of the folding. The asymmetry of folds is determined largely by the behavior of the layer contacts and the sense of layer-parallel shear during folding.

Different fold forms can be produced in identical viscous multilayers by changing the behavior of contacts between layers. Kink or box folds form if the resistance to slip at layer contacts varies with position along the contacts, and the rate of slip is a nonlinear function of the shear stress at layer contacts. Variable resistance to slip produces slip which is localized along segments of layer contacts. Concentric or chevron folds form if the resistance to slip is constant all along layer contacts, and the rate of slip is a linear function of the shear stress at layer contacts. Constant resistance to slip ranges from infinite, in which case contacts are bonded, to zero, in which case contacts slip freely. Constant, finite resistance to slip produces slip which is distributed all along layer contacts. The analysis shows that multilayer folds may have the same form regardless of whether the layer contacts are bonded or freely slipping.

Relative stiffnesses of the multilayer and media also determine fold shapes. Parallel folds, such as concentric and kink folds, form in finite multilayers confined by soft media. Constrained, internal folds, in which amplitudes of anticlines and synclines decrease to zero at upper and lower boundaries, form in multilayers confined by rigid media.

The forms of folds in multilayers confined by media with different viscosities above and below depend on the viscosity contrast of the media. For no medium above and a rigid medium below, the forms are concentric-like in the upper part and internal in the lower part of the multilayer. For no medium above and a soft medium below, the folds are concentric-like throughout the multilayer.

The theory also shows that different forms of folds can be produced in identical viscous multilayers by changing the wavelength of folds relative to the thickness of the multilayer being folded. Parallel folds, including concentric and kink forms, develop if the thickness of the multilayer is on the order of the folding wavelength. Similar folds, including chevron and box forms, develop if the thickness of the multilayer is large compared to the folding wavelength.

Asymmetric folds form in multilayers subjected to combined layer-parallel compression and shear; compression produces folding and shear produces asymmetry. For a given sense of layer-parallel shear stress, the sense of asymmetry of folds can be reversed by changing the behavior of the layer contacts. If

the resistance to slip is constant all along interfaces, folds develop the sense of asymmetry of drag folds. If the resistance to slip varies with position along interfaces, folds can develop the sense of asymmetry of monoclinal kink folds.

For a given variable resistance to slip at layer contacts, the sense of asymmetry depends on the sense and magnitude of the layer-parallel shear and on the thickness-to-wavelength ratio of the multilayer.

ORIGIN OF PLANETARY WRINKLE RIDGES - AN OVERVIEW. Ted A. Maxwell, Center for Earth and Planetary Studies, National Air and Space Museum, Smithsonian Institution, Washington, D.C. 20560

> 1958: "These low ridges are obviously flow markings, undoubtedly formed when the floors of the maria were in a hot viscous condition." (1).
>
> 1965: "It is thus probable that some wrinkle ridges, like some rilles, follow faults rather than just fractures. Possibly, the reason why definite throws or offsets are difficult to detect in wrinkle ridges is that displacements would be largely masked by the extrusions that built up the ridges." (2).
>
> 1966: "Turning now to the subject of mare ridges,... they have been caused by intrusions, presumably of lava, from below. The intrusive material is presumed to have risen through fissures, but failing to reach the surface, it spread out horizontally, instead, at some specific depth or depths, thereby raising the surface into the forms that we observe." (3).
>
> 1976: "... it is clear that concentric systems of mare ridges form close to scarp-like rings on the basin floors." (4).
>
> 1987: "... most ridges originate basically by compression resulting from vertical tectonism, although some are probably of volcanic origin." (5).

Although interpreted by Gilbert as anticlinal and monoclinal forms in 1893 (6), it was not until the mid-1960's that the details of wrinkle ridge structures began to be seriously considered as a key to understanding the structural and volcanic history of the Moon. Recognizing them as part of the "lunar grid", Strom (7) divided the structures into mare ridges, 0.5 to 5 km wide, sharply crenulated topographic highs; and arches, subdued elevated linear highs up to 40 km wide, only visible under low sun illumination. Through the acquisition of metric and panoramic photography from Apollo missions 15 through 17, debates on the origin of lunar ridges and arches ranged over whether they formed by purely volcanic means by intrusion or extrusion (3,8,9,10), or by tectonism (11,12,13). In addition to photography, Apollo results provided several lines of evidence that favored a tectonic origin for at least some classes of ridges systems: X-ray and Gamma-ray experiments had the spatial resolution to define unique chemical signatures associated with ridges, and thus to determine whether an extrusive origin was favored. No anomalies associated with ridge systems were found. Detailed topography from photogrammetric results and from the Lunar Sounder provided evidence that some concentric ridge systems within basins were at the sites of topographic offsets. Gravity models for mascon basins indicated that concentric basin ridges marked the location of the best-fit surface disc models for the mascons, suggesting subsurface involvement (14). Subsurface reflectors detected by the Lunar Sounder indicated an anticlinal rise in the horizons beneath the location of ridges in Mare Serenitatis.

With a tectonic origin strongly indicated, the potential for constraining geophysical models of lunar tectonism was recognized, and subsequent studies used the radial placement of ridges to determine the structural history of Mare Serenitatis (15, 16). Two models were used: a thin shell model to approximate stress imposed by subsidence of a cylindrical load on a spherical elastic shell, and a finite element model to determine the magnitude of elastic deformation. Using the position of ridges to constrain the location of compressive stress, the maximum compressive stress levels were found to be on the order of 200-400 bars, much less than the compressive strength of basalt (16). Thus, either global contraction was needed, or another method for concentrating stress at the radial location of the concentric ridge systems, such as subsurface basin ring structure causing zones of thin fill, or thin layers of competent material separated by weaker interbeds (17). While the finite element model successfully predicted the location of the ridge systems, it too failed to provide reasonable stress levels (15).

With the investigations of Mariner 10 and Viking data, these results became especially important for 3 reasons: 1) Ridges were found to be present not just on the Moon, but on Mercury and Mars, and the high resolution lunar photography had the potential for defining morphologic indicators of their origin, 2) The presence or absence of ridges could be used as supplemental evidence for a basaltic composition of plains units, and 3) Their recognition as primary tectonic landforms that could be used to constrain tectonic and thermal history models provided the need for detailed mapping of other planetary ridge systems. On Mercury, the relatively low resolution images from Mariner 10 revealed ridges in smooth plains materials, particularly in the Caloris basin. Recognized as a part of the Mercurian scarp system (18), investigators found that the predominant northerly orientation of ridges in the intercrater plains was similar to that of scarps, consistent with stresses that would result from tidal despinning coupled with global contraction (19). Ridges in the Caloris basin were found to be concentrated in the same radial location as those of lunar basins (20), lending support to a similar mechanism of formation. The extensive fracture system of the inner part of Caloris remained a problem, though it could be explained by loading of the basin as a ring annulus (21).

Investigations of the radial fault system surrounding the Tharsis region of Mars, coupled with gravity studies of the load initially suggested uplift as a source of stress to produce extensional faulting (22), which was later found to be not applicable based on stress trajectories (23). Ridges display a concentric arrangement surrounding Tharsis, and stress trajectories in models involving isostatic support and flexural loading best fit the observed distribution (24). Unlike ridge systems of lunar basins, however, those surrounding Tharsis show no apparent relationship to basement structure (25), and formed before at least the last episodes of extensional faulting (26).

The use of ridges to constrain geophysical models is highly dependent on which particular model of formation is employed. If

folding of the upper few kilometers of material is the primary cause, then surface deviatoric compressional stress trajectories should be normal to the orientation of the ridge systems. If faulting is considered to precede folding or is invoked solely, then such comparisons may not be valid, as shear failure would result. Thus, recent investigations into the exact mechanism of ridge formation (27, 28) are a prerequisite to the use of these features as constraints on models for basin evolution and thermal evolution of planets.

Despite the number of papers listed here (and omitted), several problems remain unresolved: 1) Not all ridges are of tectonic origin; detailed mapping and criteria need to be derived to tell them apart (to the extent possible) on a case by case basis. 2) The influence of subsurface structure (basin rings and fracture systems) is unconstrained. 3) Tectonic implications of ridges with no obvious regional or local controlling factors remain uncertain. Those on the Moon and Mercury can be explained by contraction and despinning, but the origin of many Martian ridges remains problematic.

(1) Whipple, F.L. (1958) Earth, Moon and Planets, New York, Grosset and Dunlap, p. 135. (2) Fielder, G. (1965) Lunar Geology. London, Lutterworth Press, p. 112. (3) Whitaker, E.A. (1966) The Surface of the Moon, in The Nature of the Lunar Surface, W. N. Hess, D. H. Menzel and J. A. O'Keefe, eds., Baltimore, Johns Hopkins Press, p. 89. (4) Brennan, W.J. (1976) Proc. Lunar Planet. Sci. Conf. 7th, p. 2833-2843 (p. 2840). (5) Wilhelms, D.E. (1987) U.S. Geol. Survey Prof. Paper 1348, p. 111. (6) Gilbert, G.K. (1893) Philosoph. Soc. Wash. Bull., v. 12, p. 241-292. (7) Strom, R.G. (1964) Ariz. Univ. Lunar and Planet. Lab. Commun., v. 2, no. 39, p. 205-221. (8) Strom, R.G. (1972) Modern Geology, v. 2, p. 133-157. (9) Young, R.A. et al. (1973) Apollo 17 Prelim. Sci. Rept., NASA SP-330, p. 31-1 - 31-11. (10) Hodges, C.A. (1973) Apollo 17 Prelim. Sci. Rept., NASA SP-330, 31-12 - 31-21. (11) Howard, K.A. and W.R. Muehlberger (1973) Apollo 17 Prelim. Sci. Rept., NASA SP-330, p. 31-22 - 31-25. (12) Schaber, G.G. (1973) Proc. Lunar Sci. Conf. 4th, p. 73-92. (13) Muelhberger, W.R. (1974) Proc. Lunar Sci. Conf. 5th, p. 101-110. (14) Maxwell, T.A. et al. (1975) Geol. Soc. Amer. Bull., v. 86, p. 1273-1286. (15) Maxwell, T. A. (1978) Proc. Lunar Planet. Sci. Conf., 9th, p. 3541-3559. (16) Solomon, S.C. and J.W. Head (1979) Jour. Geophys. Res., v. 84, p. 1667-1682. (17) Solomon, S.C. and J.W. Head (1980) Rev. Geophys. Space Phys., v. 18, p. 107-141. (18) Dzurisin, D. (1980) Jour. Geophys. Res., v. 83, p. 4883-4906. (19) Melosh, H.J. and D. Dzurisin (1978) Icarus, v. 35, p. 227-236. (20) Maxwell, T.A. and A.W. Gifford (1980) Proc. Lunar Planet. Sci. Conf., 11th, p. 2447-2462. (21) McKinnon, W.B. (1979) EOS, v. 60, p. 871. (22) Wise, D.U., M.P. Golombek and G.E. McGill (1979) Icarus, v. 38, p. 458-472. (23) Solomon, S.C. and J.W. Head (1982) Jour. Geophys. Res., v. 87, p. 9755-9774. (24) Watters, T.R. and T.A. Maxwell (1986) Jour. Geophys. Res., v. 91, p. 8113-8125. (25) Maxwell, T.A. (1982) Proc. Lunar Planet. Sci. Conf., 13th Part 1, p. A97-A108. (26) Watters, T.R. and T.A. Maxwell (1983) Icarus, v. 56, p. 278-298. (27) Plescia, J.B. and M.P. Golombek (1986) Geol. Soc. Amer. Bull., v. 97, p. 1289-1299. (28) Watters, T.R. (1988) Jour. Geophys. Res., v. 93, p. 10,236-10,254.

TERRESTRIAL ANALOGUES FOR PLANETARY EXTENSIONAL STRUCTURES

George E. McGill, Department of Geology and Geography, University of Massachusetts, Amherst, MA 01003.

Extensional structures have received much attention in recent years, and are among the "hottest" topics in structural geology. This is primarily a result of field studies indicating their importance in tectonic settings hitherto believed to be entirely characterized by compression. For several reasons, a thorough review of structures resulting from extensional stresses is not practical here; in fact, many of these structures have limited relevance as analogues for planetary features. What will be attempted is a rough classification of extensional structures, primarily based on scale, and an evaluation of their usefulness as analogues. Specific citations are intentionally sparse because of space constraints.

On the earth, extensional structures range in scale from features seen in thin section to features of global significance. Although beloved of many structural geologists, joints, boudinage, stretching lineations, dismembered bedding, and other indicators of extension seen in outcrop, hand specimen, and thin section are of little relevance to planetary studies because they range from one to four orders of magnitude below the resolution of the best orbital images. It is convenient to separate structures that are large enough to be resolved on orbital images into two categories: 1) those that are of crustal to global scale, and 2) those that are generally of less than crustal scale. The first group is intended to include structures associated with globally significant tectonic regimes, the second group incorporates a variety of more local structures generally not directly related to global tectonics. Structures from both categories are potentially useful as planetary analogues because they can provide clues to the kinematics and mechanics of their formation, and thus constrain hypotheses for the origin of similar structures on other planets. However, a major problem yet to be resolved is whether it is sound practice to transfer the specific crustal and tectonic environments associated with analogue structures from the earth to other planets. My bias is that this is, in general, a dangerous thing to do.

Structures of crustal to global scale: The importance of extensional structures within the earth's tectonic system has been greatly enhanced by some very exciting discoveries that have occurred in just the past few years. It is now apparent that extension is an important element in the structural evolution of all types of plate boundaries, not just divergent ones (1). The following paragraphs comment briefly on important terrestrial extensional structures, and on their probable value as analogues.

1. Mid-ocean ridges and rifts: The global system of oceanic divergent boundaries is the most prominent tectonic feature on the earth. In addition to the gross topography, there are several associated characteristics that derive from the specific processes occurring at mid-ocean ridges: positive Bouguer gravity anomalies, magnetic "stripes", elevation decrease with distance from the ridge that is correlated with age, high heat flow, ridge offsets across transforms, shallow seismic activity, and "anomalous" mantle. Furthermore, the great length of the mid-ocean ridge system clearly depends on the earth's dynamic plate tectonics; consequently, it seems risky to use mid-ocean ridges as analogues for short, discontinuous ridges with axial troughs on other planets. Even the presence of one of the associated characteristics does not help very much. For example, cross-structural offsets that, on another planet, might be interpreted as mid-ocean ridge transforms, also occur on the earth as synkinematic features in foreland thrust belts and belts of metamorphic core

collapse structures could serve as potential analogues for studies of elevated terrain on other bodies.

4. Transform boundaries: Oblique movement vectors commonly produce transtensional basins on the earth, but their value as analogues is problematical because of the almost total absence of strike-slip faults on other bodies.

Structures of "local" scale: These include grabens and normal faults due to: 1) bending, 2) lateral slip or flow along a discontinuity, and 3) adjustments of surficial materials to topography or movements in underlying rocks.

1. From considerations of simple plate bending, shallow normal faults and grabens can form in the hinge regions of structural arches and domes, and along the anticlinal hinges peripheral to basins. Numerous examples are discussed in the literature. Because most of these structures are of less than crustal scale, and because most involve the bending of layered rocks, the total extensional strain developed is not very large.

2. If local conditions permit, surface materials can slide or flow laterally along a subsurface discontinuity, with the extension accommodated by the formation of normal faults and grabens. Even though the specific geologic conditions are unlikely to be duplicated on another body, these stuctures are useful analogues because they demonstrate that the spacing and width of geometrically simple grabens provide direct evidence for the thickness of the faulted layer (9).

3. Sediments deposited over a high-relief surface will develop drape structures when they compact. Drape anticlines ("supratenuous" anticlines) formed this way have been known for a long time. Normal faults are mechanically possible in the hinge regions of these drape anticlines, but I am not aware of any published studies describing them. In structurally active areas, poorly consolidated surface materials must adjust to bending and faulting in consolidated rocks buried beneath them. One common result is the development of collapse grabens in the surface materials such as the shallow grabens formed in gravels overlying bedrock gjáu that were opened in the winter of 1975-76 by rifting in northern Iceland.

Many of these "local" structures are geometrically and mechanically useful as analogues, and they have been used to infer the mechanisms of formation of faults and grabens on Mercury, Mars, Ganymede, and the Moon. The primary problem is one of scale -- most of the planetary features are larger than the earth analogues. There are good reasons why this might be so, but this scale difference requires that we use structural analogues with care. However, it is entirely possible that crustal-scale equivalents of smaller structures on the earth appear so important on other planets and moons simply because there are no dynamic tectonic and degradational systems to mask them.

References Cited

1) Hamilton, W.B., *Geol. Soc. America Bull., 100*, 1503-1527, 1988.
2) Mohr. P., in Pálmason, G., ed., *Continental and Oceanic Rifts*, American Geophys. Union, 293-309, 1982.
3) Bott, M.H.P., in Illies, J.H. ed., *Mechanism of graben formation*, Elsevier, 1-8, 1981.
4) Illies, J.H., in Illies (Ibid), 249-266, 1981.
5) Morgan, P., & G.H. Baker, *Tectonophysics, 94*, 1-10, 1983.
6) Bohannon, R.G. et al., *J. Geophys. Res., 94*, 1683-1701, 1989.
7) Rehrig, W.A., *Geol. Soc. America Sp. Pap. 208*, 97-122, 1986.
8) Dewey, J.F., *Tectonics, 7*, 1123-1139, 1988.
9) McGill, G.E., & A.W. Stromquist, *J. Geophys. Res., 84*, 4547-4563, 1979.

complexes, and are common as later modifications of most of the earth's Archean tectonic belts.

2. Continental rifts: These are very promising analogues, because some on the earth appear to "fail", and thus are not required to be part of a dynamic global plate-tectonic system. The extension normal to the long axes of continental rifts is too great to be explained by bending and membrane strains generated by the associated uplift, but is generally less than a few 10's of km. (2). Gravity anomalies, high heat flow, and seismic data suggest that continental rifts overlie regions where the mantle lithosphere has been thinned, and some calculations suggest that this thinning is a necessary precursor to crustal-scale brittle failure (3). Brittle graben faults in the shallow crust thus pass downward into a more ductile regime. By making reasonable assumptions concerning fault attitude, the widths of continental rifts provide an upper bound on the effective elastic thickness of the crust or lithosphere (4), the best estimates coming from places where extension is least. Continental rifts have been used as analogues for inferring near-surface rheology and the existence of lateral tectonic movements on Venus.

There is a major controversy concerning the ultimate causes of continental rifts: either they are "passive", with extension and rifting caused by far-field stresses and with uplift following later as a result of lithospheric thinning; or they are "active", with uplift, lithospheric thinning, and rifting directly caused by a mantle thermal anomaly (5). Both types seem mechanically feasible, and the evidence needed to choose between them must come from geological and geophysical studies, as along the Red Sea rift where fission-track ages in rocks adjacent to the Red Sea demonstrate that uplift followed both rifting and the initiation of volcanism by 10-15 my. (6), requiring a passive formation mechanism. The distinction is of some importance, because the active mechanism implies vertical tectonics (at least locally), whereas the passive mechanism is more consistent with horizontal tectonics. At present, we cannot easily obtain diagnostic geological or geophysical data on other planets needed to distinguish between these, but such data are not totally out of reach when field work with landers begins.

3. Convergent plate boundaries: Extensional structures occur in a variety of tectonic environments associated with convergent boundaries. Normal-fault earthquakes occur oceanward of trenches as a result of tensional bending stresses in the upper part of the elastic lithosphere. Extension occurs behind many island arcs, commonly producing "back-arc basins", because the motion vector for the subducting slab is steeper than the slab itself (1), requiring that the hinge migrate away from the arc (this is sometimes inappropriately called "trench suction"). The value of either of these types of extensional structures for analogue studies is unclear. The Basin and Range and metamorphic core complex structures in the North American Cordillera may be continental equivalents of back-arc structures in the oceans, or they may be related in a more complex way to changes in relative plate motions (7). Recognition of either type of structure on another body would be strong evidence for horizontal tectonic movement. Despite the "blobby" distribution of exposed metamorphic core complexes, their origin requires large (>100%) horizontal extension, with proportionately less vertical movement. Consequently, we must avoid assuming automatically that planetary tectonic topography characterized by dome-like features is necessarily due to vertical movements.

Excessively elevated topography produced by collision commonly fails by extension simply due to gravity (8); in fact, there is a major young, low-angle normal fault cutting Mount Everest! Because gravitational failure of high topography does not depend on the mechanism for creating the topography, these

DO PIT-CRATER CHAINS GROW UP TO BE VALLES MARINERIS CANYONS?

Richard A. Schultz, Geodynamics Branch, NASA Goddard Space Flight Center, Greenbelt, MD 20771.

No.

The Valles Marineris (VM) canyon system on Mars is a spectacular planetary rift [1-3]. It has been proposed that the canyons nucleated and grew as collapse structures from a set of initially tiny pit-crater chains [4], but this scenario is not supported by structural relationships seen in Viking images.

A distinction should be made between canyons controlled by normal faulting and pit-crater chains that look superficially like canyons controlled by normal faulting. Structural mapping on enlarged 1:2 million scale photomosaics confirms that the original structural canyons are much narrower (factor of 3) than the present canyon width, and that normal faulting has controlled the lengths and depths of these canyons. Some canyons are controlled by 2 long, mutually parallel, inward dipping normal faults (Ius, western Tithonium Chasmata). Other canyons are defined by one continuous normal fault scarp faced by several discontinuous, echelon scarps (Coprates). Structures forming one or both graben walls can be inferred in Ophir and Melas Chasmata only by extrapolating along isolated spurs and massifs on canyon floors or by examining canyon terminations. These wide canyons are probably composed of several parallel grabens and are terminated in many cases by oblique trending normal faults.

In contrast, pit-crater chains (PCC) are restricted in extent and differ in morphology and structure from the canyons. Whereas grabens are found throughout VM plateaus, large PCC only occur north of Ius and South of Coprates Chasmata, respectively (Fig. 1). PCC distribution is neither random nor uniform but antisymmetric about the canyon system. Where PCC appear to merge into canyons, such as eastern Tithonium Chasma and Candor Chasma, the structure of each is distinct. Candor is defined by several parallel and oblique grabens, whereas eastern Tithonium is an echelon array of closed to partly closed depressions. Indeed, PCC are characterized by their segmented, echelon geometry [5], limited extent, and lack of clear fault control.

Mapping shows a variety of PCC trends along the canyon system. PCC north of Coprates Chasma are independent of (not parallel to) VM grabens and, somewhat surprisingly, are linked in orientation and location to wrinkle ridges (Fig. 1). In contrast, many large PCC nearest the major canyons parallel them, although the PCC south of Coprates are crosscut by oblique, northeast trending grabens. This implies that the stress state associated with the growth of PCC varied spatially along the canyon system, and certain PCC may record a set of early, pre-VM regional stress states. Valles Marineris and associated structures are said canonically to be oriented "radial to Tharsis" and this is taken to indicate some profound geometric, and presumably genetic mechanical, relationship [6]. Although a good correlation exists between principal stresses calculated from Tharsis loading models and the overall trend of VM canyons, the variety of structure locations, trends, and relative ages underscores the limited applicablility of available geophysical models to canyon tectonics. Indeed, classification of structures as "radial or nonradial to Tharsis" probably is no longer a useful or precise exercise.

Structural relationships listed above suggest that pit-crater chains have a different origin than canyons. Echelon geometry indicates that the chains of pit craters behaved mechanically as interacting cracks. This suggests that pit-crater chains may be the surface expression of laterally propagating subsurface dikes or hydrofractures. The pits themselves may be surficial collapse depressions. Systematic locations of PCC in the canyon system and growth early in the rifting

PIT-CRATER CHAINS AND VALLES MARINERIS

Schultz, R.A.

process [7] perhaps suggest a magmatic (dike) origin as the more likely. Thus, the principal Valles Marineris canyons and pit-crater chains both have a structural origin, but canyons appear controlled by normal faulting (not dikes or cracks) and pit-crater chains by subsurface dikes or cracks (not normal faulting).

REFERENCES: [1] Sharp (1973) JGR 78, 4063-4073. [2] Blasius et al. (1977) JGR 82, 4067-4091. [3] Frey (1979) Icarus 37, 142-155. [4] See discussions by Croft (1989), 4th Intern.Mars Conf. (4IMC), 88-89; Spencer et al. (1989) 4IMC, 193-194; and Lucchitta et al. (1989) 4IMC, 36-37. [5] Pollard and Aydin (1988) GSA Bull. 100, 1181-1204. [6] For example, Wise et al. (1979) Icarus 38, 456-472; Plescia and Saunders (1982) JGR 87, 9775-9791; and Banerdt et al. (1982) JGR 87, 9723-9733. [7] Schultz and Frey (1988) EOS 69, 389-390; Schultz (1989) Lunar Planet. Sci. XX, 974-975.

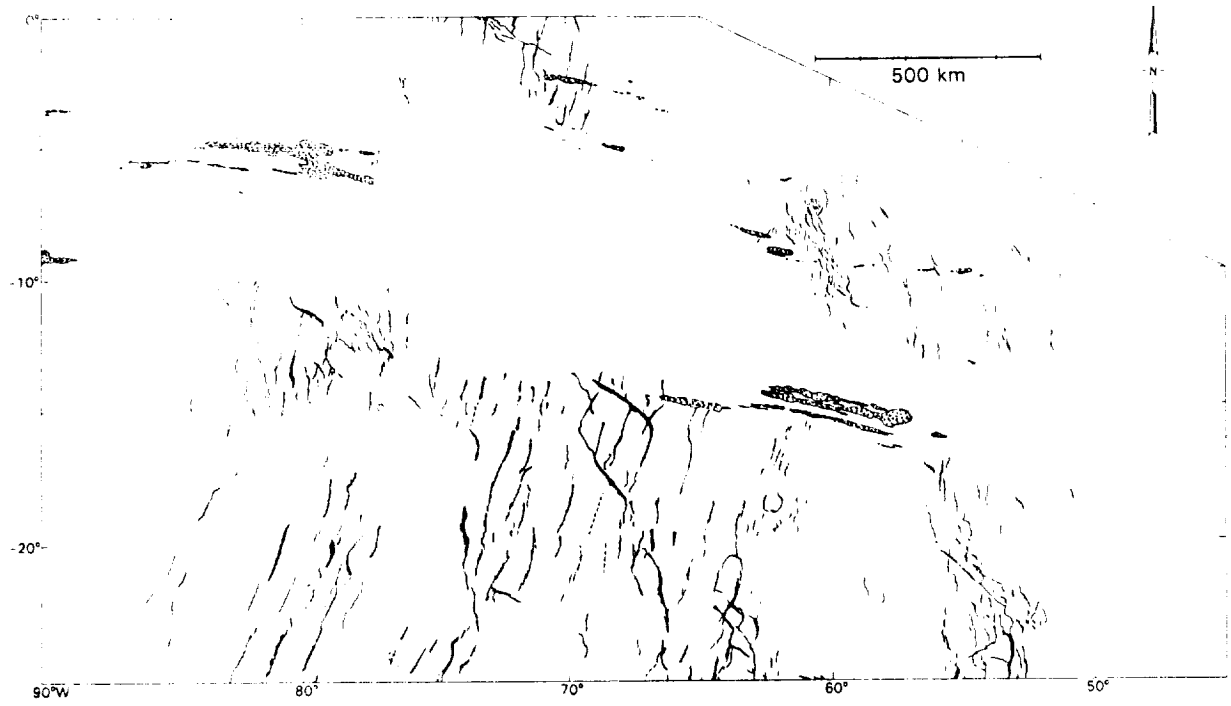

Figure 1. Distribution of wrinkle ridges and pit-crater chains (stippled) in the Valles Marineris region. Canyon outlines omitted for clarity.

STRIKE-SLIP FAULTING IN THE RIDGED PLAINS OF MARS. *Richard A. Schultz, NASA Goddard Space Flight Center, Greenbelt, MD 20771.*

The surface of Mars shows abundant evidence of extensional and contractional deformation in the form of normal faults, grabens, and wrinkle ridges [1]. In contrast, strike-slip faults have been considered to be extremely rare or absent on Mars [2,3]. However, careful study of Viking Orbiter images is revealing that strike-slip faults were produced on Mars [4]. Here I document several well-preserved examples of martian strike-slip faults, examine their relationships to wrinkle ridges, and discuss their tectonic significance.

The strike-slip faults presented here deform moderately cratered plains of presumed volcanic origin southeast of Valles Marineris (Fig. 1)[5]. North-south striking wrinkle ridges also deform plains materials throughout the area. The strike-slip faults are defined by a series of localized plateaus whose overall trend is oblique to the dominent trend of the wrinkle ridges. These polygonal or rhombohedral plateaus are connected by linear structures that are arranged en echelon. The arrays of echelon structures and plateaus are distinct morphologically from typical wrinkle ridges on the Moon and Mars [6]. The plateaus do not appear to result from disruption and lateral offset of pre-existing wrinkle ridge topography because the ridges do not match up across the echelon structures. Further, the location of plateaus within stepovers argues against simple offset because not all echelon arrays are associated with wrinkle ridges or other high topography outside the stepover. Thus, the presence of polygonal plateaus within the stepovers of echelon structures suggests that the plateaus formed as a result of mechanical interaction between those structures. Extensional basins can occur within stepovers along dilatant echelon cracks [7] and extensional stepovers along strike-slip faults [8]; stepovers between dip-slip faults are not generally associated with basins or uplifts. [9]. The rhombohedral shape of many plateaus is consistent with the geometry of rock fracture in a strike-slip stepover. Hence, the linear echelon structures are probably strike-slip faults and the plateaus correspond to uplifts within contractional stepovers.

The echelon structures and plateaus on Mars are similar geometrically to strike-slip faults and push-up ranges on the Earth (Fig. 2). Dimensions of overlap and separation of echelon faults are comparable for martian and terrestrial strike-slip faults, although overlaps along the martian contractional stepovers are somewhat smaller than those along terrestrial extensional stepovers of similar separation. However, smaller overlaps for contractional vs. extensional stepovers may be produced during the growth of strike-slip faults in echelon arrays [10], so the mechanics of strike-slip faulting on Mars does not appear to differ significantly from that on Earth.

Determination of the sense of slip along echelon strike-slip faults is straightforward given the type of stepover and sense of step. For example, contractional stepovers occur for right steps along a left lateral fault or left steps along a right lateral fault. The northwest trending strike-slip faults (Fig. 3) step consistently to the right, implying left lateral slip along the echelon array. The northeast trending faults to the south step consistently to the left, implying right lateral slip along that array. Secondary structures such as end-cracks, joints, and normal faults or stylolites, folds, and reverse faults can grow near strike-slip fault terminations as a result of fault slip [11], and the locations of these structures depend on the sense of slip. For a right lateral fault, large horizontal compressive stresses build up in the north-east and south-west quadrants, promoting nucleation and growth of folds and reverse faults. The right lateral fault arrays are associated with wrinkle ridges in the north-east and south-west quadrants, and left lateral faults join wrinkle ridges in north-west and south-east quadrants. Wrinkle ridges are notably absent in the opposing, extensional quadrants of these faults. These relationships

suggest that these wrinkle ridges may have nucleated in response to slip along the strike-slip faults and propagated away from the fault termination regions. High-angle (but not orthogonal) intersections between wrinkle ridges and the strike-slip faults are consistent with this hypothesis. In some cases, small crenulations that extend away from some fault terminations are superimposed on larger ridges, perhaps implying multiple stages of contractional deformation and local uplift. The location and orientation of wrinkle ridges near terminations of strike-slip faults provide independent evidence that wrinkle ridges represent contractional deformation such as folding or reverse faulting.

The amount of overlap provides a rough estimate of the magnitude of lateral offset along echelon faults with extensional stepovers [12]. Applying this relationship to contractional stepovers, the cumulative lateral offset along each martian strike-slip fault array appears to be several tens of kilometers. This kinematic estimate probably underestimates fault slip because it assumes rigid materials with no internal deformation in the stepover region and neglects shortening within wrinkle ridges located near fault terminations. However, it demonstrates that significant lateral displacement of the martian crust has indeed occurred. Relationships between several strike-slip faults and wrinkle ridges suggest that strike-slip faulting predated growth of at least some wrinkle ridges. In a few cases, however, apparent superposition of fault-termination wrinkle ridges on much larger ridges implies the reverse sequence. No examples were found that would suggest strike-slip faulting that clearly postdated wrinkle ridge formation. Thus, it appears that strike-slip faulting predated and overlapped the episodes of wrinkle ridge growth.

The remote stress state associated with the martian strike-slip faults is inferred from their orientations and sense of slip. Using typical values of fault friction [13] and a Coulomb slip condition, the direction of maximum horizontal compressive principal stress σ_3 would be oriented 30° to the faults, or approximately east-west (Fig. 3). Remote stress states associated with wrinkle ridge formation are usually obtained by assuming that σ_3 is oriented normal to the overall trend of the ridges [14]. The orientations of σ_3 defined by both sets of structures are very similar. This result is consistent with the relative timing of strike-slip faults and wrinkle ridges discussed above and suggests that magnitudes of the other two principal stresses varied spatially or temporally within the region.

The strike-slip faults and associated wrinkle ridges may be related to isostatic adjustments in Tharsis. However, Tharsis principal stress trajectories [14] differ by 10-30° from those derived from structure orientations (Fig. 3). One possibility is that the differences between Tharsis geophysics and structure orientations arise from idealizations or assumptions in the models. On the other hand, the region south-east of Valles Marineris is tectonically complex, and Tharsis-related remote stress states may have been modified by more local stresses. More refined geophysical modeling of Tharsis deformation and analysis of local deformation will help resolve these alternatives. The age of strike-slip and wrinkle ridge deformation is early Hesperian, or about 3-3.5 b.y. ago [15]. Strike-slip faulting south-east of Valles Marineris was either roughly comparable in age or younger than that inferred along the Gordii Dorsum escarpment west of Tharsis [4]. However, principal stress trajectories from Tharsis deformation models [14] do not appear to be suitably oriented to drive left lateral slip along Gordii Dorsum faults. Thus, there were probably at least two episodes of strike-slip faulting in widely separated regions of Mars. Given the complexity of deformation observed in many ancient terrains, it is possible that strike-slip faulting was fairly common on Mars.

REFERENCES: [1] Plescia & Saunders, JGR, 87, 8775 (1982); Solomon & Head, JGR, 87, 9755 (1982); Chicarro et al., Icarus, 63, 153 (1985). [2] Wise et al., Icarus, 38, 456 (1979); Golombek, JGR, 90, 3065 (1985). [3] Mars is considered to be a "one-plate" planet [Solomon, GRL, 5, 461 (1978)] with predominently vertical motions of its lithosphere. [4] Forsythe & Zimbelman, Nature, 336, 143 (1988); R. Schultz, in prep. [5] See Blasius et al. [J. Geophys. Res., 82, 4067 (1977)] for review. [6] Sharpton & Head, PLPSC 18th, (Cambridge Univ. Press), 307 (1988); Watters, JGR, 93, 10,236 (1988). [7] Pollard & Aydin [JGR, 89, 10,017 (1984)] and Sempere & Macdonald [Tectonics, 5, 151 (1986)]. [8] Aydin & Nur, Tectonics, 1, 11 (1982). [9] Aydin & Nur [in Strike-Slip Deformation, Basin Formation, and Sedimentation (ed., Biddle and Christie-Blick, SEPM SP-37), p. 35 (1985)] discuss important kinematic differences between along-strike and down-dip stepovers. [10] Aydin & R. Schultz, in Proc. U.S.G.S Workshop on Fault Segmentation and Controls of Rupture Initiation and Termination, USGS Open-File Report, in press (1989); and J. Struct. Geol., in press, (1989). [11] Rispoli, Tectonophysics, 75, 29 (1981); Segall & Pollard, JGR, 85, 4337 (1980); Aydin & Page, GSA Bull., 95, 1303 (1984). [12] Quennell, in Tectonics of the Dead Sea Rift, Intern. Geol. Congress, 20th, Mexico City (1959), p. 385; Garfunkel, Tectonophysics, 80, 81 (1981). [13] Coefficients of static friction along well-slipped faults are commonly lower (f=0.6) than those of unfaulted rock (f=0.85). See Byerlee [Pure Appl. Geophys., 116, 615 (1978)], Rudnicki [Ann. Rev. Earth Planet. Sci., 8, 489 (1980)], Rice [Pure Appl. Geophys., 121, 443 (1983)], and Li [in Fracture Mechanics of Rock (Academic Press, London), 351 (1987)]. [14] Banerdt et al. [JGR, 87, 9723 (1982)]; Sleep & Phillips [JGR, 90, 4469 (1985)]. [15] Tanaka, PLPSC 17th, part 1, in JGR, 91, E139 (1986).

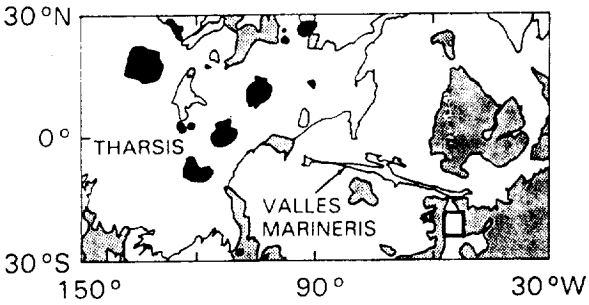

Fig. 1. Location of strike-slip faulting (inset).

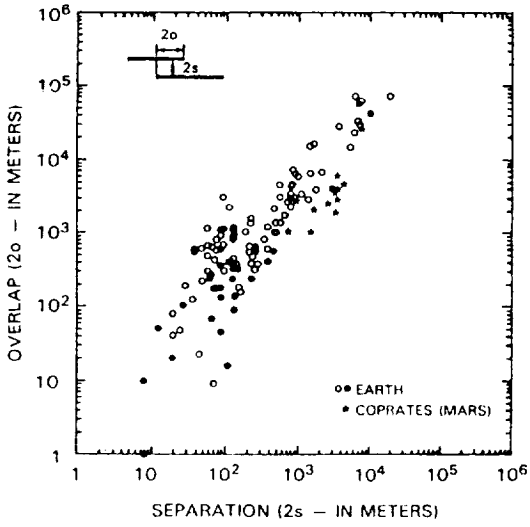

Fig. 2. Geometry of echelon strike-slip faults from Earth and Mars. Filled symbols, contractional stepovers; open, extensional.

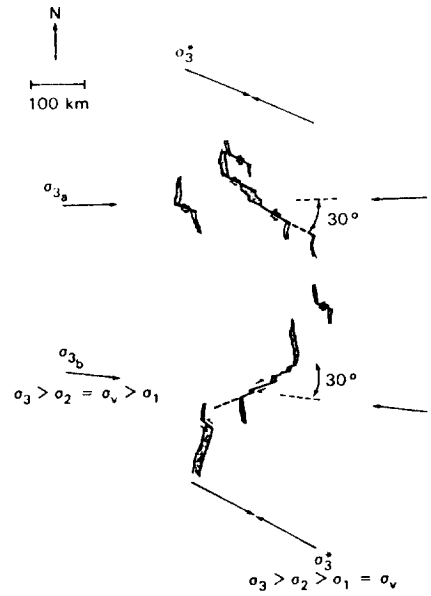

Fig. 3. Relationships between strike-slip faults and wrinkle ridges. Orientations of maximum compressive principal stress inferred from left lateral faults (σ_3a), N90W; from right lateral faults (σ_3b), N80-85W. These trajectories are consistent with orientations of wrinkle ridges. Principal stress trajectories calculated from Tharsis isostasy models (σ_3*) differ by 10-30° from those inferred from structure orientations and would predict reverse faulting or folding normal to σ_3*.

NEW EVIDENCE--OLD PROBLEM: WRINKLE RIDGE ORIGIN; David H. Scott, U.S. Geological Survey, Flagstaff, AZ 86001.

Wrinkle ridges characterize lava plains on the Moon, Mars, and Mercury. Although they are recognized as structural features, different interpretations as to their origin have been advanced. Some investigators have thought that they were formed by compressional forces (1-5); others have suggested that the ridges result from crustal extension followed by lava intrusions along fractures and faults (6-8).

One of the least rewarding pursuits is the search for new information from a much-used data bank that has been long unreplenished. Thus, the fortuitous discovery of fresh evidence contributing to the understanding of a problem is stimulating. During the large-scale (1:500,000) geologic mapping of the Kasei Valles-Lunae Planum region of Mars (MTM 25057), a continuous progression was observed in the transition from a wrinkle ridge to a chain of collapse pits (a catena) to grabens (Fig. 1). A similar but more limited association of structural elements occurs in places on the lunar maria where wrinkle ridges lead into linear rilles or grabens (Fig. 2) which, in turn, are commonly associated with catenae. On Mars, too, grabens and catenae are either coincident or intergradational in many places. However, the occurrence of a tripartite transition between ridges, catenae, and grabens is probably rare, because it apparently has not been observed previously. The relations of these structures in this local area seem to be most plausibly explained by their having common origins that involve crustal extension, surface fracturing and collapse, magma intrusions, and the formation of dikes that have breached surface layers.

Wrinkle ridges having nearly orthogonal intersections occur in ridged plains material south of Valles Marineris. The cross-cutting patterns formed by these ridges are similar to those of fractures and grabens transecting ridged plains material north of Kasei Valles. Crustal extension rather than compression may be the best explanation for the development of these structures.

References

(1) Howard, K.A., and Muehlberger, W.R. (1973) Apollo 17 Preliminary Science Report, NASA SP-330, sec. 31, p. 22-25; (2) Plescia, J.B., and Golombek, M.P. (1986) GSA Bull., 97, p. 1289-1299; (3) Raitala, J.T. (1987) Lunar and Planet. Sci. Conf. 18, p. 816-817; (4) Waters, T.R. (1987) Lunar and Planet. Sci. Conf. 19, p. 1243-1244, p. 1245-1246; (5) Colton, G.W., Howard, K.A., and Moore, H.J. (1972) Apollo 16 Preliminary Science Report, NASA SP-315, sec. 29, p. 90-93; (6) Young, R.A. et al. (1973) Apollo 17 Preliminary Science Report, NASA SP-330, sec. 31, p. 1-11; (7) Hodges, C.A. (1973) Apollo 17 Preliminary Science Report, NASA SP-330, sec. 31, p. 12-21; (8) Scott, D.H. (1973) Apollo 17 Preliminary Science Report, NASA SP-330, sec. 31, p. 25-28.

WRINKLE RIDGE ORIGIN
Scott, D. H.

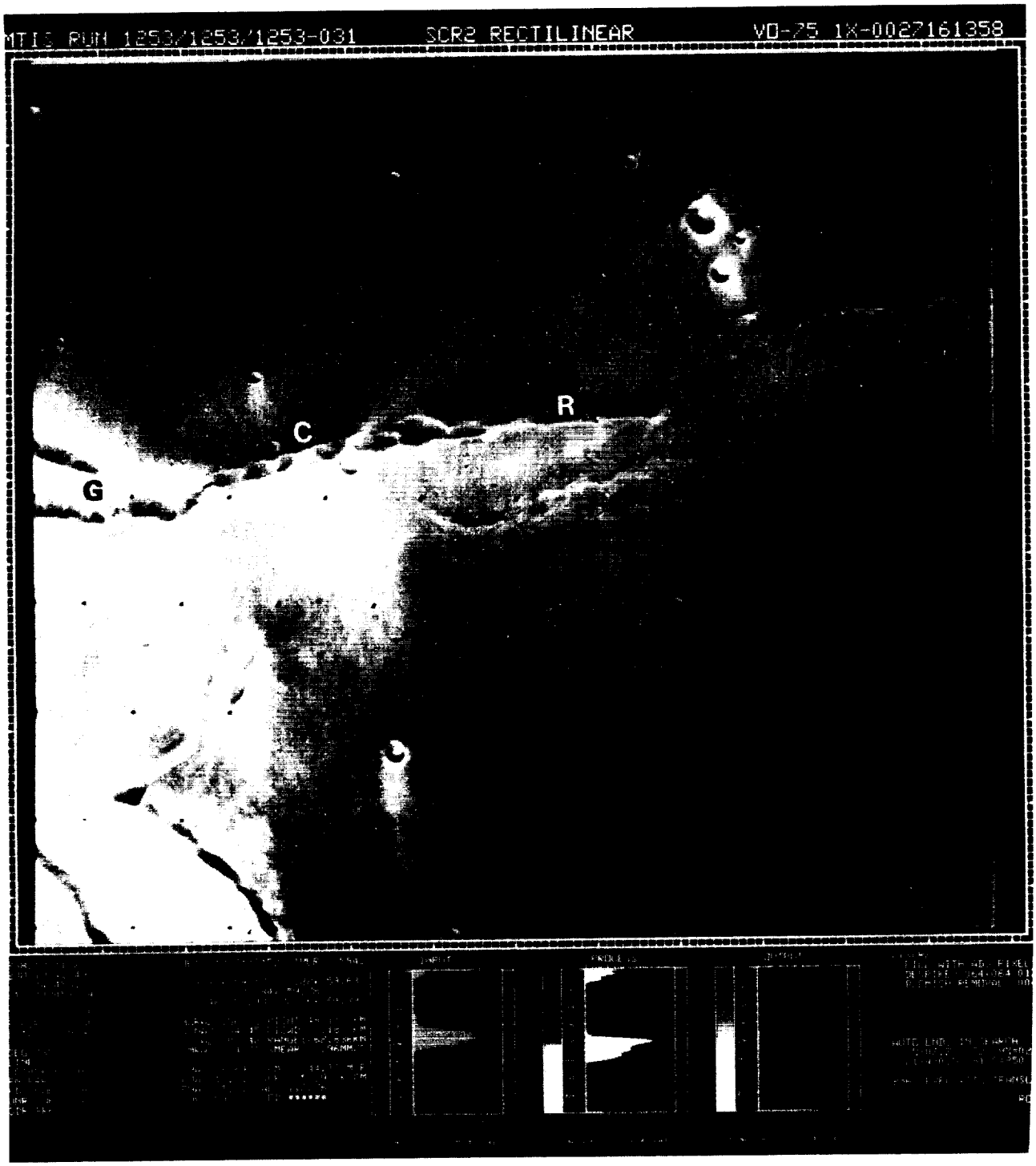

Figure 1. Ridged plains material of Lunae Planum (Viking frame 064A41). G-graben, C-catena, R-ridge.

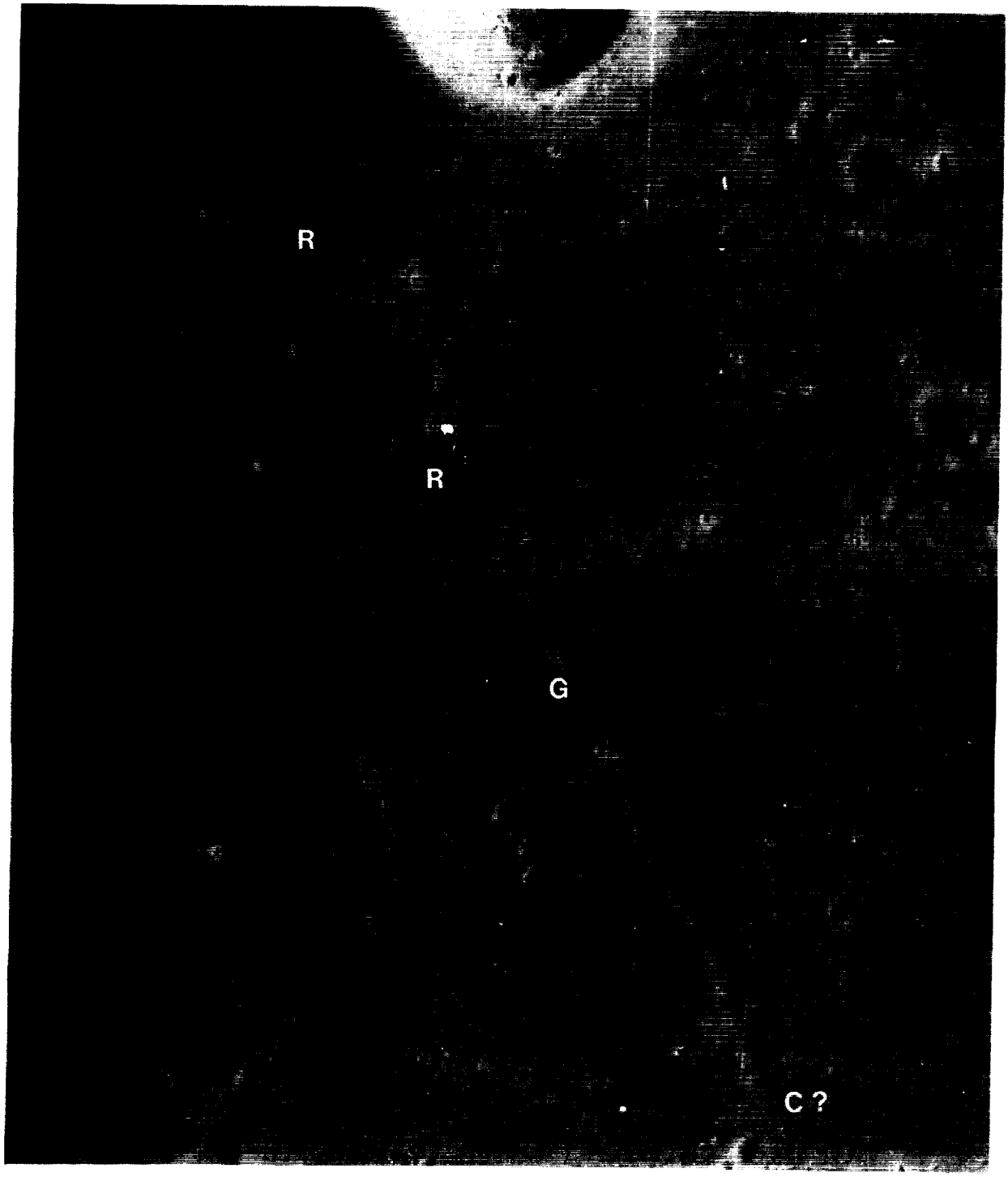

Figure 2. Mare Serenitatis (Apollo 15 9303 Panoramic). G-graben (rille), R-ridge, C?-questionable catena. Picture width about 8 km.

FAULT-RELATED FOLDING ON THE EARTH WITH APPLICATION TO WRINKLE RIDGES ON MARS AND THE MOON;

J. Suppe[1,2], and W. Narr[2], [1]Division of Geological and Planetary Sciences, Caltech, Pasadena CA 91125, [2]Department of Geological and Geophysical Sciences, Princeton University, Princeton NJ 08544.

Quantitative analysis of high-quality seismic, well, and surface geologic data over the last decade demonstrates that many, if not most, large-scale folds in the upper crust are formed in response to faulting. The most important mechanisms that have been identified are fault-bend folding (Suppe, 1983) and fault-propagation folding (Suppe and Medwedeff, 1984; Suppe, 1985; Woodward et al., 1985).

Fault-bend folds are produced by bending of the hanging-wall fault block as it slides over a non-planar fault surface; both compressional and extensional fault-bend folds are common. In contrast fault-propagation folding takes place at the tip of a propagating thrust fault (note that some thrusts propagate slowly as slip increases with folding at the fault tip whereas others propagate rapidly by Coulomb fracture). Quantitative geometric and kinematic relationships between fault shape and fold shape have been derived for both fault-bend and fault-propagation folds based on knowledge of the small-scale deformation mechanisms. For example layer thickness is generally conserved in compressional fault-bend folding because most of the deformation is by bedding slip, whereas layer thickness is generally not conserved in extensional fault-bend folding because most of the deformation is by slip on small normal faults that cut bedding. These quantitative relationships between fault and fold shape have been successfully tested in many cases in which the entire shape is well known. The theory has been applied successfully to complex situations with excellent data, including wedge-shaped faults, multiple folds and faults, and folding of faults.

Major modification of fold shapes takes place within strata deposited during deformation, that is within growth strata. Actual examples agree well with theoretical predictions. In the case of deposition faster than the structural uplift, little or no surface expression exists (for example Lost Hills anticline; Medwedeff, 1988, 1989). At lower depositional rates, substantial topography

or bathymetry can develop, but the surface is generally a time-transgressive angular disconformity, which has a shape quite different from the underlying layers (for example Wheeler Ridge anticline, Medwedeff, 1988). The deposition of rock over such growing structures provides a complete record of the deformation which allows quantitative kinematic reconstruction of the deformation. However subsurface data are required and surface data alone can be deceptive.

All the fault-related folding mechanisms involve kink-band migration, with the band boundaries pinned to hangingwall or footwall cutoffs on the faults. At small displacements relative to the thickness of the stratigraphic cover, the kink band may assume a shape that is quite different from the simple theory. An example from Casper Mountain is given, which may be analogous to some wrinkle ridges. The kink band undergoes substantial widening vertically such that the surface dips are quite shallow whereas at depth they are nearly vertical. The vertical component of the deep displacement does reach the surface, whereas the horizontal component is dissipated such that the surface fold shape cannot be simply related to deep structure.

Medwedeff, D.A., 1988, PhD Thesis, Princeton University, 184p.
Medwedeff, D.A., 1989, Amer. Assoc. Petroleum Geol. Bull. 73, 54.
Suppe, J., 1983, Am. J. Sci. 283, 684.
Suppe, J., 1985, Principles of Structural Geology, Prentice-Hall, 537p.
Suppe, J., D.A, Medwedeff, 1984, Geol. Soc. Amer. Abstr. Prog. 16, 670.
Woodward, N.J., S.E. Boyer, J. Suppe, 1985, An Outline of Balanced Cross-Sections, Univ. Tenn. Dept. Geol. Sci., Studies Geol. 11, 170p.

DEVELOPMENT OF GRABENS, TENSION CRACKS, AND PITS SOUTHEAST OF ALBA PATERA, MARS; **Kenneth L. Tanaka and Philip A. Davis**, U.S. Geological Survey, Flagstaff, AZ 86001 and **Matthew P. Golombek**, Jet Propulsion Laboratory, Caltech, Pasadena, CA 91109.

The two major regions on Mars that are dominated by grabens and collapse features (e.g., pits, pit chains, and troughs) are the regions surrounding Valles Marineris and Alba Patera. Most of these collapse features formed along or parallel to graben floors and walls. Possible genetic relations among grabens, tension fractures, and pits can be better studied in the Alba Patera region because (1) the pit chains at Valles Marineris show progressive enlargement and coalescence into troughs due to mass-wasting and erosional processes that are as yet poorly understood, and (2) volcanism and tectonism in the Valles Marineris region were long lived, and they have obscured crustal stratigraphy, tectonic history, and relations among pit and pit-chain size and distribution and fracture size and distribution.

The pits near Alba Patera, on the other hand, appear to have undergone only minor modifications. The pits formed chiefly in fractured lava flows on the southeast flank of Alba Patera over an area of several hundred kilometers. Pit development postdates Alba Patera volcanism and faulting, and it appears to be related to the latest tectonic activity in the region, which was centered on Ascraeus Mons [1]. The pits show no indication of significant alteration by other processes, although their walls appear to have been eroded back by mass wasting and the pits have possibly been partly filled with eolian material. Only a few of the southernmost pits may have been buried by late lava flows of Ceraunius Fossae and Acraeus Mons.

Four major pit chains (the longest of which is 1100 km) on the southeast flank of Alba Patera parallel the dominant northeast strike of the grabens and are of similar age to the grabens; spacing between the chains (about 150 km) is fairly uniform. Many smaller pit chains, mostly within grabens, occur between the four large chains. Because the grabens that contain pits were formed by regional tectonic activity, we infer that the drainage of the pits was also initiated by tectonic processes. The model by [2] proposes that major tension cracks developed in intact megaregolith (ejected breccia whose impact-induced fractures were healed by carbonate cementation and which may have had pore-fluid pressure if water was present). The open tension cracks provided voids into which weaker, overlying material (such as uncemented megaregolith) may have collapsed to form pits. Also, the model indicates that the cracks would originate at the same subsurface mechanical discontinuity at which faults bounding grabens intersect. This model is consistent with the general association of pits with grabens and the tectonic setting and likely crustal stratigraphy where pits formed.

The minimum pit spacings within the four large chains mentioned above average about 1 to 2 km. According to laboratory experiments [3], this distance may also represent the thickness of unconsolidated material above a tension crack. (However, these laboratory experiments used unconsolidated material that may not be completely analogous to the material involved in vertical pit drainage on Mars.) A probable measure of the thickness of the unconsolidated material above tension cracks is the depth to the mechanical discontinuity where faults bounding grabens initiated, which is suggested by the model of [2] and the laboratory results of [3]. This mechanical discontinuity in Lunae, Syria, and Sinai Plana was recently estimated to be between 1 and 1.5 km deep, which is close to the modal depth value for measured pits and troughs in these three regions [4]. If the faulted-layer

thickness around Alba Patera (which we are currently investigating) is similar to that estimated for these other regions, then the tension-fracture model proposed by [2] explains graben and pit development in which both faulting and fracturing initiated at the same mechanical discontinuity.

Certain predictions can be made regarding faulting on Mars on the basis of the Griffith failure criteria that describes the formation of tension cracks and shear faults in intact rock, Byerlee's law that describes failure in shear for prefractured material, and a crustal stratigraphy in which prefactured material (e.g., ejected breccia) overlies intact material (e.g., cemented breccia). Shear faults bounding grabens will form in the prefractured material and connect with tension cracks that may form in the underlying intact rock, if the stresses are high enough to form tension cracks [2]. The shear faults will form at lower deviatoric stresses than those required to form tension cracks. This suggests that the faults bounding grabens will initiate at the controlling subsurface mechanical discontinuity and propagate to the surface before tension cracks initiate at the same discontinuity and propagate down. Subsurface drainage of unconsolidated breccia into sufficiently large tension cracks beneath the grabens would result in the formation of pits along graben traces. Because most grabens on Mars do not have drainage pits associated with them, the material below the mechanical discontinuity either does not fail due to its greater strength or forms tension cracks that are too small to allow the subsurface drainage of material. However, grabens will always form above subsurface tension cracks, provided the overlying material is prefractured (suggested by the presence of the grabens) and thus weaker than the underlying intact rock. This model is in accord with the observation that most pits occur along the trace of grabens.

Some smaller pit chains near Alba Patera are not spatially associated with grabens, which requires either lateral changes in mechanical properties or formation by a different process such as gas venting. The latter alternative seems unlikely because of the apparent lack of coeval volcanic deposits in the area (the pits clearly postdate the volcanism of Alba Patera), the lack of rims on the pits, and the linear alignment of the pit chains. Note that pits produced by gas venting generally have raised rims and form sinuous chains [5,6].

We therefore propose that the mechanical properties of the crustal material determines where tension cracks may form in subsurface material without forming grabens that breach the surface above them. The general stratigraphy of Syria, Sinai, and Lunae Plana may be similar to that near Alba Patera and may therefore provide some insight into the mechanical properties of the crustal materials that control graben, tension fracture, and pit formation in the latter region. We interpret from recent studies of depths to various erosional and mechanical discontinuities [4, 7, 8] that the stratigraphy within those three plana consist, from top to bottom, of a layered sequence of lava flows, sedimentary rock, and ejected breccia (about 0.5 km thick), a relatively pristine ejected breccia layer (about 0.5 km thick), a cemented, resistant ejected breccia layer (about 1.5-2.0 km thick), and a healed basement. The correspondence between head depths of sapping valleys and the depth of the cemented ejected breccia layer (about 1 km) suggests that water (either ice or liquid) was present. Tension fractures could develop in the cemented breccia layer regardless of the presence or absence of water; pore-fluid pressure in the cemented breccia would augment the development of tension fractures.

Some areas of the shallow crust around Alba Patera where there are pits

apparently impeded graben formation, and therefore differ from the above stratigraphy. If the surficial layers were intact and sufficiently strong such that tensile stresses adequate to crack the cemented breccia were below those required to crack the stronger overlying rocks, faults would not propagate to the surface. Locally, lava flows near Alba Patera thus may be without throughgoing thermal-contraction fractures to satisfy this strength requirement. Failure criteria [2] indicate that pore-fluid pressure in the cemented breccia and basement rocks is probably required so that their tensile strengths at depth are lower than the surficial volcanic rocks. In this case, subsurface drainage of the layer of unconsolidated breccia into the tension cracks would, at some point, cause overburden failure in the volcanic rocks and result in collapse, without associated graben development.

References

[1] Rotto, S.L. and Tanaka, K.L. (1989) Lunar and Planet. Sci. XX, Abstracts, 926-927.
[2] Tanaka, K.L. and Golombek, M.P. (1989) Proc. Lunar Planet. Sci. Conf. 19th, p. 383-396.
[3] Horstman, K.C. and Melosh, H.J. (1989) Fourth Intl. Conf. Mars, Abstracts, 128.
[4] Davis, P.A. and Golombek, M.P. (1989) Lunar and Planet. Sci. XX, Abstracts, 224-225.
[5] Siegal, B.S. and Gold, D.P. (1973) Moon 6, 304-336.
[6] Schumm, S.A. (1970) Geol. Soc. America Bull. 81, 2539-2552.
[7] Tanaka, K.L. and Davis, P.A. (1988) J. Geophys. Res. 93, 14,893-14,917.
[8] Robinson, M.S. and Tanaka, K.L. (1988) MEVTV Workshop, LPI Tech. Rept. 88-05, pp. 106-108.

FLANK TECTONICS OF MARTIAN VOLCANOES

P.J. Thomas[1], S.W. Squyres[1] and M.H. Carr[2]

[1]Center for Radiophysics and Space Research, Cornell University, Ithaca, NY 14853 USA; [2]US Geological Survey, Astrogeology Branch, Menlo Park CA 94025.

Olympus Mons exhibits a series of terraces on its slopes, concentrically distributed around the caldera. The base of each terrace is marked by a modest but abrupt change in slope. Above the base, the slope decreases gradually with height, creating a gentle, convex topographic profile. In some locations, several terraces are located one above another. They occur in a region roughly 20% to 55% of the radius from summit to base, at altitudes of 20 – 12 km above Mars datum.

The sharp break in slope at the base of the terraces and the apparent dislocation of some flows suggests an origin by faulting. However, the faulting does not appear to be analogous to the "pali" around the periphery of the Hawaiian shields, which result from normal faulting associated with outward movement of the shield flanks. Normal faults typically are marked by a steep escarpment with sharp breaks in slope at their base and crest. This is true of the peripheral faults on Kilauea and Mauna Loa, and is true also of the numerous normal faults on Mars. In contrast, the terraces on Olympus Mons have a sharp break in slope at their base, and gentle convex upward profiles. Here we explore the possibility that the breaks in slope are caused by thrust faults that formed penecontemporaneously with emplacement of the flows on the volcano flanks, due to compressional failure of the cone.

In an attempt to understand the mechanism of faulting and the possible influences of the interior structure of Olympus Mons, we have constructed a numerical model for elastic stresses within a martian volcano using an incompressible, Eulerian finite element formulation (1,2).

For Olympus Mons, our model represents the volcano as an axisymmetric truncated cone, 21 km in height, with upper and basal radii of 50 km and 250 km, respectively. The cone rests upon a base 100 km thick and 500 km in radius. The base is constrained below and at its outer edge by rigid boundary conditions. Numerical tests show that the base is sufficiently large to completely avoid edge effects.

The model incorporates a magma chamber. The magma chamber has a diameter equal to that of the caldera, $\approx$ 100 km. Given this diameter, the magma chamber clearly is far from spherical; we model it as an oblate spheroid. For the case of Kilauea, accurate measurements of surface tilting are best explained by pressurization of a magma chamber at a depth of 2 – 6 km (3). This requires that the chamber be within the edifice, raised above the surrounding plains. The vertical location of the magma chamber probably is controlled by the buoyancy of the magma, as it ascends though material of decreasing density (4). The variation in density with depth is predominantly due to the closing of voids by hydrostatic pressure at depth. Scaling the depth of the Kilauea magma chamber (4) for gravity, we find that an appropriate vertical extent is 5 – 15 km below the summit. This implies that the magma chamber is elevated over 10 km above the surrounding plains.

The magma chamber in the model may be vacant, filled but unpressurized, or pressurized. Pressurization of the magma chamber is simulated by specifying normal stresses as boundary conditions on the magma chamber walls. The density of the material throughout the volcano is 2050 kg m^{-3}, and a value of Young's modulus appropriate to basalt, 9×10^{10} Pa s, is adopted.

For a full magma chamber, the stress environment at the surface is dominated

by a region of compressive stress occupying the upper two thirds of the slope, appropriate to the formation of thrust faults there. Maximum compressive stresses are ~250 MPa. These stresses arise from the general elastic deformation of the cone, and represent a net reduction in surface area. In addition to these prominent stress features, there is a region of compressive tangential stress at the summit, ringed by a region of extensional stress. However, the stresses here are much smaller (~10 MPa). The location of the greatest extensional stresses is found on the lower slopes of the cone when the chamber is filled, occupying roughly the lowest third of the flanks. The stresses here are < 30 MPa.

A similar stress distribution is observed when the cone contains a vacant magma chamber. In this case, however, compressive stresses tend to be more equally distributed over the volcano slopes, and no extensional stress is evident on the lower slopes. This is apparently because the presence of a vacant magma chamber permits increased compression of the edifice and, accordingly, more pronounced compression on the slopes. Assuming that the escarpments on Olympus Mons are indeed the expressions of the thrust faults, we find that a full chamber produces a stress distribution most consistent with the observed distribution.

If the magma chamber is pressurized, additional extensional stresses can occur at the summit and the upper slopes of the cone. For a magma chamber pressure of 100 MPa (twice the overburden), the maximum extensional stress is ~80 MPa. While such stresses could readily cause extensional faulting, it is unlikely that the material of the volcano could support such large overpressures without extrusion taking place. We find that the location of the expected zone of thrust faulting is a complicated function of the size and shape of the volcano and magma chamber and the internal pressures within the chamber, but to a limited extent the position of the faults may be used to derive information about the internal structure of the volcano at the time of faulting.

Terraces like those on the flanks of Olympus Mons are also observed on three other martian volcanoes: they are very prominent on Ascraeus Mons, and present but less well-developed on Arsia Mons and Pavonis Mons. Alba Patera, which has a diameter over twice that of Olympus Mons, does not have them. If the occurrence of these features, which we believe are due to thrust faulting, is related to edifice size, then clearly large diameter alone is not a sufficient requirement. We therefore considered the influence of both diameter D and mean slope h/D, where h is the edifice height, on flank stresses.

Calculations for a range of h/D and D show that the maximum compressive stress found on the flanks is a simple linear function of these parameters. By modeling volcanoes with various diameters and slopes, then, we can extend the results obtained for Olympus Mons to the other martian volcanoes. We find that the four volcanoes with the largest stresses are the only ones on which concentric flank terraces are observed, lending considerable support to the view that these features form by thrust faulting.

It is useful to compare our calculated maximum stresses to laboratory data for the strength of basalt. Estimates for the unconfined uniaxial compressional strength of basalt vary from 124 MPa (5) to 262 MPa (6) for basalts with densities similar to that assumed for this model. Figure 1 shows the range of edifice dimensions h/D and D that will produce flank stresses that meet or exceed this failure strength. Dimensions of the major martian volcanoes are shown, using topographic data from Pike (8). All four volcanoes that exhibit flank terraces lie well within the region where failure, and hence thrust faulting, is expected. All other martian volcanoes, which are free of terraces, have flank stresses below the failure strength

of basalt. Simplifying assumptions of this model, in particular incompressibility (7) and neglect of lithospheric flexure, have the effect of understimating stresses on the volcano flanks, and do not alter our major conclusions.

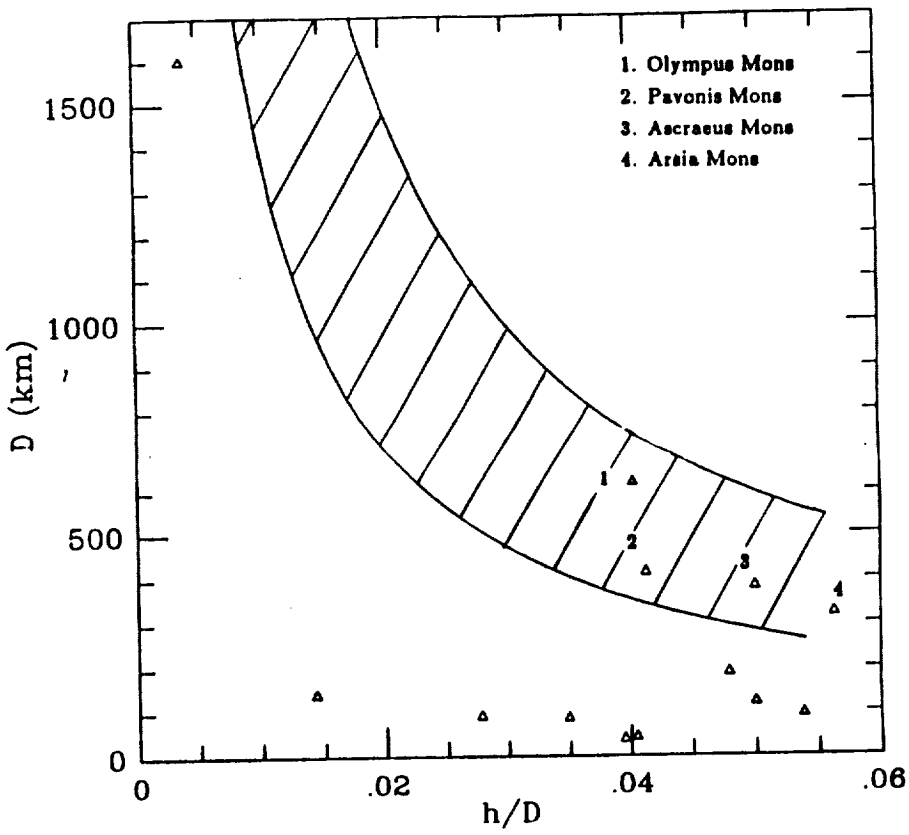

Figure 1. Volcano diameter *vs.* average slope for all major martian volcanoes. The range where maximum flank stresses equal compressional strength values for basalts are indicated by the hatched region.

References: (1) Thompson, E.G. & M.I. Haque (1973) *Int. J. Num. Methods Eng.*, 6, 315-321. (2) Thompson, E.G. (1975) *Int. J. Num. Methods Eng.* **9**, 925-932. (3) Macdonald, G.A. (1961) *Science*, **133**, 673-679. (4) Ryan, M.P. (1987) *U.S. Geol. Surv. Prof. Pap. 1350*, vol. 2, 1395-1447. (5) Hathaway, A.W. & G.A. Kiersch (1982) in *Handbook of physical properties of rock*, CRC Press. (6) Handin, J. (1966) in *Handbook of Physical Constants*, GSA Memoir 97. (7) Deterich, J.H. (1988) *J. Geophys. Res.*, **93**, 4258-4270, 1988. (8) Pike, R.J. (1979) in *Proc. 9th Lunar Planet. Sci. Conf.*, pp. 3239-73, Pergamon, New York.

ORIGIN AND CHARACTERISTICS OF DEXTRAL STRIKE-SLIP FAULTS WITHIN THE YAKIMA FOLD BELT, COLUMBIA RIVER FLOOD-BASALT PROVINCE, USA

Terry L. Tolan, Geology Department, Portland State University, P.O. Box 751, Portland, Oregon 97207, James Lee Anderson, Department of Geology, University of Hawaii at Hilo, 523 W. Lanikuala St., Hilo, Hawaii 96720, Marvin H. Beeson, Geology Department, Portland State University

The presence of northwest-trending, dextral strike-slip faults within the Yakima Fold Belt (YFB) has been firmly established and recent studies (1,2,3,4,5,6,7) suggest that these faults can be informally grouped into 3 categories based on their physical characteristics and mode of origin: 1) tear faults local to ridge uplift, 2) faults or shear zones of limited extent and minor displacement that do not influence ridge-fold geometry, and 3) wrench faults of regional extent that can be traced across ridge uplifts and interridge basins. The first two categories of dextral strike-slip faults can be found throughout the YFB while the last category of faults occurs mainly in the southwestern and southern portions of the YFB.

The first category of dextral strike-slip faults consists of tear faults (and associated folds) which commonly define the boundaries of anticlinal ridge segments within the YFB (1,2,4,7). These faults and associated folds are typically confined to the area of ridge uplift and do not extend any appreciable distance into adjacent basins (2,7,5). Trend of these structures is variable, ranging from N 10 degrees to 60 degrees W. Faults of this first category are thought to originate in response to differences in developing anticlinal fold geometry along the ridge trend and do not necessarily reflect the presence of pre-Columbia River basalt structures (8,2,5).

The second category consists of faults that typically have small displacements and do not appear to have exerted any control on ridge-fold geometry. The trend of these faults is variable, ranging from N 5 degrees to 65 degrees W. Fault planes are typically near vertical to vertical and have narrow (<1 m-wide) breccia/gouge zones. Lateral displacement on these faults is generally thought to be on the order of a few meters to tens of meters (1) and vertical displacement is commonly less 5 m. Because of their subtle topographic and geologic expression, this category of fault is often difficult to recognize except in areas of excellent exposure or where the trace of these faults have been accentuated by erosion and/or vegetation. These faults are known to occur throughout the YFB, but appear to increase in frequency of occurrence in the southwestern portion of the YFB (9,1). Faults of this category are an expected consequence the development and growth of the YFB. However it has been postulated that these faults could have also originated as part of a broader "distributed shear" system operating on western North America (10).

The last category consists of at least 12 northwest-trending, dextral wrench fault zones. These zones typically strike between N 30 degrees to 50 degrees W and usually exceed 40 km in length (4,5,6). Where these zones transect an anticlinal ridge they often mark ridge-segment boundaries. But unlike tear faults of the first category, these features can be traced into, and often through, adjacent basins. Within the interridge basins these fault zones commonly display a combination of structural features(4,5,6) including:

- en echelon faults, with reversal of apparent dip-slip separation along strike commonly observed;
- transpressive, en echelon, faulted, asymmetric, doubly-plunging anticlines (flower structures);
- transtensional horsts and grabens.

Amount of lateral displacement on these wrench fault zones is estimated to be generally less than 1 km (5). Evidence indicates that these dextral wrench fault zones are the present expression of older strike-slip faults that existed prior to the emplacement of Columbia River basalt flows in middle Miocene time (3,5,6) and therefore not a direct consequence of YFB development(5).

References Cited

(1) Bentley, R.D., Anderson, J.L., Campbell, N.C., and Swanson, D.A., U.S. Geol. Surv. Open File Rep. 80-200, 1980. (2) Reidel, S.P., Am. Jour. Sci., 284, 942-978, 1984. (3) Beeson, M.H., Fecht, K.R., Reidel, S.P., and Tolan, T.L., Oregon Geol., 47, 87-96, 1985. (4) Anderson, J.L. and Tolan, T.L., Geol. Soc. Am. Abstr. Programs, 18, 82, 1986. (5) Anderson, J.L., Ph.D. dissertation, Univ. Southern Calif., Los Angeles, CA, 1987. (6) Beeson, M.H., Tolan, T.L., and Anderson, T.L., in Geol. Soc. Am. Sp. Paper: Volcanism and Tectonism in the Columbia River Flood-Basalt Province, in press. (7) Reidel, S.P., Fecht, K.R., Hagood, M.A., and Tolan, T.L., in Geol. Soc. Am. Sp. Paper: Volcanism and Tectonism in the Columbia River Flood-Basalt Province, in press. (8) Davis, G.A., Wash. Public Power Supply System, Nucl. Proj. 2, FSAR, ammendment 18, subappendix 2.5-N, 1981. (9) Bentley, R.D. and Anderson, J.L., EOS trans. AGU, 60, 961, 1979. (10) Sheriff, S.D., Tectonics, 3, 397-408, 1984.

STRUCTURAL GEOMETRY, STRAIN DISTRIBUTION AND FOLD MECHANICS WITHIN EASTERN UMTANUM FOLD RIDGE, SOUTH CENTRAL WASHINGTON; A.J. Watkinson, Geology Department, Washington State University, Pullman, WA 99164 USA
E.H. Price, CER Corporation, P.O. Box 94977, Las Vegas, NV 89193

Umtanum Ridge is one of the best-exposed Yakima ridges formed by folded basalt flows in south-central Washington. An analysis was made of the structural geometry and strain distribution in the deformed basalt layers exposed on the ridge at Priest Rapids. The purpose of the analysis was to gain an understanding of the distribution and orientations of the small-scale structures [faults, breccias and joints] around the anticlinal structure. From this we can assess the relative strain intensity and distribution around the fold and use this information, along with the mapped profile shape of the fold and associated faults, to construct a balanced section leading to constraints on the tectonic models of the Columbia Plateau.

The strain distributions and structural geometries within the Umtanum fold accord well with an asymmetric kink-fold geometry with predominantly flexural strains in the steep limb; however, the internal cataclastic flow in the steep limb is not penetrative at field observation scale. Discrete flexural slip has occurred, both within and long flow contacts, along with some internal shatter brecciation and faulting between and at angles to the flow-parallel faults.

Two major faults are associated with the fold. The upper, the Buck thrust, appears to be specifically associated with the change in trend of the anticline, and as such is interpreted to be an accommodation structure. The other major fault, the Umtanum fault, is conjectured to have formed out of the kink-like fold at depth. Slickenside striae orientations on faults developed during folding are generally perpendicular to the fold axis.

Our fold reconstruction is based on the following constraints:

1. The Cold Creek syncline on the south side of the Umtanum anticline is structurally higher than the Wahluke syncline on the north side.

2. Because the Buck thrust dies out along strike, and appears to be formed as a result of the bend in the trace of the anticline, we assume that the major fault is the Umtanum fault. We therefore use the southerly dip [20-25] of the southern back limb of the fold structure as a guide for the extrapolated dip of the Umtanum fault at a lower structural level.

3. The southern limb and hinge zone has a very low fracture intensity, and therefore we do not believe that the fold has travelled far up and over any series of ramps or flats.

4. We assume that the dip of the Umtanum fault is very low at the surface, based on the observations made further along strike.

5. The resulting section has be be compatible with the strain distributions estimated from the small-scale structures.

6. We have no drill data through the structure, or access to any geophysical information to constrain the deeper levels.

7. We place 'pin' lines, perpendicular to bedding, in the low strain areas of the syncline to the north and the back limb of the anticline.

Our partially restored section showing the Umtanum fault to be an out-of-fold fault does balance and is one of the most conservative models in terms of amount of fault displacement.

Owing to the lack of subsurface information, detailed boundary conditions are hard to specify, making it difficult to constrain the exact mechanics of folding. The characteristic shape of the fold is presumably as much a function of the layer properties (1) as it is the specific structural environment.

If low angle thrust faults are regionally developed (although there is no clear seismic, drill or field evidence that they are), other viable geometric models are possible such as fault bend folds (2), fault propagation folds (3), or detachment folds (4).

The current state of stress (5), measured by hydrofracturing techniques, is below that estimated for the critical buckling stress (6) for initiation of periodic, sumisoidal, elastic buckling of a uniform multilayer on a weaker substrate from sinusoidal

$$EI\frac{d^4v}{dx^4} + P\cdot\frac{d^2v}{dx^2} + Kv = 0 \quad (7)$$

Attenuated folding (of form $v = Ce^{\beta x} \sin \alpha x$) at lower values of differential stress could occur at sites of localized shear (8) (from reactivated faults at depth?) or localized bending moments (9) (from propagating kink/buckle folds?).

The flat synclines separating the anticlines suggests a regional model of local décollement folding (10), perhaps initiated in the N/S stress field, in part gravitationally generated in an actively subsiding basin? [cf (11).]

REFERENCES

1. Johnson, A.M., 1977. Styles of Folding.
2. Suppe, J., 1983. Am. Journ. Sci., p. 684-721.
3. Suppe, J., 1985. Principles of Structural Geology.
4. Jamison, W.R., 1987. Journ. Struct. Geol., p. 207-219.
5. Kim, K., Dischler, S.A., Aggson, J.R., and Hardy, M.P., 1986. RHO-BW-ST-73 P.
6. Watters, T.R., 1989, in press. Geol. Soc. Am. Spec. Paper.
7. Hetenyi, M., 1946. Beams on Elastic Foundation.
8. Johnson, A.M., 1970. Physical Processes in Geology.
9. Watkinson, A.J., and Cobbold, P.R., 1978. Bull. Geol. Soc. Am., p. 448-450.
10. Blay, P., Cosgrove, J.W., and Summers, J.W., 1977. Journ. Geol. Soc., p. 329-342.
11. Dixon, J.M., and Summers, J.W., 1983. Can. Journ. Earth Sci., p. 1843-1861.

CROSSCUTTING PERIODICALLY SPACED FIRST-ORDER RIDGES IN THE RIDGED PLAINS OF HESPERIA PLANUM: ANOTHER CASE FOR A BUCKLING MODEL

Thomas R. Watters and D. John Chadwick, Center for Earth and Planetary Studies, National Air and Space Museum, Smithsonian Institution, Washington, D.C. 20560

Hesperia Planum (20°S, 250°W) is one of the largest contiguous areas of ridged plains on Mars outside of the Tharsis Plateau. Ridged plains units on Mars are characterized by the presence of landforms analogous to those in mare wrinkle ridge assemblages (1). Like the ridged plains of Tharsis, those of Hesperia Planum are associated with a volcanic center. Tyrrhena Patera is a relatively small, heavily degraded shield volcano, surrounded and embayed by ridged plains material (2). The first-order ridges of Hesperia Planum are morphologically and dimensionally analogous to those on Tharsis. However, the spatial relationship of the ridges is much more complex. Many of the ridges crosscut one another at nearly orthogonal angles forming what have been termed as reticulate ridge patterns (3,4).

The ridged plains of Hesperia Planum with prominent reticulate ridge patterns lie to the east and southeast of Tyrrhena Patera. The reticulate pattern has been separated into two sets of first-order ridges, one with a predominant NW-SE trend and the other with a predominant NE-SW trend. Using the 1:2,000,000 Controlled Photomosaics as a base, ridge spacing was determined using a series of sampling traverses spaced at roughly 12 km intervals oriented perpendicular to the predominant trend of each set of ridges. Since the method used to determine ridge spacing includes all measurements between any two ridges along the sampling traverse including spacings between ridges that are not immediately adjacent, and the frequency distribution of ridge spacing is generally asymmetric, the mode is the most reliable measure of the average spacing. Based on the results of this study, both the NW-SE and the NE-SW trending ridge sets have an average spacing of 30 km.

The near consistent spacing of both sets of first-order ridges can be explained by two superimposed episodes of buckling of the ridged plains material at a critical wavelength where the maximum compressive stress direction has changed by roughly 90°. In this fold model (5), it is assumed that the ridged plains material: 1) deformed at the free surface under little or no confining pressure and, 2) behaves like a series of thin linearly elastic plates with essentially frictionless contacts. An elastic rheology was chosen over linearly viscous or power-law flow (see 6) because at low temperatures and pressures, ductility is rarely observed in rock (7). Free slip between layers is assumed based on the likely presence of regolith interbeds in the ridged plains volcanic sequence. The presence of such interbeds in a flood basalt sequence is consistent with subsurface data in Mare Serenitatis and Mare Crisium on the Moon and the Columbia Plateau.

CROSSCUTTING RIDGES
WATTERS, T.R. AND CHADWICK, D.J.

The multilayer rests on a mechanically weak regolith substrate of finite thickness which is in turn resting on a rigid boundary. The rigid basement does not participate in the deformation, thus no assumption of whole lithosphere deformation is necessary to explain the periodically spaced ridges. In the model proposed here, the basement is assumed to have elastic properties equal to the ridged plains material. This is not unreasonable since it is assumed that the deformation involving the ridged plains is limited to the upper crust of Mars (< 10 km). The observed wavelengths of many of the ridges can be explained by this model, at critical stresses below the maximum compressive strength envelope of a basalt-like material, given that: 1) the ratio in Young's modulus between the ridged plains material and the underlying regolith $E/E_o \geq 1000$; 2) the thickness of the ridged plains material is between roughly 2,000 and 4,100 m; and 3) the average thickness of a layer in the sequence is between 250 and 500 m (figure 2).

The origin of compressional stress that resulted in crosscutting ridges in Hesperia Planum is not clear. In the case of the ridged plains of the Tharsis Plateau, compressional stress may be the result of isostatic uplift (8,9,10). However, in the absence of a "Tharsis-like" uplift or load in Hesperia Planum and other ridged plains provinces on Mars (i.e., Syrtis Major Planum, Malea Planum), other mechanisms must be sought. Compressional stress may result from local subsidence due to loading from the ridged plains material (see 4). However, local subsidence will likely generate only a single dominant trend related to the geometry of the basin. A combination of local subsidence and a later superimposed regional tectonic event could account for the crosscutting ridge pattern.

References Cited

(1) Watters, T.R., JGR, 93, 10236-10254, 1988. (2) Carr, M.H., R. Greeley, K.R. Blasius, J.E. Guest, and J.B. Murray, JGR, 82, 3985-4015, 1977. (3) Saunders, R.S. and Gregory, T.E., Reports of Planet. Geol. and Geophys. Program, 1980, NASA Tech. Mem. 82385, 93-94. 1980. (4) Raitala, J., Earth, Moon and Planets, 40, 71-99, 1988. (5) Watters, T.R., in Fourth International Conference on Mars, Program and Abstracts, 206-207, 1989. (6) Zuber, M.T. and L.L. Aist, in Fourth International Conference on Mars, Program and Abstracts, 215-216, 1989. (7) Jaeger, J.C., and N.G.W. Cook, Fundamentals of rock mechanics, 3rd ed., 593 pp., Chapman and Hall, London, 1979. (8) Banerdt, W.B., R.J. Phillips, N.H. Sleep, and R.S. Saunders, JGR, 87, 9723-9733, 1982. (9) Sleep, N.H. and R.J. Phillips, JGR, 90, 4469-4489, 1985. (10) Watters, T.R. and T.A. Maxwell, JGR, 91, 8113-8125, 1986.

Figure 1. Crosscutting first-order ridges in the ridged plains of Hesperia Planum.

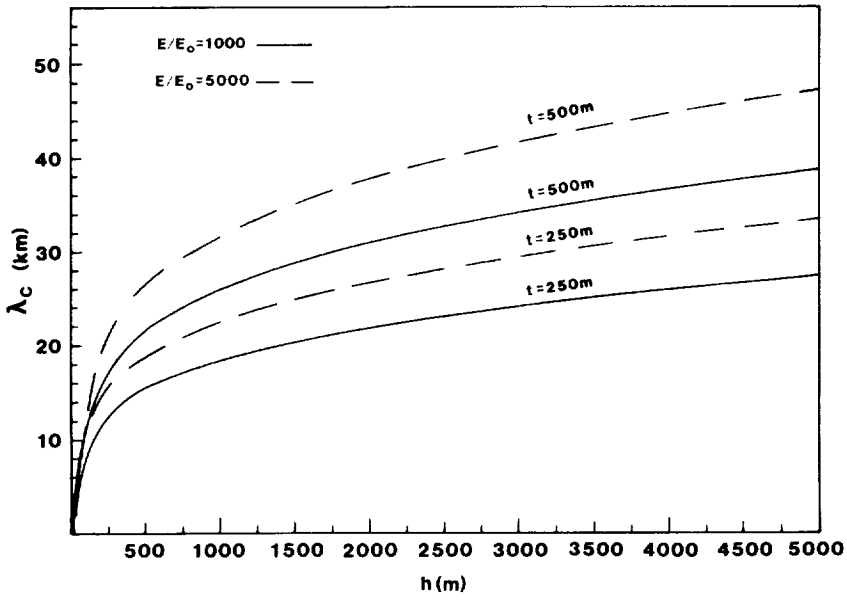

Figure 2. Critical wavelength of buckling as a function of thickness of the ridged plains material.

STRIKE-SLIP FAULTING ASSOCIATED WITH THE FOLDED COLUMBIA RIVER BASALTS: IMPLICATIONS FOR THE DEFORMED RIDGED PLAINS OF MARS

Thomas R. Watters and Michael J. Tuttle, Center for Earth and Planetary Studies, National Air and Space Museum, Smithsonian Institution, Washington, D.C. 20560

The anticlinal ridges in the continental flood basalts of the Columbia Plateau (or Columbia Basin) are long, narrow, periodically spaced structures with broad relatively undeformed synclines. The orientation and spacing of the anticlines varies throughout the Yakima Fold Belt, but is consistent within certain domains (1). Associated with the steeply dipping vergent side of the asymmetric anticlines are reverse to thrust faults. Mechanisms suggested for the origin of the anticlines or Yakima folds include: 1) drape folding over high angle reverse faults (2); 2) buckling over shallow detachments in the basalt sequence followed by reverse to thrust faulting (3); 3) buckling of the basalt sequence simultaneously with the emplacement of the oldest flows followed by dominantly reverse to thrust faulting (4); and 4) initial buckling in response to a horizontal compressive load coupled with a layer instability between the basalts and sub-basalt sediments (1,5).

In addition to the anticlines, numerous strike-slip faults have been mapped in the fold belt. Anderson (6) reports 35 right-lateral strike-slip faults (mean strike N40°W) and 10 left-lateral (mean strike N13°E) in the southern portion of the fold belt. The lateral displacement along the most extensive faults is typically small (< 1 km). Tolan et al. (7) suggest that the strike-slip faults can be classified as either tear faults, faults of limited extent or regional faults. Based on paleomagnetic data, Reidel et al. (8) observe a clockwise rotation in the anticlines relative to the synclines that they attribute to rotation along a localized NW trending right-laterial shear system developed in the anticlines as they grew.

In an effort to find additional evidence of strike-slip faults within the fold belt, Landsat Thematic Mapper (TM) data (30 m/pixel), Seasat SAR (25 m/pixel) and topographic data are being examined for prominent lineaments. The TM data has been geometrically corrected and edge enhanced to optimize the discrimination of linear features. Mapped lineaments are then digitized to facilitate statistical analysis using double angle method. To date over 80 lineaments have been mapped, 73 of which are located in the southern domain of the fold belt. Many of these correspond to previously mapped right-lateral strike-slip faults. The mean direction of the known and suspected strike-slip faults in the southern domain is N37°W (circular variance = 0.15) (figure 1). No predominant secondary trend corresponding to conjugate left-lateral strike-slip faults is present in our data.

Tectonic domains where major fold trends are transected by conjugate strike-slip faults have been documented (9,10). Because of the limited extent and lateral displacements of the strike-slip faults in the fold belt, a pure shear rather than a simple shear mechanism should best explain the geometric relationships between the structures. Pure shear is consistent with the development of relatively short (< 100 km) conjugate sets of strike-slip faults (see 10). Given a N-S directed compressive stress, the system of structures possible includes E-W trending first-order folds and first-order right-lateral and conjugate left-lateral strike-slip faults with a angle θ to the primary stress direction (figure 2). The angle θ is constrained by the Coulomb-Navier criterion where θ is related to the coefficient of internal friction μ. For typical values of μ between 0.58 and 1.0, θ is in the range of 22.5°-30°. In the southern domain of the fold belt, the mean direction of the ridges is roughly N80°W. Taking the normal to this to be the approximate direction of the compressive stress, the mean direction of the known and suspected right-lateral strike-slip faults is within the range for θ. Although the regional faults are thought to predate the Columbia River basalts (7), their orientation and extent are consistent with the expected system of tectonic features.

The anticlinal ridges in the Yakima Fold Belt have been shown to be good analogs to first-order ridges in wrinkle ridge assemblages that occur in the ridged plains material on Mars (5). If the ridged plains material has deformed in a similar style to the basalts of the Yakima Fold Belt, then strike-slip faults and their associated secondary structures may be common on Mars. In contrast to the Gordii Dorsum escarpment, interpreted by Forsythe and Zimbelman (11) to be a major transcurrent fault, the strike-slip faults associated with the first-order ridges, like their analogs in the Yakima Fold Belt, would be expected to be limited in extent, accommodating a portion of the relatively low bulk strain apparent in the ridged plains.

Reference Cited

(1) Watters, T.R., in Geol. Soc. Am. Sp. Paper: Volcanism and Tectonism in the Columbia River Flood-Basalt Province, in press, 1989. (2) Bentley, R.D., in Geology excursions in the Pacific Northwest, Western Washington Univ., Bellingham, WA, 339-389, 1977. (3) Price, E.H., Ph.D. dissertation, Washington State Univ., Pullman, WA, 1982. (4) Reidel, S.P., Am. Jour. Sci., 284, 942-978, 1984. (5) Watters, T.R., JGR, 93, 10,236-10,254, 1988. (6) Anderson, J.L., Ph.D. dissertation, Univ. South. CA, 1987. (7) T.L. Tolan, J.L. Anderson and M.H. Beeson, this volume. (8) Reidel, S.P., G.R. Scott, D.R. Bazard, R.W. Cross, and B. Dick, Tectonics, 3, 251-273, 1984. (9) Tirrul, R., I.R. Bell, R.J. Griffis and V.E. Camp, Geol. Soc. Am. Bull., 94, 134-150, 1983. (10) Sylvester, A.G., Geol. Soc. Am. Bull., 100, 1666-1703, 1988. (11) Forsythe R.D. and J.R. Zimbelman, Nature, 336, 143-146, 1988.

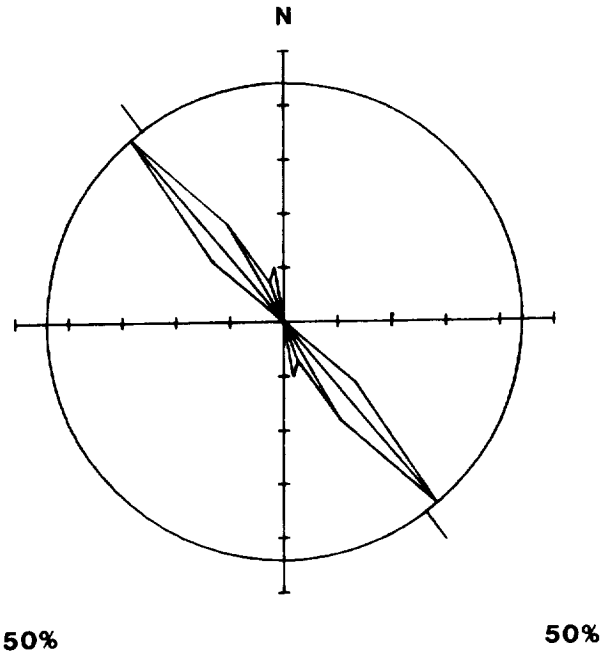

Figure 1. Rose diagram of known and suspected right-lateral strike-slip faults.

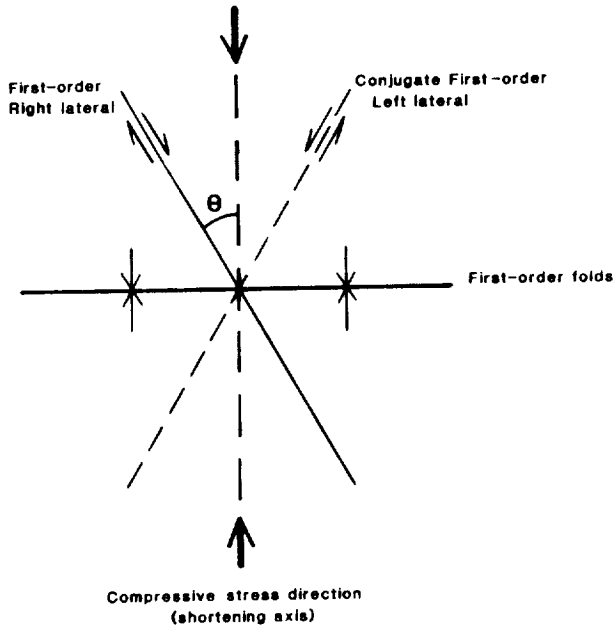

Figure 2. Geometric relationships between system of structures. θ = Arctan(μ^{-1})/2

*U.S.GOVERNMENT PRINTING OFFICE:1989-661-008/00106

THE DEPTH OF THE OLYMPUS MONS MAGMA CHAMBER AS DETERMINED FROM THE SPATIAL DISTRIBUTION OF TECTONIC FEATURES. *M.T. Zuber*[1] *and P.J. Mouginis-Mark*[2], [1]Geodynamics Branch, NASA/Goddard Space Flight Center, Greenbelt, MD 20771, [2]Planetary Geosciences Division, Hawaii Institute of Geophysics, University of Hawaii, Honolulu, HI 96822.

The summit caldera of Olympus Mons exhibits one of the clearest examples of tectonic processes associated with shield volcanism on Mars [1,2]. Within the 80 km diameter structure there are six nested calderas that indicate that the Olympus Mons edifice has undergone multiple collapse episodes [1]. Also found within the caldera are numerous wrinkle ridges and graben. Analysis of the topography of the caldera as derived from stereophotogrammetry [3] shows that the central portion of the caldera, where the majority of the ridges are located, represents a topographic low, while topographically high points around the caldera perimeter are characterized by circumferential graben (Figure 1). The relationship of the summit topography to the tectonic features, in combination with photogeologic evidence for basalt-like resurfacing of the caldera floor [4], is believed to indicate that a large lava lake has cooled and subsided as magma from the underlying chamber was withdrawn by flank eruptions [1].

The characteristics of the tectonic features in the Olympus Mons caldera contain information about the nature of the subsurface magmatic reservoir. Specifically, the radial locations of the ridges and graben can be used as a constraint on the magma chamber depth. If we assume, as suggested above, that the tectonic features developed in response to caldera subsidence associated with magma withdrawal, then we can obtain first order constraints on the subsurface structure of the volcanic edifice by calculating the radial surface stresses (σ_{rr}) corresponding to a given subsurface pressure distribution, and comparing the results to the radial positions of compressional (ridges) and extensional (graben) tectonic features within the caldera.

One of the simplest approaches is to treat the evacuating magma chamber as a simple horizontal line source in a linear elastic halfspace of uniform rigidity. The line source is modeled as an imposed stress condition that represents an instantaneous pressure drop of constant radial magnitude [5]. In the first case considered the source is assumed to have the same horizontal dimension as the caldera, as observed for Kiluea [6]. The problem is solved using a finite element approach assuming axisymmetric deformation. A sample grid is shown in Figure 2. For the model shown, the following boundary conditions were imposed: vanishing horizontal (u) displacements at the center of symmetry of the caldera; vanishing vertical (w) displacements at depths much greater than the caldera radius; and vanishing horizontal and vertical displacements at radial distances far from the caldera rim. Numerical analyses were performed to assure that solutions were not sensitive to the far field boundary conditions.

Examples of the radial stress distributions for magma chamber source depths of 0.1, 0.25, 0.5, 1.0, and 1.5 times the caldera radius are shown in Figure 3. Negative stresses are compressional and positive stresses are extensional. Because the mechanical properties of Olympus Mons' subsurface are not known, stress magnitudes are scaled by Young's Modulus. The state of stress as inferred from the radial locations of ridges and graben in Figure 1 changes from compression to extension at a radial distance of 0.5r, where r is the caldera radius. For the largest of the Olympus Mons calderas (shown in Figure 1), r is approximately 30 km. The corresponding best-fit pattern of stresses determined from our simple model indicates that the top of the Olympus Mons magma chamber was located at a depth of about half the caldera radius (about 15 km) at the time the ridges and graben formed, and is thus within the volcanic construct. A similar depth/radius ratio is also observed for the magma chamber in the Kiluea caldera [6], which suggests a gross similarity of internal structure of the two shields.

In order to better understand the magma chamber mechanics and subsurface structure of Olympus Mons and other martian shield volcanoes, we are currently in the process of examining more detailed magma chamber geometries, as well as more complicated rheological structures. Preliminary results for linear elastic volcanic edifices that contain filled magma chambers with simple 2-D geometries have yielded results that are consistent with those of the simpler model.

References: [1]Mouginis-Mark, P.J., *Proc. Lunar Planet. Sci. Conf. XII*, 1431-1447, 1981. [2]Mouginis-Mark, P.J., L. Wilson, and M.T. Zuber, submitted to *Mars*, University of Arizona Press, Tucson, 1989. [3]Wu, S.S.C., P.A. Garcia, R. Schafer, and B.A. Skiff, *Nature, 309*, 432-435, 1984. [4]Greeley, R., and P.D. Spudis, *Rev. Geophys., 19*, 13-41, 1981. [5]Dieterich, J.H., and R.W. Decker, *J. Geophys. Res., 80*, 4094-4102, 1975. [6]Ryan, M.P., J.Y.K. Blevins, A.T. Okamura, and R.Y.

Koyanagi, *J. Geophys. Res.*, *88*, 4147-4181, 1983. [7]Mouginis-Mark, P., and A. Mathews, *EOS Trans. Am. Geophys. Un.*, *68*, 1342, 1987.

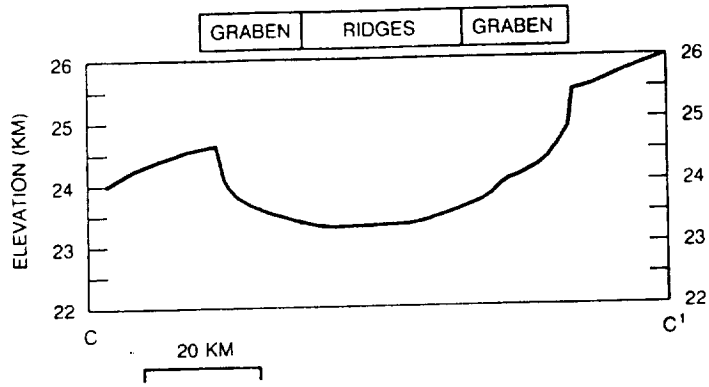

Figure 1. Topography and radial distribution of ridges and graben in the largest caldera of the Olympus Mons caldera complex. The profile traverses only one of the six calderas in the attempt isolate tectonic features associated with a single deformational episode. After [7].

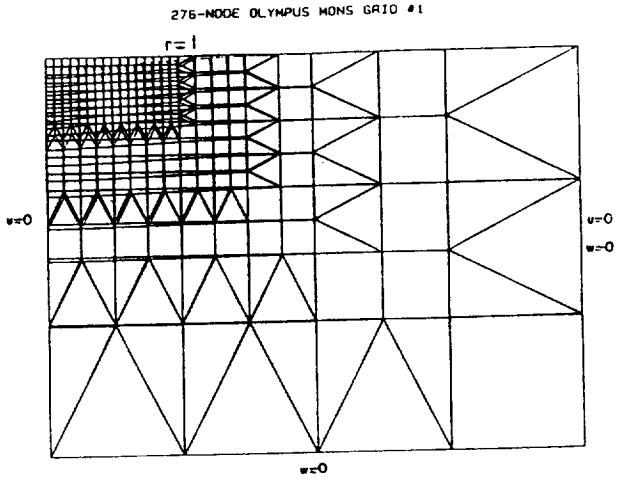

Figure 2. Finite element grid (before and after deformation). The caldera rim is located at r=1.

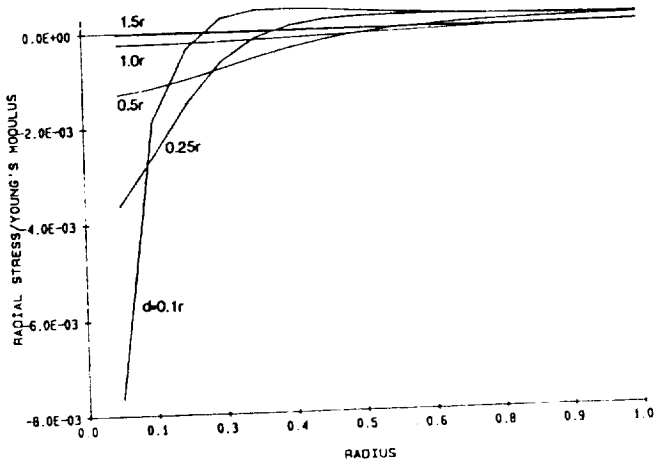

Figure 3. Plot of normalized radial surface stress (σ_{rr}/E) as a function of distance from the caldera center for a line source uniform pressure drop of width r=1 at a range of depths (d) beneath the surface. Negative stresses are compressional and positive stresses are extensional.

FIELD GUIDE

FIELD GUIDE

Lunar and Planetary Institute MEVTV Workshop on Tectonic Features on Mars

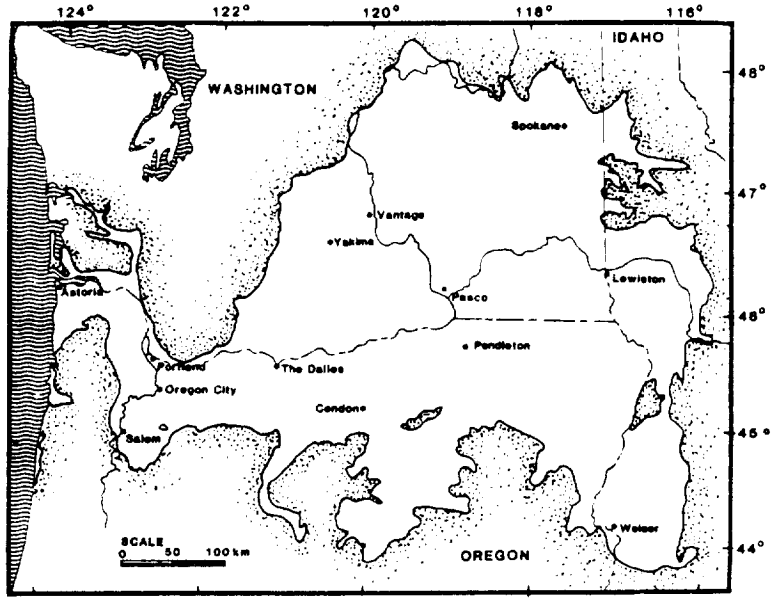

APRIL 20–22, 1989
RICHLAND, WASHINGTON

FIELD GUIDE TO THE LUNAR AND PLANETARY INSTITUTE MEVTV WORKSHOP ON "TECTONIC FEATURES ON MARS"

STRUCTURAL FEATURES OF THE YAKIMA FOLD BELT, COLUMBIA PLATEAU, CENTRAL WASHINGTON

April 22, 1989

Stephen P. Reidel and Karl R. Fecht
Geosciences Group, Westinghouse,
Richland, Washington 99352

and

Terry L. Tolan
Department of Geology
Portland State University
Portland, Oregon 97207

INTRODUCTION

The Yakima Fold Belt is a series of anticlinal ridges and synclinal valleys that covers about 14,000 km^2 of the western Columbia Plateau (Fig. 1). The fold belt formed as basalt flows of the Columbia River Basalt Group, and intercalated sediments of the Ellensburg Formation were folded and faulted under north-south directed compression. Many structural and tectonic models have been proposed to explain the origin and geologic evolution of the Columbia Plateau (e.g. Laval, 1956; Davis, 1977, 1981; Bentley, 1977, 1980; Barrash and others, 1983; and Reidel, 1984) but no one model has gained general acceptance because of differing interpretations of the nature of the geologic structures, extrapolation of structures to depth, character of basement involvement, and the timing and rates of deformation.

The primary emphasis of this field trip will be to examine the geometry of the anticlinal ridges in the central part of the Yakima Fold Belt and the mechanical response of the basalts to folding and faulting. Because the folds have undergone very little erosion, the geomorphology of the ridge closely reflects the geometry. The first 5 stops examine the overall geometry of the ridges. The 6th stop is a traverse through the Saddle Mountains anticline near Sentinel Gap where the Columbia River has eroded completely through the fold. The Saddle Mountains stop affords an excellent place to examine the internal structure of the anticline.

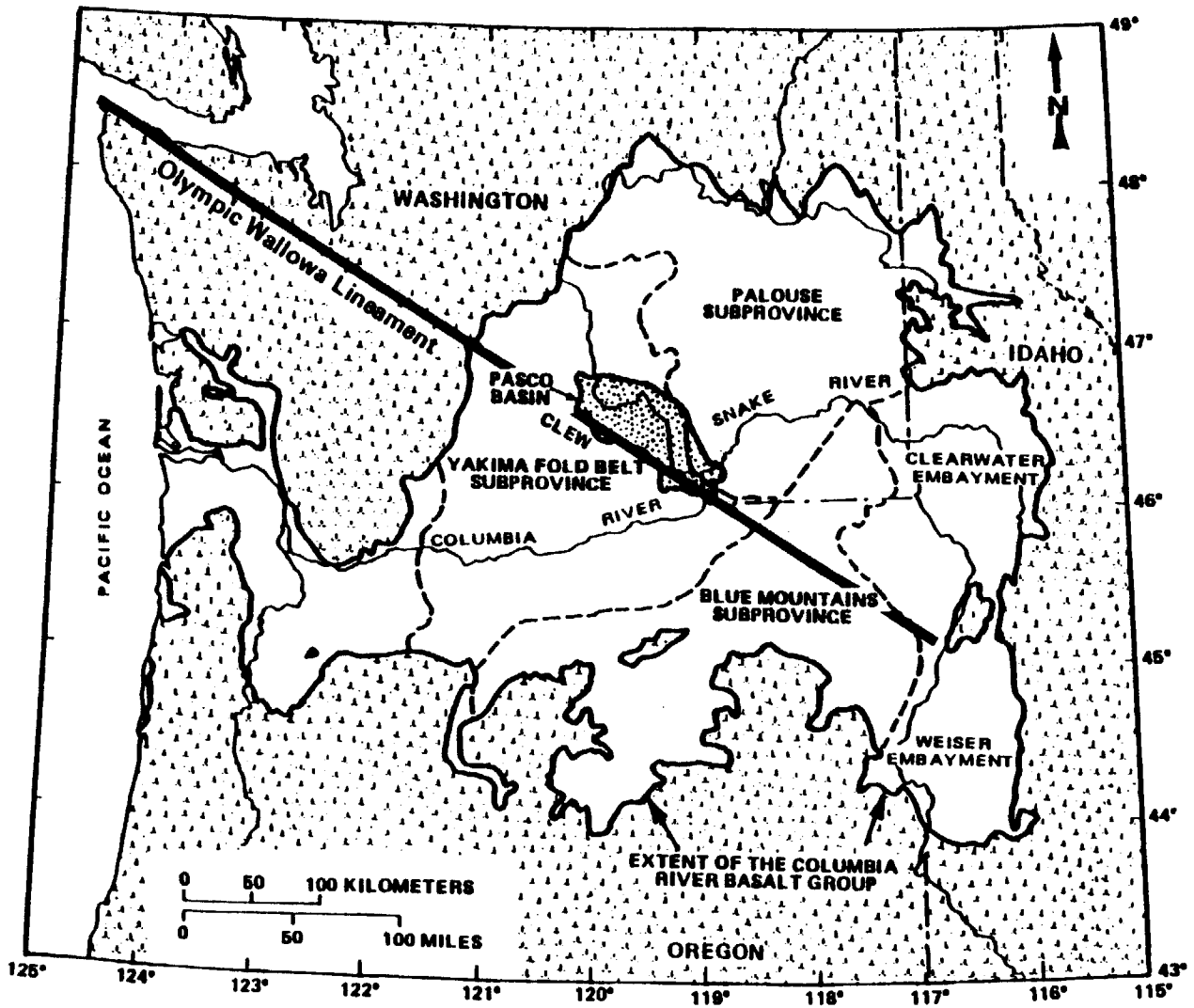

Fig. 1. The Columbia Plateau. Shown are the areal extent of the Columbia River Basalt Group, the four major structural-tectonic subprovinces, the Pasco Basin, the Olympic-Wallowa lineament, and the CLEW, the central portion of the OWL that passes through the western part of the Columbia Plateau.

THE REGIONAL SETTING

The Columbia Plateau is a broad plain situated between the Cascade Mountains to the west and the Rocky Mountains to the east and constructed from the Miocene Columbia River Basalt Group. In the central and western parts, the basalt is underlain predominantly by Tertiary continental sedimentary rocks and overlain by late Tertiary and Quaternary fluvial and glaciofluvial deposits.

The Columbia River Basalt Group covers four general structural-tectonic regions or subprovinces of the Columbia Plateau, each of which has a distinctly different structural style: the Yakima Fold Belt, the Palouse Slope, the Blue Mountains, and the Clearwater, St Maries, and Weiser embayments (Fig. 1). The Yakima Fold Belt consists of a series of generally east-west trending (ranging from N 50° W to N 50° E) anticlinal ridges and synclinal valleys (Fig. 2). The Palouse Slope is the least deformed region with only minor faults and low amplitude, long wavelength folds on an otherwise gently westward dipping paleoslope (Swanson and others, 1980). The Palouse paleoslope marks the eastern boundary of the Yakima Fold Belt and has been a relatively stable feature since at least the middle Miocene (Swanson and Wright, 1976). The Blue Mountains are a northeast trending anticlinorium that extend 250 km from the Cascades to the eastern part of the Plateau. The Blue Mountains form the southern boundary of the Yakima Fold Belt.

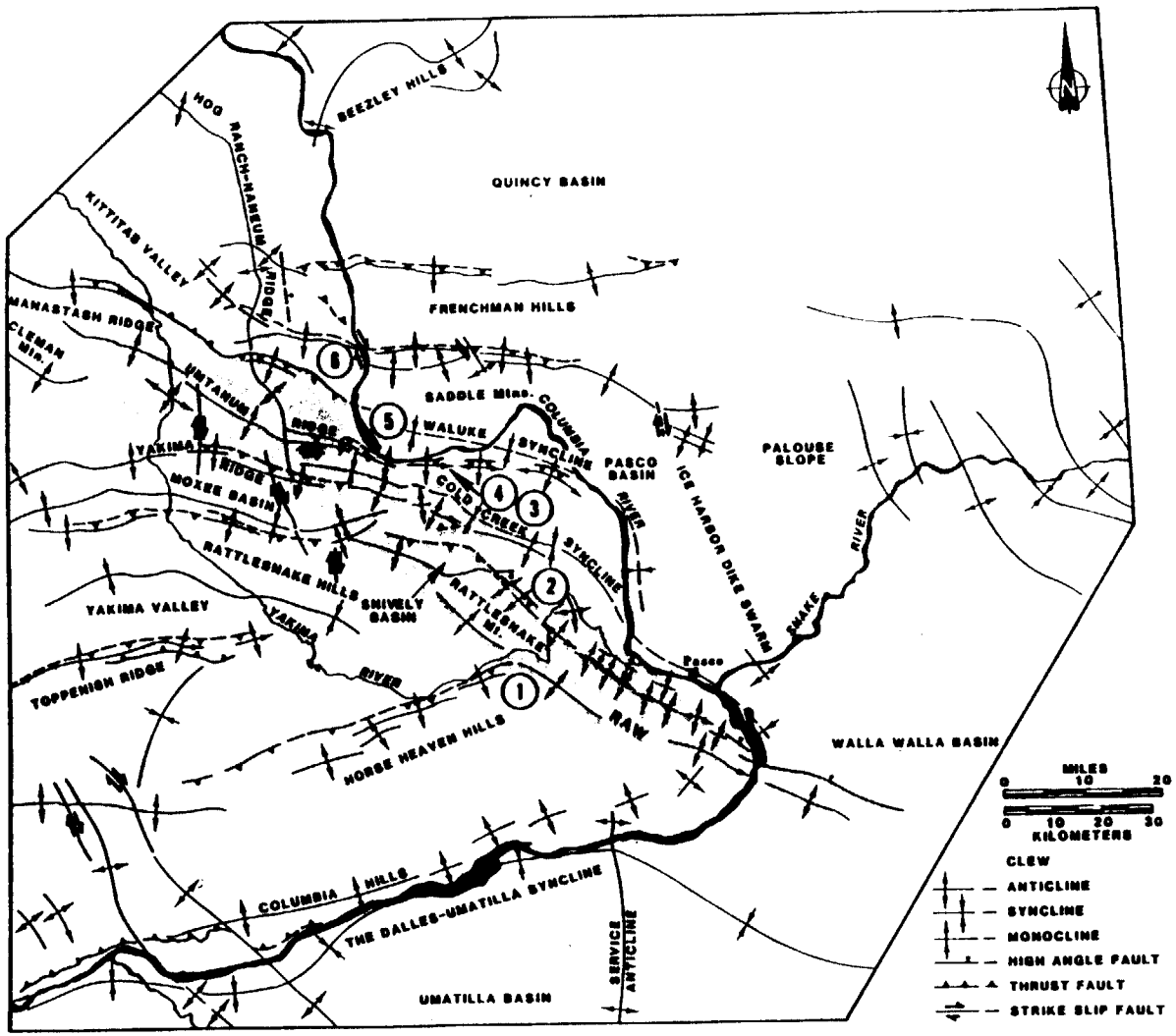

Fig. 2. Major faults and folds in the central part of the Yakima Fold Belt and the western part of the Palouse Slope (from Reidel and others, in press[b]). Shown are the Hog Ranch-Naneum Ridge anticline that forms the western boundary of the Pasco Basin, the Cle Elum-Wallula Deformed zone (CLEW, stippled), and the Rattlesnake-Wallula alinement (RAW) that forms that portion of the OWL and CLEW in the Pasco Basin. GB is Gable Butte, GM is Gable Mountain, and SE is the Southeast anticline along the Umtanum anticline; H.C.A. is the Hansen Creek anticline.

Two regional structures cross cut the central and western part of the Columbia Plateau: the Olympic-Wallowa lineament (OWL) (Figs. 1 and 2), and the Hog Ranch-Naneum Ridge (HR-NR) anticline (Fig. 2). The segment of the OWL that crosses the Yakima Fold Belt is referred to as the Cle Elum-Wallula deformed zone (CLEW, Keinle and others, 1977) and is marked by a rather diffuse zone of anticlines with a N 50° W orientation (Fig. 2). The Hog Ranch-Naneum Ridge anticline is a basement controlled anticline that extends southward from the North Cascades (Tabor and others, 1984) and forms the western boundary of the Pasco Basin (Reidel, 1984), one of the larger basins in the fold belt (Figs. 1 and 2).

STRATIGRAPHY

The generalized stratigraphy of the Yakima Fold Belt and western margin of the Columbia Plateau is shown in Figure 3. The dominant rocks of the area are the Columbia River Basalt Group and intercalated sedimentary rocks of the Ellensburg Formation. These are overlain by younger sedimentary rocks of the Ringold Formation and the Pleistocene catastrophic flood deposits of the Hanford formation (informal). Sedimentary and volcanic units of the Naches, Ohanapecosh, and Fifes Peak formations underlie the basalt along the western margin and extend under the basalt.

Pre-Columbia River Basalt Group Units

In the central Cascade Range west of Yakima, early Tertiary

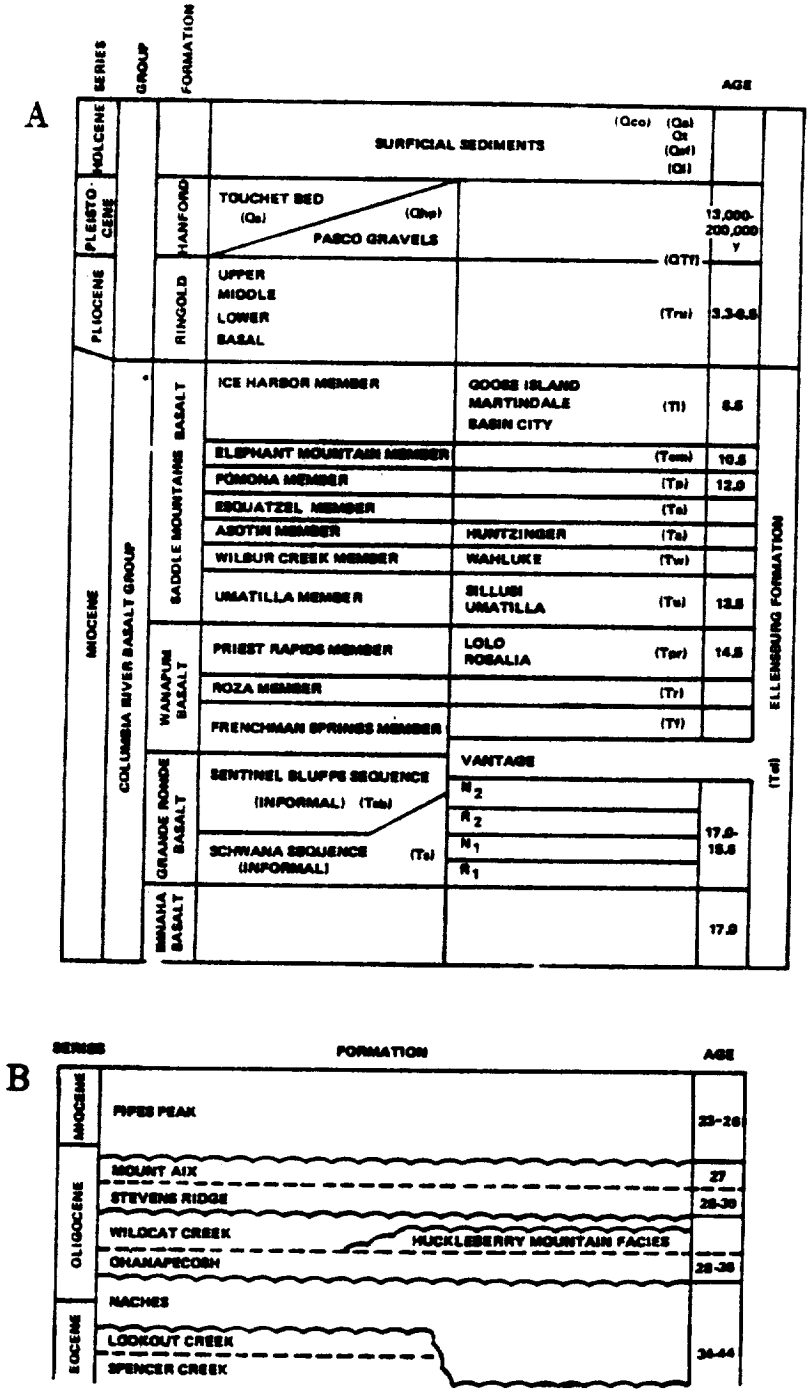

Fig. 3. Major Tertiary stratigraphic units in the area covered by the field guide. A. Units of the Columbia River Basalt Group, intercalated sediments, and overlying sediments. B. Units older than the Columbia River Basalt Group that are exposed along the margin of the Columbia River basalt. Symbols in () are used on geologic maps of Figs. 12, 13, and 14. Recent sediments are generalized as: alluvium (Qa), talus (Qt), alluvial fans (Qaf), colluvium (Qco), and loess (Ql). Older alluvial fans of uncertain age are shown as (QTf).

sedimentary and volcanic rocks underlie the mid-Miocene Columbia River Basalt Group (Fig. 3). The late Eocene Naches Formation is composed of fluvial, feldspathic sandstones and rhyolite flows and tuffs, with basalt and andesite flows in the upper part. K-Ar age dates near the base of the Naches Formation give ages of 40-44 Ma. (Tabor and others, 1984). The Naches Formation is principally confined to the area bounded on the south by the White River-Naches River fault zone and on the north by splays of the Straight Creek fault (Fig. 4).

Younger volcanic rocks of the Ohanapecosh and Fifes Peak formations are found along the western margin of the basalt. The Ohanapecosh Formation consists of multicolored andesitic tuffs and volcaniclastic sediments interbedded with rhyolite and andesite flows. Fission track ages on zircons range from 28-36 Ma. (Vance and others, 1987). Ohanapecosh rocks are more voluminous south of the White River-Naches River fault (Fig. 4). The Fifes Peak Formation consists of three or more eroded volcanic cones along the eastern flank of the Cascade Range. These rocks range in age from about 23-26 Ma. (Vance and others, 1987).

Columbia River Basalt Group

The Columbia River Basalt Group, the principal rock unit in the Yakima Fold Belt, is a sequence of tholeiitic flood basalt flows that were erupted between 17 and 6 Ma. The Columbia River

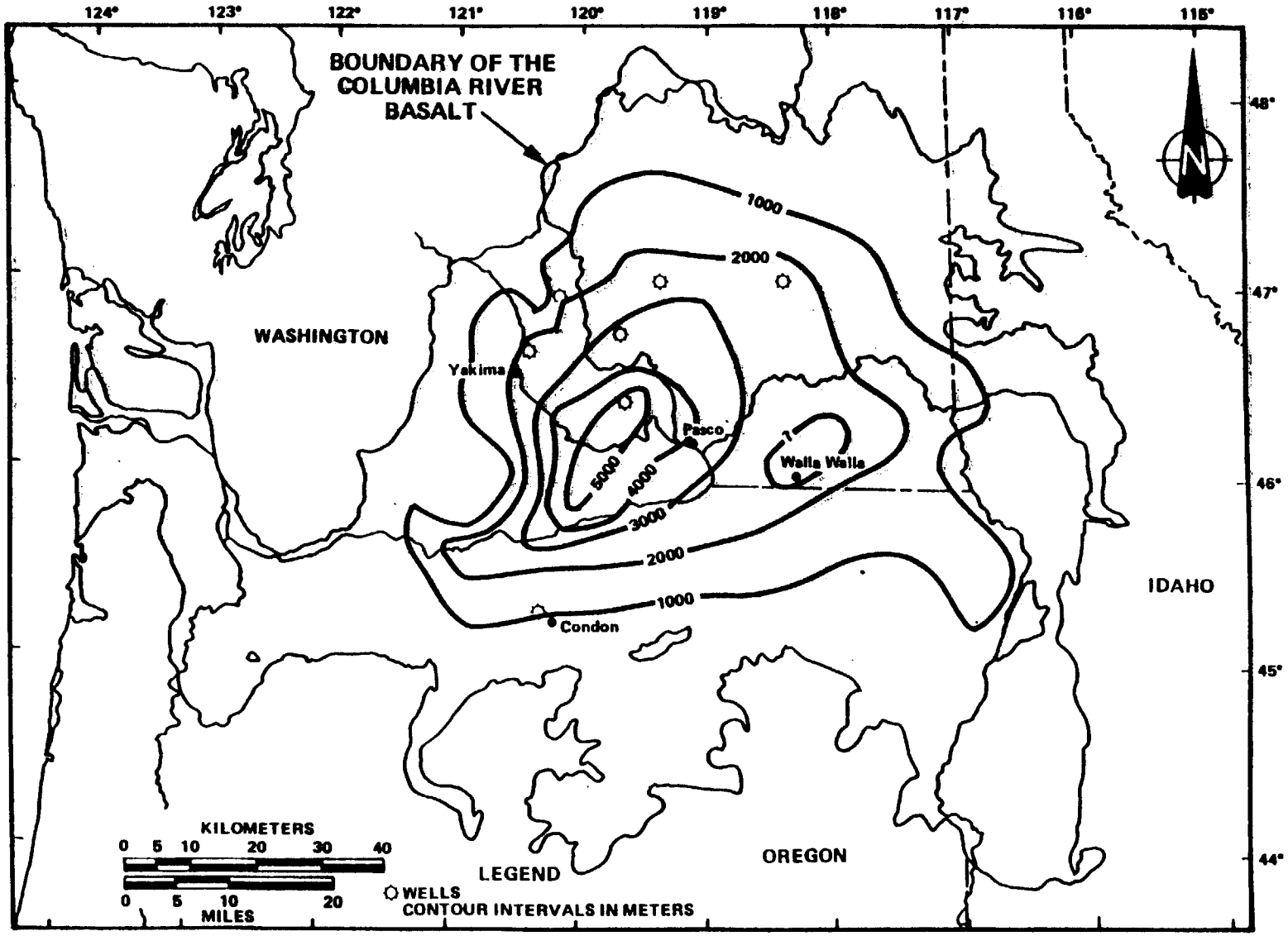

Fig. 4 Map showing the thickness of the Columbia River Basalt Group.

Basalt Group now covers approximately 164,000 km^2 and consists of 174,000 km^3 of basalt (Tolan and others, 1987, in press). The Columbia River Basalt Group has been divided into five formations (Swanson and others, 1979a) (Fig. 3; Picture Gorge Basalt is not shown on this figure but intercalates with the Grande Ronde Basalt); only the Grande Ronde Basalt, the Wanapum Basalt and the Saddle Mountains Basalt are exposed within the western Columbia Plateau.

The basalt flows of the Columbia River Basalt Group are recognized using a combination of lithology, chemistry, and paleomagnetic data (Swanson and others, 1979a). Chemical composition and paleomagnetic data have proven to be the most reliable criteria for flow recognition and correlation; lithology is reliable for many flows primarily within the Wanapum and Saddle Mountains basalts but chemical compositions are still used to confirm identifications. Chemical composition and paleomagnetic data are most important in identifying flows within the Grande Ronde Basalt because of the similarity of lithology. In the field the Grande Ronde Basalt has been divided into four magnetostratigraphic units (msu) (Fig. 3) which, from oldest to youngest are: Reversed 1 (R_1), Normal 1 (N_1), Reversed 2 (R_2), and Normal 2 (N_2) (Swanson and others, 1979a). The composition has been broadly subdivided into two groups based on relative concentrations of MgO (Swanson and others, 1979a) (Fig. 3, High Mgo is Sentinel Bluffs and low MgO is Schwana) but recent studies

have provided more detailed compositional subdivisions (Reidel, 1983; Mangan and others, 1986; Reidel and others, in press[b]).

Ellensburg Formation

The Ellensburg Formation includes epiclastic and volcaniclastic sedimentary rocks that are intercalated with and overlie the Columbia River Basalt Group (Waters, 1961; Swanson and others, 1979a). Most volcaniclastic material in the Ellensburg Formation was produced by volcanic events in the Cascade Mountains. Along the western margin deposition was primarily by volcanic debris flows (lahars) and related stream and sheet floods. Some air fall and pyroclastic-flow deposits are also present. The age of the formation along the western margin in the Naches drainage is between 16.5 and 7.4 Ma. (Smith and others, 1988). The bulk of the material in the Naches River drainage was derived from a single source near Bumping Lake (Fig. 4). Farther east in the central Plateau, Ellensburg Formation is mixed with sediments deposited by the ancestral Clearwater and Columbia rivers (Fecht and others, 1982, 1987).

Suprabasalt Sediments

Sediments continued to be deposited in most synclinal valleys long after the eruptions of the Columbia River basalt. During the late Neogene epiclastic and volcaniclastic rocks of the Ringold Formation were deposited in the central Columbia Plateau. The Ringold Formation of Pliocene age represents main

and side-stream facies of the ancestral Columbia River. The Ringold has been divided into four units (Fig. 3) based primarily on texture. The basal unit represents a complete fining-upward fluvial cycle deposited by a braided-river system associated with the ancestral Columbia River system (Fecht and others, 1982, 1987). The lower and upper units are fine-grained sediments that were deposited in a low-energy lacustrine and/or fluvial overbank depositional environment. The middle unit is composed of stream gravels which were also deposited by the ancestral Columbia River system.

The most recent sediments were deposited by cataclysmic flood waters during the Pleistocene, and post-flood alluvium and eolian deposits. The flood deposits are called the Hanford formation (informal) and are divided into the fine-grained, slack-water sediments, the Touchet beds, and the Pasco gravels.

Regional thickness variations of units and tectonic implications

The greatest thickness of both pre-Columbia River Basalt Group Tertiary rocks (Campbell, in press) and Columbia River basalt (Reidel and others, 1982; Reidel, 1984; Reidel and others, in press[a]) occurs in the central Columbia Plateau (Fig. 4). Magnetotelluric data (Berkman and others, 1987) and seismic-reflection data (Catchings and Moody, 1988) suggest that both the Columbia River Basalt Group and subbasalt sediments thicken from the Palouse slope into the area covered by Yakima Fold Belt (Fig.

5). The Columbia River Basalt Group ranges from 500 to 1500 m thick on the Palouse slope but abruptly thickens to more than 4000 m in the Pasco Basin area (Reidel and others, 1982; in press[a]). Although the total thickness of the subbasalt sediments is not known, these sediments appear to thicken dramatically beneath the Yakima Fold Belt (Campbell, in press; Reidel and others, in press[a].

The regional thickness pattern of both the Columbia River Basalt Group and underlying Tertiary sediments indicate that prior to the eruption of the Columbia River Basalt Group, the area encompassing the present day Yakima Fold Belt had subsided relative to the Blue Mountains and Palouse Slope and filled with sediments. There is no evidence of encroachment by the sea into the central Columbia Plateau during the Tertiary. The continental nature of the sediments (Campbell, in press) suggests that aggradation kept pace with subsidence, and the subaerial nature of the Columbia River Basalt Group (Reidel and others, 1982, in press[b]) indicates that subsidence continued through the eruption of the basalts and basalt accumulation kept pace with subsidence. Furthermore, the suprabasalt sediments from the Pasco Basin indicate that subsidence continued beyond the Miocene and into the Pliocene. Evidence for the thinning and pinchouts of basalt flows onto the Blue Mountains (e.g. Ross, 1978; Hooper and Camp, 1981; Fox and Reidel, 1987) indicates that the Blue Mountains were growing during the eruption of the Columbia River

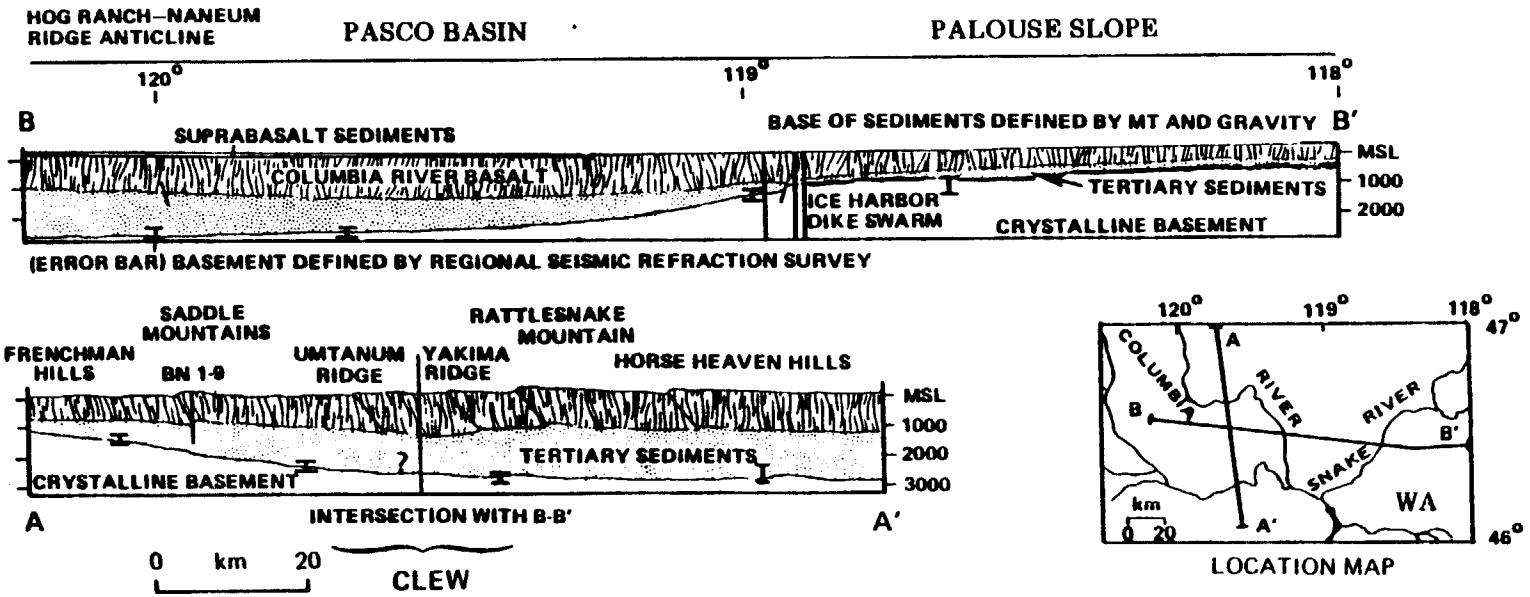

Fig. 5 North-south and east-west cross sections through the central Columbia basin (from Reidel and others, in press).

Basalt Group and while the central Plateau was subsiding. The regional tectonic setting of the central Columbia Plateau throughout much of the Cenozoic, therefore, appears to be one of a subsiding intermontane basin (graben or rift?) that is bounded on the west by the rising Cascade Range, on the south by the slowly growing Blue Mountains, and on the east by a relatively stable westward dipping paleoslope.

GEOLOGY ALONG THE NORTHWEST MARGIN OF THE COLUMBIA PLATEAU

The principal structural elements that border the basalt include the Straight Creek fault, faults thought to be associated with the Olympic-Wallowa lineament, and the White River-Naches River fault zone (Fig. 6). All are potential structures that could extend under the basalt.

Straight Creek Fault

The Straight Creek fault of the Cascade Range is a major fault zone extending from north of the Canadian border to at least as far south as Snoqualmie Pass in central Washington. There is little or no evidence to extend this fault south of the drainages of the White River-Naches River fault zone (Fig. 6). Instead, the Straight Creek fault turns southeastward, splaying into a series of sub-parallel faults (Tabor and others, 1984; Frizzel and others, 1984). These fault splays pass under the Columbia River Basalt Group and align with northwest trending folds in the Yakima Fold Belt (Manastash Ridge). However, at the

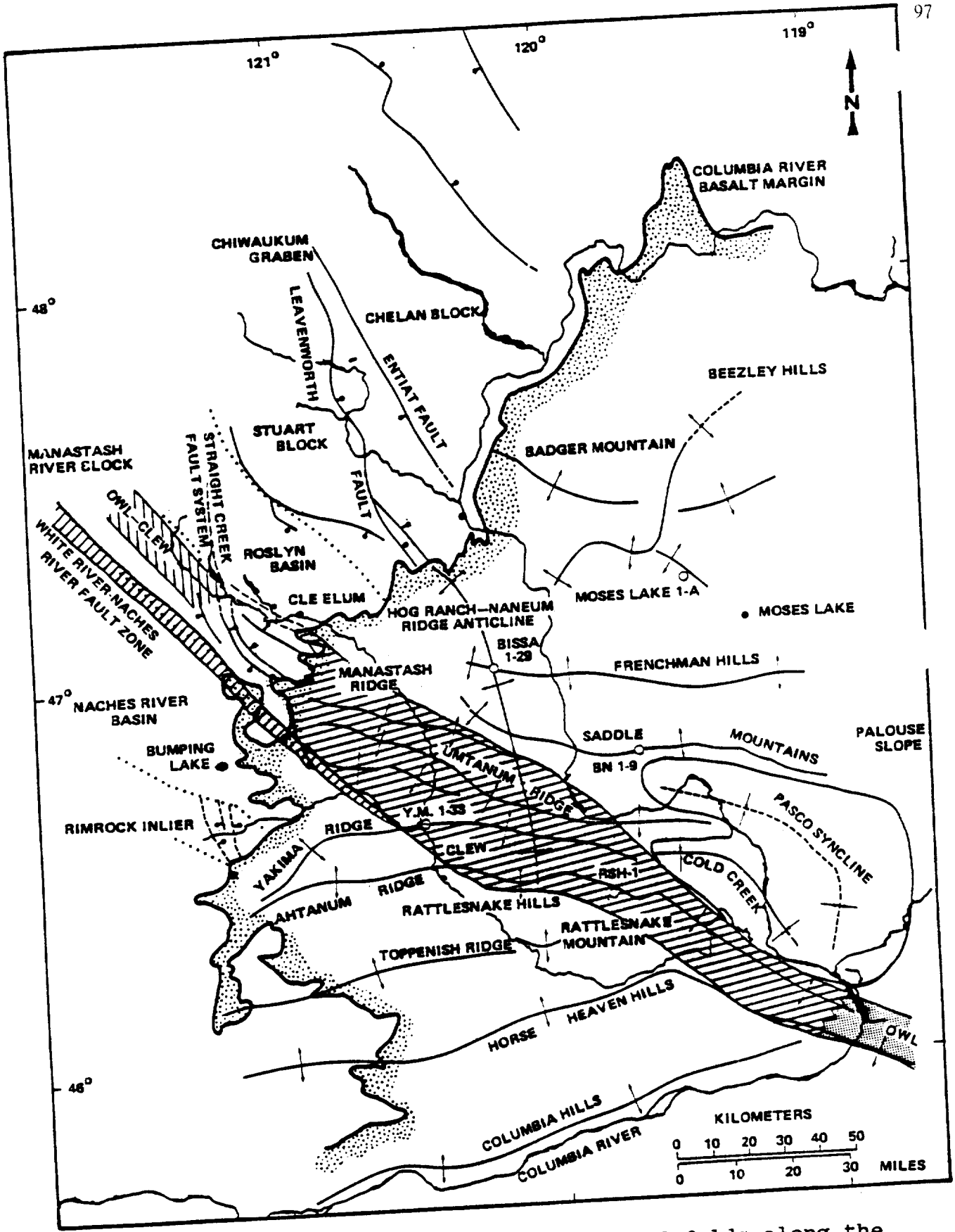

Fig. 6. Generalized map of major faults and folds along the western margin of the Columbia Plateau and Yakima Fold Belt. Hydrocarbon exploration boreholes are shown as open circles.

plateau margin, only small, low displacement faults and broad, flat folds are present in subbasalt rocks. Farther to the southeast, within the Yakima Fold Belt, the deformation becomes more intense.

The Olympic-Wallowa lineament

The Olympic-Wallowa lineament has been recognized as a major through-going topographic feature in Washington (Raisz, 1945; Fig. 1). This feature aligns with pre-basalt structural trends northwest of the Columbia Plateau and in the Columbia Plateau. Within the Yakima Fold Belt, deformation along Manastash Ridge and abrupt bending of the eastern ends of Umtanum Ridge, Yakima Ridge, and Rattlesnake Ridge (Fig. 2) are considered to be evidence for Miocene or younger deformation along the OWL. This portion of the OWL is called the Cle Elum-Wallula deformed zone (CLEW).

Just northwest of the Columbia River basalt margin, on Manastash Ridge, numerous northwest trending faults and shear zones of the Straight Creek fault system occur subparallel to the OWL (Tabor and others, 1984). It is not known whether the OWL affects Tertiary rocks here or if deformation is solely related to the Straight Creek fault system.

White River-Naches River Fault Zone

The Naches River and Little Naches River flow in a rather

straight, southeasterly direction from near the crest of the Cascade Range toward Yakima, Washington (Fig. 7). The White River-Naches River fault zone (WR-NR) is a major fault zone and is aligned with this 50 km-long valley system (Naches-Little Naches rivers) that separates two terranes of dissimilar structure, stratigraphy, and topography (Campbell, 1988). Northeast of the White River-Naches River fault zone, faults and folds in pre-Tertiary through Pliocene rocks parallel (N 60° W) splays of the Straight Creek fault zone. Southwest of the White River-Naches River fault zone, faults in pre-Tertiary rocks trend N 5° E to N 20° W. Middle and late Tertiary rocks in this area reflect Miocene folding and are commonly aligned east-west.

Within the basalts the White River-Naches River fault zone appears to influence fold development in the Yakima Fold Belt as far southeast as Yakima. The fault zone separates a domain of east-northeast trending folds on the southwest from dominantly northwest trending folds on the northeast, and defines structural low points along the Yakima Ridge and Rattlesnake Hills anticlines. The fault zone can be shown to offset flows of the Columbia River Basalt Group for several kilometers southeast of the margin (Campbell, 1988).

The White River-Naches River fault zone derives its name from an alignment northwest of this area between this fault zone in the Naches River and the White River fault (Hammond, 1963;

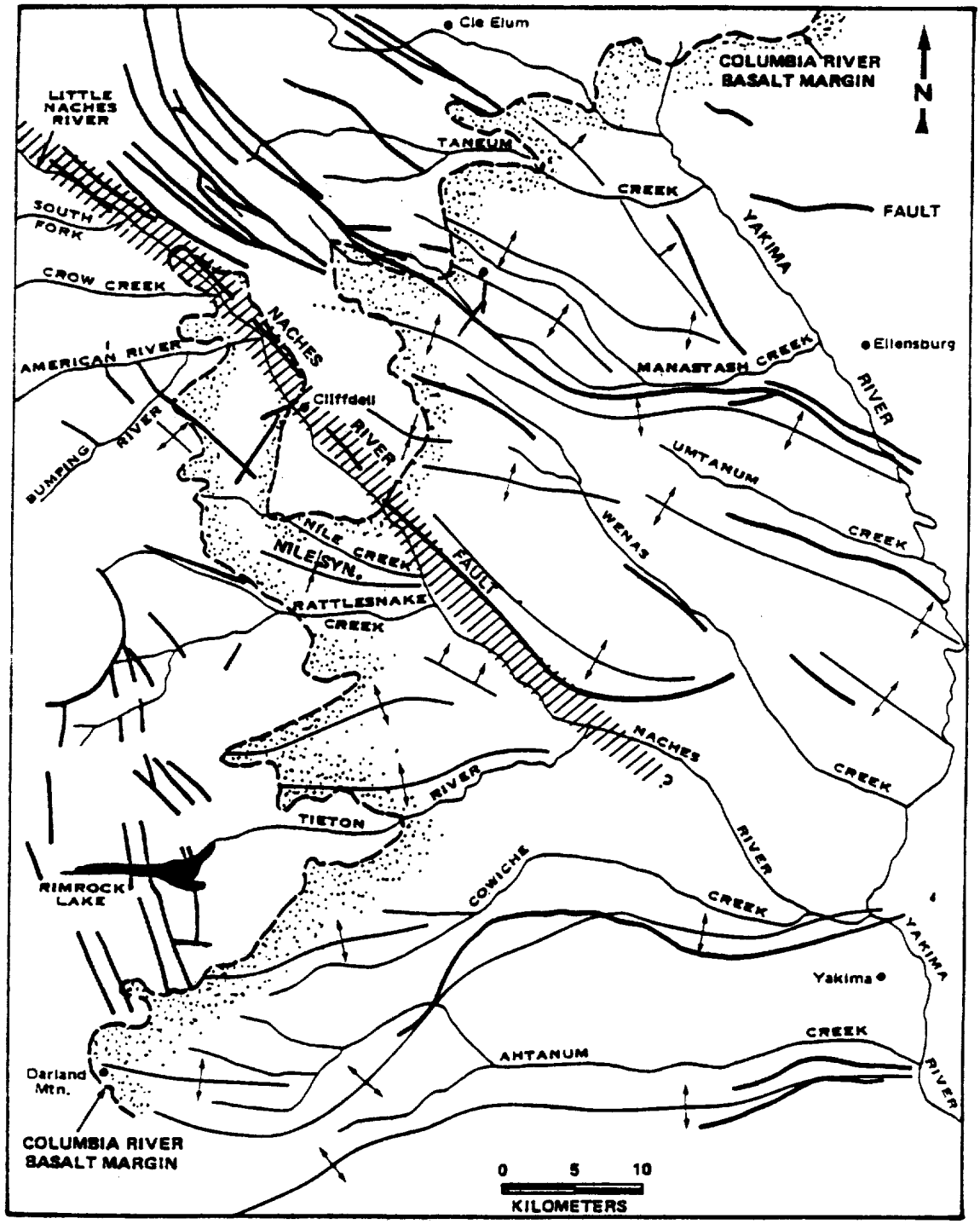

Fig. 7. Comparison of drainage and geologic structural patterns on both sides of the Naches-Little Naches rivers. The Naches River-White River Fault Zone is the striped pattern superimposed on the map. Thin lines are drainage systems, and heavy lines are major faults.

Frizzell and others, 1984), a major fault that continues at least 50 km west-northwest of the area. The total length of the entire fault zone, from Enumclaw to Naches, exceeds 90 km.

THE YAKIMA FOLDS

Introduction

The anticlines of the Yakima Fold Belt consist of non-cylindrical, asymmetrical anticlinal ridges and synclinal valleys. The anticlines are typically segmented and usually have a north vergence, although some folds such as the Columbia Hills have a south vergence. Synclines are typically asymmetrical with a gently dipping north limb and a steeply dipping south limb. Fold length is variable ranging from several km to over 100 km; fold wavelengths range from several kilometers to as much as 20 km. Structural relief is typically about 600 m but varies along the length of the fold. The greatest structural relief along the Frenchman Hills, the Saddle Mountains, Umtanum Ridge, and Yakima Ridge occurs where they intersect the north-south trending Hog Ranch-Naneum Ridge anticline (Fig. 2).

In general, the axial trends produce a "fanning" pattern across the fold belt (Figs. 2 and 6). Anticlines on the western side of the fold belt generally have a N 50° E trend (Swanson and others, 1979b). Anticlines in the central part of the fold belt have east-west trends except along the CLEW where a N 50° W trend

predominates. The Rattlesnake Hills, Saddle Mountains, and Frenchman Hills have overall E-W trends across the fold belt but Yakima Ridge and Umtanum Ridge change eastward from E-W to N 50° W in the zone of the CLEW. In the central part of the fold belt, the Horse Heaven Hills, the Rattlesnake Hills and the Columbia Hills have eastward terminations against the CLEW. There is no evidence for continuation of any anticline to the northeast across the CLEW.

Fold and Fault Geometry

Within the east-central fold belt, the fold geometry typically consists of steeply dipping to overturned north flanks and gently dipping (< 5 degrees) south flanks. Exceptions, however, include the doubly plunging anticlines within the Rattlesnake-Wallula alinement (RAW) of the CLEW (Fig. 2) and the conjugate box-fold geometry of parts of the anticlines such as the Smyrna segment of the Saddle Mountains (Reidel, 1984). The main variable in fold profiles is the width of the gently dipping limb. The widths of the gently dipping limbs vary from as little 5 km to as much as 35 km.

Segmentation of the anticlines is common throughout the fold belt and is defined by abrupt changes in fold geometry or by places where regional folds die out and become a series of doubly plunging anticlines. Segment lengths are variable but average about 12 km (ranging from 5 to 35 km) in the central Plateau;

some of the larger segments contain subtler changes in geometry such as different amplitudes that could also be considered segment boundaries. Segment boundaries are often marked by cross or tear faults that trend N 20° W to north and display a principal component of strike-slip movement (e.g. Saddle Mountains, Reidel, 1984). In the central Columbia Plateau these cross faults are confined to the anticlinal folds and usually occur only on the steeper limb, dying out onto the gentler limb. In the southwest Plateau, some cross faults can be traced as far as 100 km (Swanson and others, 1979b) (also see the Tolan, Reidel, and Fecht field guide in this volume).

Segment boundaries may also be marked by relatively undeformed areas along the fold trend where two fold segments plunge toward each other. For example the Yakima River follows a segment boundary where it crosses the RAW at the southeast termination of Rattlesnake Mountain (Fig. 2) (Stop 2).

The steep limb of the asymmetrical anticlines in the east-central fold belt is almost always faulted (Fig 8). In the eastern portion of the Yakima Fold Belt, the steep limb is typically the northern flank, but elsewhere, as at the Columbia Hills (Swanson and others, 1979b), the south limb is faulted. Where exposed, these frontal fault zones have been found to be imbricated thrusts as, for example, at Rattlesnake Mountain, Umtanum Ridge near Priest Rapids Dam (Bentley, 1977; Goff, 1981;

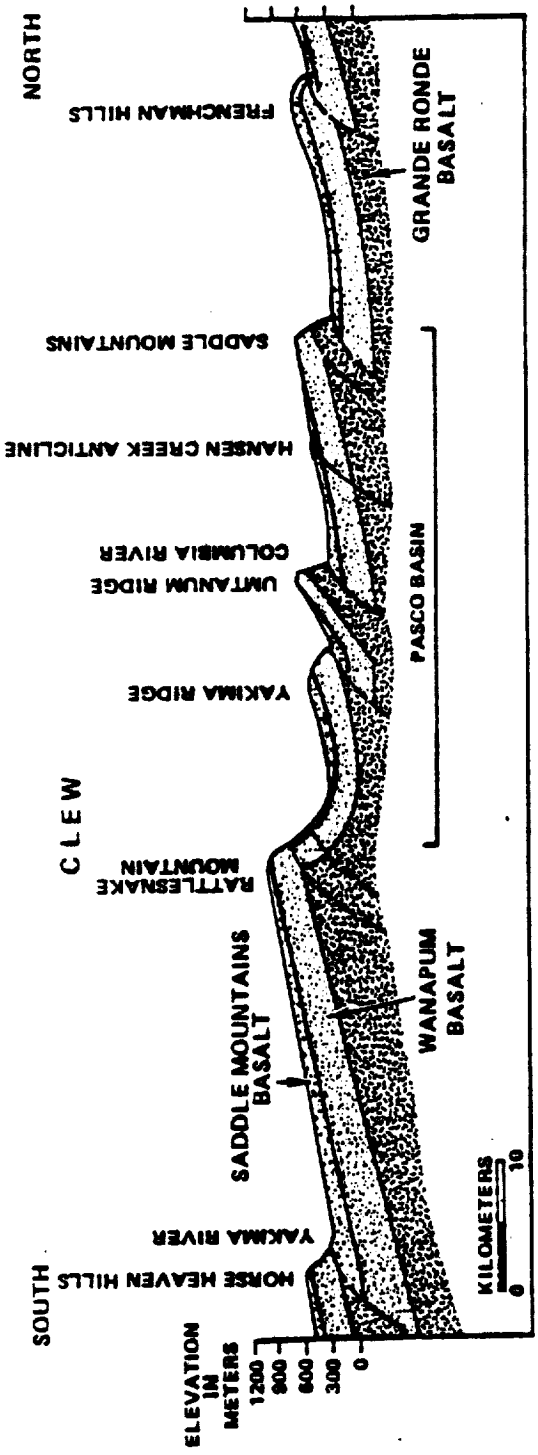

Fig. 8. Schematic cross section through the Yakima Fold Belt in the central Columbia Plateau at about 120 degrees longitude.

Bentley in Swanson and others, 1979b), the Horse Heaven Hills near Byron Road (Hagood, 1986) and the Saddle Mountains near Sentinel Gap (Reidel, 1984).

Yakima folds of the central Columbia Plateau have emergent thrust faults at the ground surface (Fig. 8). The tops of the youngest lava flows at the earth's surface serve as a plane that becomes a low angle thrust fault; the structural attitude of the surface flow controls the angle of the emergent fault plane. This type of apparent structural control led many investigators to conclude that faults associated with the Yakima Folds are low-angle thrust faults with detachment surfaces either within the Columbia River Basalt Group, in the sediments below the basalts, or at the basalt-sediment contact. Where erosion provides deeper exposures into the cores of folds, the frontal faults are observed to be reverse faults (e.g. the Columbia water gap in the Frenchman hills, 45 degrees south (Grolier and Bingham, 1971); the Columbia Hills at Rock Creek, WA, 50-70 degrees north (Swanson and others, 1979b)).

Subsurface Structure

The dip of the frontal fault plane and the structure of the anticlines at depth remains controversial. A multitude of possible models (such as Suppe's (1983, 1985) fault-bend fold or fault-propagation fold, Jamison's (1987) detachment fold, and Mitchell and Woodward's (1988) kink-detachment fold) can all

produce similar surface geometries and thus have provided abundant food for thought influencing many of the models that have been proposed for the fold belt. No clear answers have come forth because of the lack of direct observations, however. We will present some information during the field trip from some of the recent hydrocarbon exploration on the Columbia Plateau that helps constrain subsurface interpretations.

STOP DESCRIPTIONS

Figure 9 shows the route covered by the road log. Swanson and others (1979b) provide excellent reconnaissance geologic maps that include areas covered by this field guide. More detailed maps are available for parts of the areas described below: the Saddle Mountains (Reidel, 1988); out of date but useful color maps by Myers and others (1979) for the Pasco Basin, and Grolier and Bingham (1971) for Franklin and Grant Counties. Bentley (1977) and Carson and others (1987) provide guides for portions of the Yakima Fold Belt. The Carson guide has been included with this guidebook.

STOP 1. OVERVIEW OF THE EASTERN PART OF THE YAKIMA FOLD BELT FROM THE CREST OF THE HORSE HEAVEN HILLS.

This stop provides an overview of the central Columbia Basin and Pasco Basin and is an excellent place to discuss the geologic history of the area.

Our view point is at the eastern termination of the Horse Heaven Hills where it intersects the CLEW (Fig. 2). There are three sets of anticlinal ridges that comprise the CLEW along this segment. The Horse Heaven Hills has the greatest structural relief here but farther to the northwest the Rattlesnake Mountain trend has the greatest structural relief. The Horse Heaven Hills is a series of low-amplitude (50-100 feet) anticlines there.

To the northeast the Palouse slope can be seen on a clear day. The slope is marked by very gentle dips (1°) into the area of the Ice Harbor dike swarm where dips increase into the Pasco Basin (Fig. 5).

This is a good locality to see the typical geometry of Yakima folds. To the north is Rattlesnake Mountain. The north side is very steep (Stop 3) but here one can observe the very gentle south slope. Even more dramatic is the very gentle south slope of the Horse Heaven Hills. The back slope extends for about 30 km to the Columbia River\Columbia Hills anticline with a gentle dip. Note the very abrupt change from a gentle south dip on the back slope to a steeper dip near the crest. This is very apparent on both Rattlesnake Mountain and the Horse Heaven Hills. Our view point is from one of the doubly plunging anticlines that mark the crest of the anticline; note how the crest of the Horse Heaven Hills

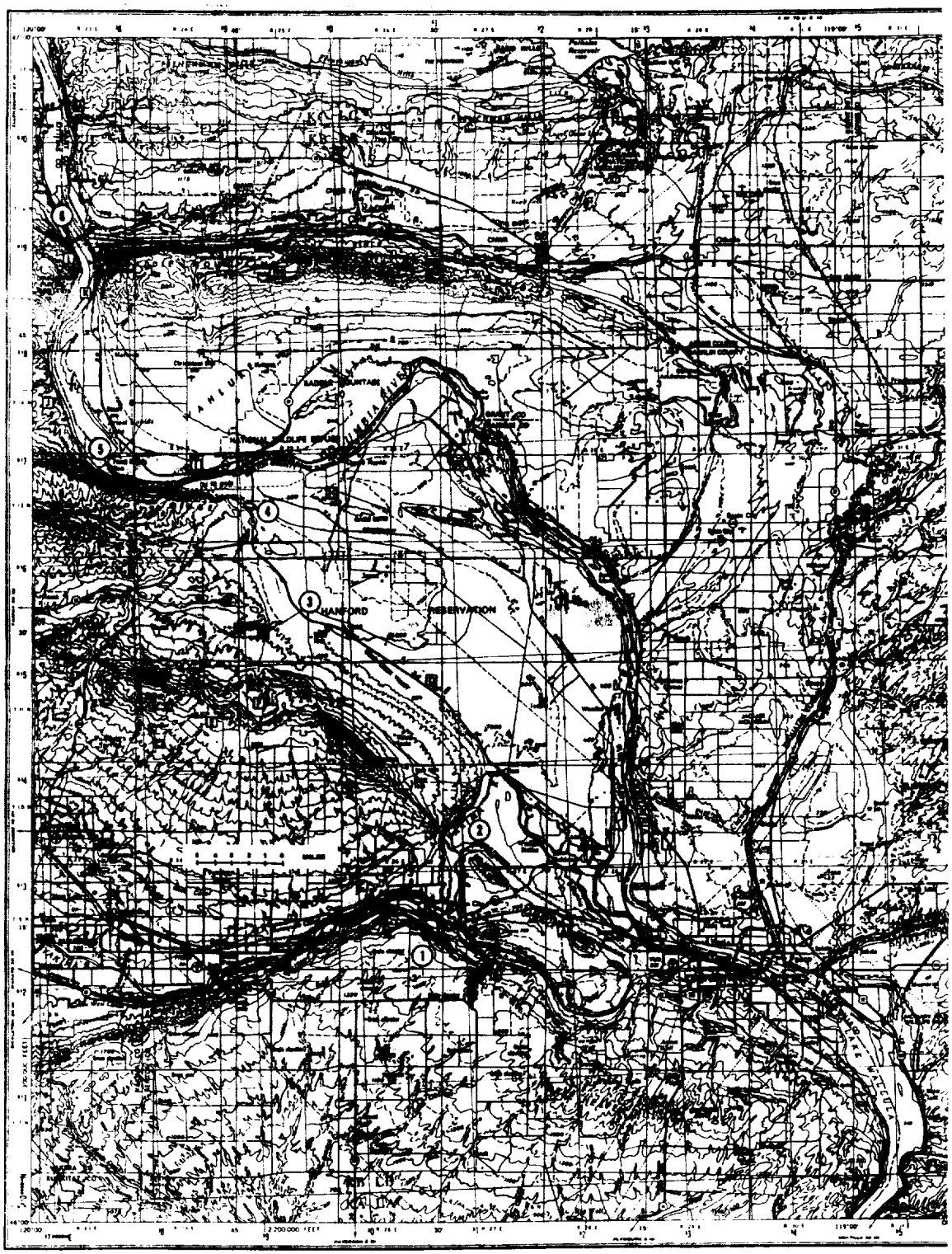

Fig. 9 Location of field trip stops. Stop locations are shown by numbers; additional points that will be referred to during the trip are shown as letters in a box. A - Badger gap road cut. B - Webber Canyon. C - Badlands anticline. D - Rattlesnake Mountain view. E - RSH-1. F - Snively Basin. G - Yakima Ridge south tear fault. H - Gable Butte. I - View of Umtanum Ridge from road. J - low amplitude folds north of Umatnum Ridge. K - Sentinel Gap. L - West side of Sentinel Gap. M - Pillow complex at Sand Hollow. N - BN 1-9.

is marked by these doubly plunging anticlines. These anticlines tend to be east-west oriented and en echelon to the trend of the Horse Heaven Hills (see Hagood, 1986, for a detailed study of the Horse Heaven Hills).

STOP 2. YAKIMA RIVER GAP IN THE CLE ELUM-WALLULA DEFORMED ZONE (PART OF THE OWL).

This stop demonstrates the discontinuity of faulting along the CLEW

This will be a brief stop. At this locality the Yakima River passes through a gap formed by the southeast plunging Rattlesnake Mountain and the northwest plunging Red Mountain anticline (Fig. 2). The basalts here are the 8.5 Ma Ice Harbor Member, the 10.5 Ma Elephant Mountain Member, and the 12 Ma Pomona Member. Within a short distance along the CLEW the amount of structural relief changes greatly. For example, the Elephant Mountain Member is at an elevation of 500 feet here but 5 miles to the northwest on Rattlesnake Mountain, it is at an elevation of 3,600 feet. The CLEW trend has been argued to be a major zone of strike-slip faulting, perhaps even the northern most fault of a series of strike-slip faults in the western United States. Detailed mapping at this locality has shown that there is no evidence of strike-slip movement since <u>at least</u> the late Miocene (12 Ma). Geophysical studies as part of the siting of nuclear power plants have shown that basement rocks and structures

can not have more than 3 miles of strike-slip offset along the CLEW. The record of deformation along the CLEW has been compressional rather than strike slip since the late Miocene. Strike-slip movement has been minimal during the geologic history of the CLEW. All faults in the area are reverse faults but these are small faults. The main frontal fault on Rattlesnake Mountain dies out before reaching this area.

STOP 3. VIEW OF RATTLESNAKE MOUNTAIN.

The purpose of this stop is to view the structure of the north flank of Rattlesnake Mountain and the Snively Basin complex.

View South

This locality provides an excellent view of the north flank of one of the largest of the Yakima anticlines, Rattlesnake Mountain. There is almost 4,000 feet of structural relief on the youngest lava flows on Rattlesnake Mountain. All basalt flows thin onto Rattlesnake Mountain which we interpret to mean that the fold was growing during the eruption of the basalt. The present relief developed in the last 10.5 m. y. but geophysical data show that even more structural relief on Rattlesnake Mountain is buried by the younger flows (Fig. 10).

The prominent bench just below the crest marks the Wanapum -

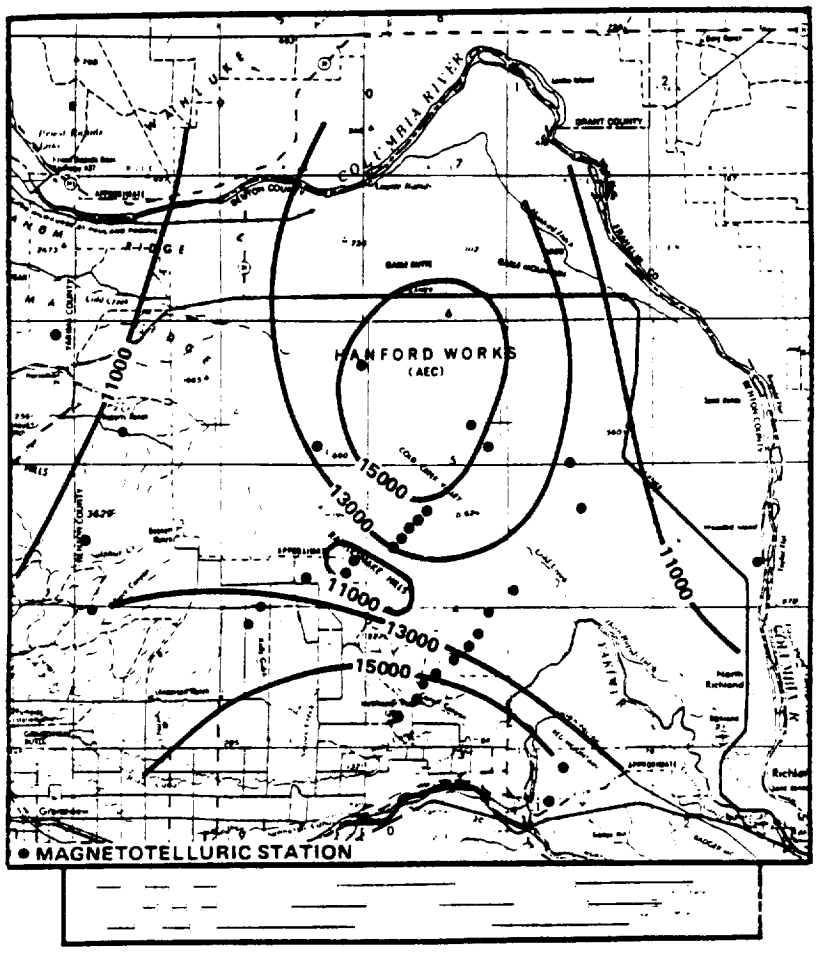

Fig. 10. Thickness of the Columbia River Basalt Group on Rattlesnake Mountain based on MT data (from Reidel and others, in press).

Saddle Mountains Basalts contact and is erosional. The contact is marked by a sedimentary unit, the Mabton interbed.

The main fault runs along the base of the north flank but is covered by sediments. As noted at stop 2, the fault dies out before reaching the river. Basalt flows along the north side dip between 50° to 70° north. The second bench marks an upper thrust fault placing gently south dipping beds above the steeply north dipping beds. The anticlinal axis has been thrust over and eroded from the present exposures. The upper thrust dies out to the southeast and northwest and is responsible for the greater structural relief along this part of Rattlesnake Mountain.

View west

The Hog Ranch-Naneum Ridge anticline marks the western boundary of the Pasco Basin (Fig. 2). To the west of this stop it is marked by a broad, low amplitude anticline and can not be seen from here. From the western boundary of the basin, the Yakima folds plunge gently eastward toward the Palouse slope. The structure of this area is complex because the CLEW trends across the area.

The first deep hydrocarbon exploration well, RSH-1 (Figs 4 and 7, location E), was drilled to a depth of 10,660 feet in

the 1950's on the Rattlesnake Hills south of here and was still in Columbia River basalt (Reidel and others, 1982). Geophysical data indicate that there is at least another 1,000 feet of basalt or more making a total thickness of at least 12,000 feet. Analysis of the chemistry of the basalt from the borehole indicates that there is no significant repeat in stratigraphy.

From this locality the eastward plunge of the Yakima folds is very apparent. In the distance only Gable Butte and Gable Mountain of the Umtanum Ridge anticline protrudes above the sediment filled basin (Fig. 2). A buried ridge east of Gable Mountain, called the Southeast anticline, marks the eastward termination of the Umtanum Ridge structural trend. Gable Mountain and Gable Butte are second order en echelon anticlines developed on the Umtanum anticline (Fecht, 1978). The Yakima Ridge anticline also plunges southeast and is buried by sediments of the Ringold Formation and Hanford formation. To the south is the intersection of the east trending Rattlesnake Hills and northwest trending Rattlesnake Mountain. Both anticlines appear to terminate at this intersection. On the north side of Rattlesnake Mountain is the old Rattlesnake Hills gas field.

STOP 4. THE NORTHERN PASCO BASIN.

The purpose of this stop is to view the structures that form the northern Pasco Basin.

The crest of the hill and our view point also marks the crest of Umtanum Ridge (Fig. 2), which is plunging to the east. The prominent basalt flow that we are on is the Pomona flow. At 12:00 is the Sentinel Gap segment of the Saddle Mountains, at 2:00 is the Smyrna Bench segment. The geometry of the Saddle Mountains anticline changes here from an open fold in the Sentinel Gap segment to a box fold in the Smyrna Bench segment. Farther east in the Saddle Gap segment, the fold geometry is that of an open fold. At about 12:00 on the crest of the Saddle Mountains is the site where Shell and ARCO drilled the BN 1-9 wildcat well (Figs. 4 and 7, location N). This well penetrated about 11,500 feet of basalt and bottomed (at over 17,000 feet) in the Chumstick Formation of Eocene age (Campbell, in press). The well had subcommercial gas shows.

STOP 5. UMTANUM RIDGE.

The purpose of this stop is to observe the structure and overturned basalt on the north side of Umtanum Ridge.

Umtanum Ridge extends about 100 km from near the western margin of the Columbia Plateau to the Palouse slope. The structural relief gradually decreases eastward to Gable Butte where it becomes a series of en echelon anticlines. In the Priest Rapids Dam area the north limb is overturned and dips 40° to the south. An upper fault, the Buck thrust, and

a lower fault, the Umtanum fault define the overturned flows of the fold (Price, 1982; Price and Watkinson, in press). The Buck thrust dies out to both the east and west but the Umtanum fault has been inferred to extend from the western edge of the anticline to just east of Midway. Drilling has constrained the angle of the Umtanum fault in the near surface to between 30° and 60°.

SENTINEL GAP.

Cohassett flow, Grande Ronde Basalt in road cuts. The internal vesicle zone of the flow is exposed along the road (McMillian and others, 1987). We will see this same flow at the next stop. This is near Site 6 of Carson and others (1987).

STOP 6. THE SADDLE MOUNTAINS FAULT ZONE AND CORE OF ANTICLINE.

The purpose of this stop is to examine the faulting and folding in the core of the of the Saddle Mountains anticline.

At this locality we will examine one of the few places where the core of the Saddle Mountains anticline is well exposed (Fig. 11). The Columbia River, which is controlled by a tear fault here, has exposed a zone of complex folding and faulting in the core of the Saddle Mountains anticline. Above the main fault, the Saddle Mountains fault, is an upper fault that does not penetrate the upper layers of

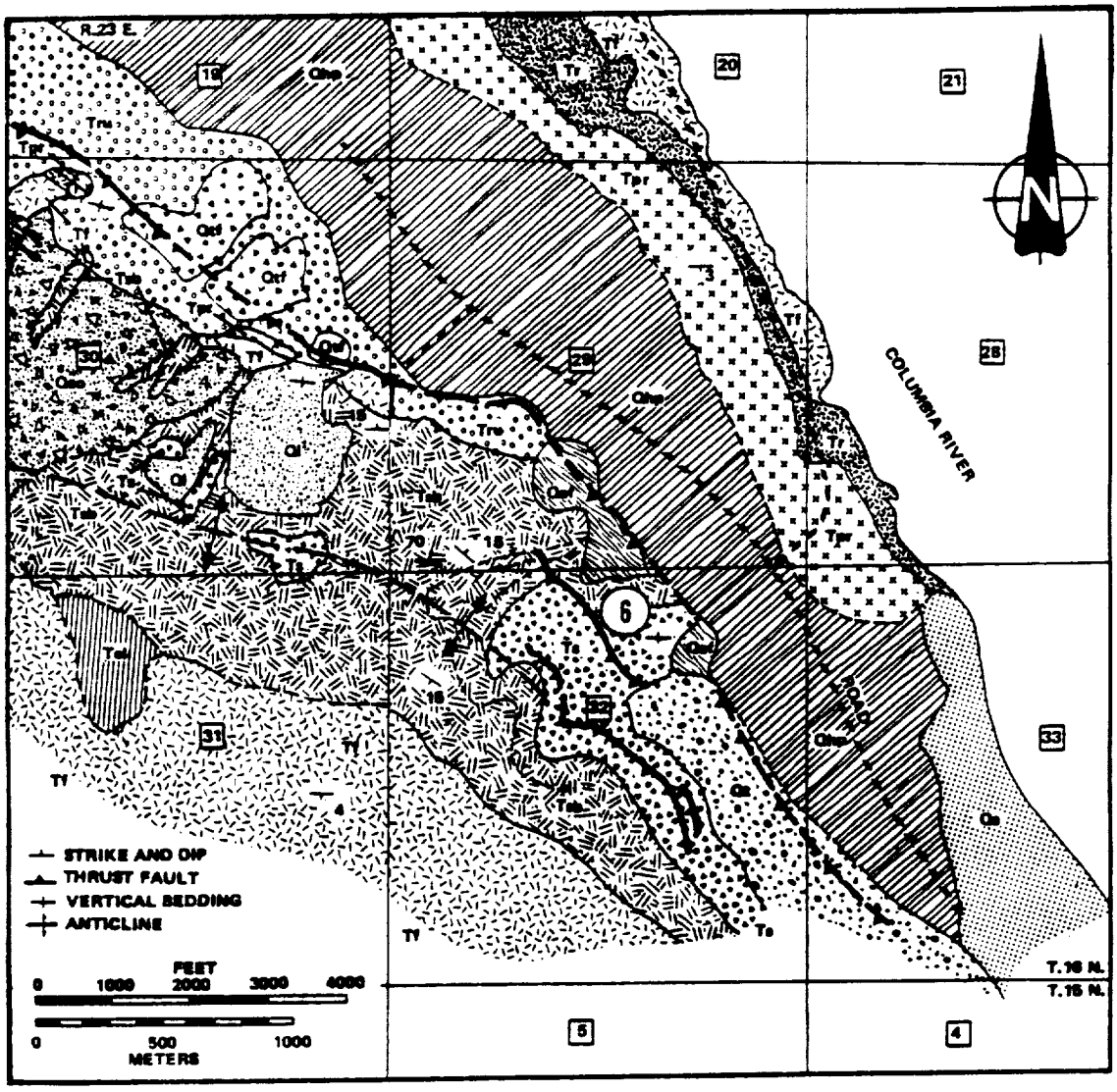

Fig. 11. Geologic map of the west side of Sentinel Gap, Saddle Mountains (from Reidel, 1988).

basalt. The basalt flows between the two faults (the hummocky exposures) are vertical and strike west. The flows are shattered and brecciated but their chemical compositions permit identification of the individual flows. Above the upper fault, the flows are relatively intact but folded. The upper fault has about 100 m of offset measured on the Umtanum flow. Total shortening across this part of the Saddle Mountains anticline is about 3 km.

About a mile north of this locality, the Saddle Mountains fault is exposed. There the Wanapum Basalt is thrust northward over the Ringold Formation. The basalt flows are steeply north dipping to vertical south of the fault and the Ringold sediments are nearly horizontal north of the fault. The youngest faulting here is older than the youngest catastrophic flooding (13,000 yr) because apparently undisturbed Hanford formation gravels overlie the fault.

SELECTED REFERENCES

Barrash, W.; Bond, J. G.; Vankatakrishnan, R.; 1983, Structural evolution of the Columbia Plateau in Washington and Oregon: American Journal of Science, v. 283, no. 9, p. 897-935.

Bentley, R. D., 1977, Stratigraphy of the Yakima Basalts and Structural Evolution of the Yakima Ridges in the western Columbia Plateau: in Brown, E. H., and Ellis, R. C. editors, Geology Excursions in the Pacific Northwest, Western Washington University Press, p. 339-389.

Bentley, R. D.; 1980, Wrench tectonic model for the late Cenozoic evolution of Oregon and Washington [abstract]: Geological Society of America Abstracts with Programs, v. 12, no. 7, p. 385.

Bentley, R.D., and Campbell, N.P., 1983, Geologic Map of the Yakima Quadrangle, Washington: Washington Division of Geology and Earth Resources Geologic Map GM-29, 1 plate, scale 1:40,000.

Berkman, E. A.; Orange, A.; Bergstrom, K. A.; Mitchell, T. H., 1987, Interpretation of magnetotelluric data, Rattlesnake Mountain, Pasco Basin, Washington: Rockwell Hanford Operations Report SD-BWI-TI-354, Richland, Washington, 31 p.

Bingham, J. W.; Londquist, D. J.; Baltz, E. H., 1970, Geologic investigation of faulting in the Hanford Region, Washington: U.S. Geological Survey Open-file Report, 103 p.

Campbell, N. P., 1975, A geologic road log over Chinook, White Pass, and Ellensburg to Yakima highways: Washington Division of Geology and Earth Resources Information Circular 54, 81p.

Campbell, N. P., 1988, Structural geology along the northwestern Columbia River basalt margin, Washington: Washington Division of Geology and Earth Resources, Open-File Report 88-5.

Campbell, N. P., in press, Structural and stratigraphic interpretation of the rocks under the Yakima Fold Belt based on recent surface mapping and well data, in Reidel, S. P., and Hooper, P. R. editors, Volcanism and Tectonism in the Columbia River flood-basalt province: Geological Society of America Special Paper 239.

Carkin, Brad, 1988, The geology and petrology of the Fifes Peak Formation in the Cliffdell area, central Cascades Washington: Masters of Science Thesis, Western Washington University, Washington 157 p., 2 plates, scale 1:24,000.

Carson, R. J.; Tolan, T.L.; Reidel, S. P., 1987, Geology of the Vantage area, south-central Washington -- an introduction to the Miocene flood basalts, Yakima Fold Belt, and Channeled Scabland: in Hill Mason, editor, Geological Society of America Centennial Field Guide - Cordilleran Section, p. 357-362.

Catchings, R. D.; Moody, W. D., 1988, Crustal structure of the Columbia Plateau -- evidence for continental rifting: Journal of Geophysical Research, v. 19, no. B1, p. 459-474.

Davis, G. A., 1977, Tectonic evaluation of the Pacific Northwest Pre-Cambrian to recent: Preliminary Safety Analysis Report, In Washington Public Power Supply System, 1977, Washington Public Power Supply System nuclear project number 2, Preliminary Safety Analysis Report: Washington Public Power Supply System, Appendix 23, Subappendix 2R C, p. 1 to 46.

Davis, G. A., 1981, Late Cenozoic tectonics of the Pacific Northwest with special reference to the Columbia Plateau, In Washington Public Power Supply System, 1977, Washington Public Power Supply System nuclear project number 2, Preliminary Safety Analysis Report: Washington Public Power Supply System, Appendix 23, Subappendix 2.5 N, p. 1 to 44.

Fecht, K. R., 1978, Geology of the Gable Mountain-Gable Butte area: Rockwell Hanford Operations Report RHO-BWI-LD-5, 70 p.

Fecht, K. R.; Reidel, S. P.; Tallman, A. M., 1982, Evolution of the Columbia River system in the central Columbia Plateau of Washington from Miocene to present [abstract]: Geological Society of America Abstracts with Program, v. 14, no. 4, p. 163.

Fecht, K. R.; Reidel, S. P.; Tallman, A. M., 1985, Paleodrainage of the Columbia River system on the Columbia Plateau of Washington State -- a summary: Rockwell Hanford Operations Report RHO-BW-SA-318p, Richland, Washington, 55p.

Fecht, K. R.; Reidel, S. P.; Tallman, A. M., 1987, Paleodrainage of the Columbia River system on the Columbia Plateau of Washington State -- a summary: in Schuster, J. E., editor, Selected Papers on the Geology of Washington, Division of Geology and Earth Resources, Bulletin 77, p. 219-248.

Fox, T. P.; Reidel, S. P., 1987, Stratigraphy of the Standard Kirkpatrick No. 1, Gilliam County, Oregon -- New insights into Tertiary tectonism of the Blue Mountains: Oregon Geology, v. 49, no. 2, p. 15-22.

Frizzell, V. A.; Jr.; Tabor, R. W.; Booth, D. B.; Ort, K. M.; Waitt, R. B. Jr., 1984, Preliminary geologic map of the Snoqualime Pass 1:100,000 quadrangle, Washington: U.S. Geological Survey Open-File Report 84-693, 43 p., 1 plate, scale 1:100,000.

Goff, F. E., 1981, Preliminary geology of eastern Umtanum Ridge, south-central Washington: Rockwell Hanford Operations Report RHO-BWI-C-21, Richland, Washington, 100 p.

Grolier, M. J.; Bingham, J. W., 1971, Geologic map and sections of parts of Grant, Adams and Franklin Counties, Washington: U.S. Geological Survey Miscellaneous Geologic Investigations Series Map I-589, scale 1:62,500.

Hagood, M. A., 1986, Structure and evolution of the Horse Heaven Hills, south-central Washington: Rockwell Hanford Operations Report RHO-BW-SA-344, Richland, Washington, 176 p., 1 plate, scale 1:24,000.

Hammond, P. E., 1963, Structure and stratigraphy of the Keechelus volcanic group and associated Tertiary rocks of the west-central Cascade Range, Washington: University of Washington Doctor of Philosophy Thesis, 294 p., 2 plates.

Hooper, P. R.; Camp, V. E., 1981, Deformation of the southeast part of the Columbia Plateau: Geology, v. 9, no. 7, p. 323-328.

Keinle, C. F.; Bentley, R. D.; Anderson, J. L., 1977, Geologic reconnaissance in the Cle Elum-Wallula Lineament and related structures, In Washington Public Power Supply System, 1977, Washington Public Power Supply System nuclear project number 2, Preliminary Safety Analysis Report: Washington Public Power Supply System v. 2A, Amendment 23, Subappendix 2R D, p. 1 to 33.

Jamison, W. R., 1987, Geometric analysis of fold development in overthrust terranes: Journal of Structural Geology, v. 9, no. 2, p. 207-220.

Laval, W. N., 1956, Stratigraphy and structural geology of portions of south-central Washington: Doctor of Philosophy Thesis, University of Washington, 221 p.

Mackin, J. H., 1961, A stratigraphic section in the Yakima Basalt and Ellensburg Formations in south-central Washington: Washington Division of Mines and Geology Report of Investigations 19, 45 p.

Mangan, M. T.; Wright, T. L.; Swanson, D. A.; Byerly, G. R., 1986, Regional correlation of Grande Ronde Basalt flows, Columbia River Basalt Group, Washington, Oregon, and Idaho: Geological Society of America Bulletin, v. 97, no. 11, p. 1300-1318.

McMillian, Kent, Cross, R. W.; Long, P. E., 1987, Two-stage vesiculation in the Cohassett flow of the Grande Ronde Basalt, south central Washington: Geology, v. 15, no. 9, p. 809-812.

Mitchell, M. M.; Woodward, N. B., 1988, Kink detachment fold in the southwest Montana fold and thrust belt: Geology, v. 16, no. 2, p. 162-165.

Myers, C. W.; and others, Geologic Studies of the Columbia Plateau -- a status report: Richland, Washington, Rockwell Hanford Operations Report RHO-BWI-ST-4, Richland, Washington, 326 p., 10 plates.

Price, E. H., and Watkinson, A. J., in press, Structural geometry and strain distribution within east Umtanum Ridge, southcentral Columbia Plateau: in Reidel, S. P., and Hooper, P. R., editors, Volcanism and Tectonism in the Columbia River flood-basalt province: Geological Society of America Special Paper 239.

Price, E. H., 1982, Structural geology, strain distribution, and tectonic evolution of Umtanum Ridge at Priest Rapids Dam, and a comparison with other selected localities within the Yakima Fold Belt structures, south-central, Washington: Rockwell Hanford Operations Report RHO-BWI-SA-138, Richland, Washington, 197 p., 3 plates.

Raisz, E., 1945, The Olympic-Wallowa-Lineament: American Journal of Science, v. 243-a, no. 5, p. 479-485.

Reidel, S. P., 1983, Stratigraphy and petrogenesis of the Grande Ronde Basalt from the deep canyon country of Washington, Oregon and Idaho: Geological Society of America Bulletin, v. 94, no. 4, p. 519-542.

Reidel, S. P., 1984, The Saddle Mountains -- the evolution of an anticline in the Yakima Fold Belt: American Journal of Science, v. 284, no. 8, p. 942-978.

Reidel, S. P., 1988, Geologic Map of the Saddle Mountains, Southcentral Washington: Washington Division of Geology and Earth Resources, Geologic Map Series GM-28, 5 plates, scale 1:40,000.

Reidel, S. P.; Long, P. E.; Myers, C. W.; Mase, Jack, 1982, New evidence for greater than 3.2 kilometers of Columbia River basalt beneath the central Columbia Plateau: EOS (Transactions of American Geophysical Union), v. 63, no. 8, p. 173.

Reidel, S. P.; Scott, G. R.; Bazard, D. R.; Cross, R. W.; Dick, B., 1984, Post-12 million year clockwise rotation in the central Columbia Plateau, Washington: Tectonics, v. 3, no. 2, p. 251-273.

Reidel, S. P.; Fecht, K. R., 1986, The Huntzinger flow: evidence of surface mixing of the Columbia River Basalt Group and its petrogenetic implications -- Geological Society of America Bulletin, v. 98, no. 6, p. 664-667.

Reidel, S. P.; Fecht, K. R.; Hagood, M. C.; Tolan, T. L., in press (a), Geologic evolution of the central Columbia Plateau, in Reidel, S. P., and Hooper, P. R., editors, Volcanism and Tectonism in the Columbia River flood-basalt province: Geological Society of America Special Paper 239.

Reidel, S. P.; Tolan, T. L.; Hooper, P. R.; Beeson, M. H.; Fecht, K. R.; Anderson, J. L.; and Bentley, R. D., in press (b), The Grande Ronde Basalt, Columbia River Basalt Group -- stratigraphic descriptions and correlations in Washington, Oregon, and Idaho: in Reidel, S. P., and Hooper, P. R., editors, Volcanism and Tectonism in the Columbia River flood-basalt Province: Geological Society of America Special Paper 239.

Ross, M. E., 1978, Stratigraphy, structure, and petrology of Columbia River basalt in a portion of the Grande Ronde-Blue Mountains area of Oregon and Washington: Doctor of Philosophy Thesis, University of Idaho, 407 p., 1 plate.

Schmincke, H.-U., 1964, Petrology, paleocurrents, and stratigraphy of the Ellensburg Formation and interbedded Yakima Basalt flows, south-central Washington: Doctor of Philosophy Thesis, The John Hopkins University, Maryland, 384 p.

Schmincke, H.-U., 1967, Flow direction in Columbia River basalt flows and paleocurrents of interbedded sedimentary rocks, south-central Washington: Geologisches Rundschau, v. 56, no. 3, p. 992-1019.

Shannon and Wilson, 1973, Geologic studies of the Columbia River basalt structures and age of deformation: Report to Portland General Electric Company, Portland, Oregon, 45 p.

Smith, G. O., 1903, Anticlinal mountain ridges in central Washington: Journal of Geology, v. 11, no. 2, p. 166-177.

Smith, G. A., 1988a, Neogene synvolcanic and syntectonic sedimentation in central Washington: Geological Society of America Bulletin, v.100, no. 9, p. 1479-1492.

Smith, G. A., 1988b, Sedimentology of proximal to distal volcaniclastics dispersed across an active fold belt -- Ellensburg Formation (late Miocene), central Washington: Sedimentology, v. 35.

Smith, G. A.; Campbell, N. P.; Deacon, M. W.; Muhammad Shafiquallah, 1988, Eruptive style and location of volcanic centers in the Miocene Washington Cascade Range: Reconstruction from the sedimentary record: Geology, v. 16, no. 4, p. 337-340.

Suppe, J., 1983, Geometry and kinematics of fault-bend folding: American Journal of Science, v. 283, no. 7, p. 648-721.

Suppe, J., 1985, Principals of Structural Geology: Prentice-Hall, Inc, New Jersey, 537 p.

Swanson, D. A.; and Wright, T. L., 1976, Field Guide to field trip between Pasco and Pullman, Washington, emphasizing stratigraphy, vent areas, and intracanyon flows of the Yakima Basalt: in Proceedings, Geological Society of America Cordillerian Section meeting, Pullman, Washington, Field Guide 1, 33 p.

Swanson, D. A.; Wright, T. L.; Hooper, P. R.; Bentley, R. D., 1979a, Revisions in stratigraphic nomenclature of the Columbia River Basalt Group: U.S. Geological Survey Bulletin 1457-G, 59 p.

Swanson, D. A.; Anderson, J. L.; Bentley, R. D.; Camp, V. E.; Gardner, J. N.; Wright, T. L., 1979b, Reconnaissance geologic map of the Columbia River Basalt Group in Washington and adjacent Idaho: U.S. Geological Survey Open-file Report 79-1363, 7 plates, scale 1:250,000.

Swanson, D. A.; Wright, T. L.; Camp, V. E.; Gardner, J. N.; Helz, R. T.; Price, S. M.; Reidel, S. P.; Ross, M. E., 1980, Reconnaissance geologic map of the Columbia River Basalt Group, Pullman and Walla Walla quadrangles, southeast Washington and adjacent Idaho: U.S. Geological Survey Miscellaneous Investigations Map I-1139, scale 1:250,000.

Tabor, R. W.; Frizzell, V. A.; Vance, J. A.; Naeser, C. W., 1984, Ages and stratigraphy of Lower and Middle Tertiary sedimentary and volcanic rocks of the central Cascade, Washington -- Application to the tectonic history of the Straight Creek Fault: Geological Society of America Bulletin, v. 95, no. 1, p. 26-44.

Tolan, T. L.; Reidel, S. P.; Beeson, M. H.; Anderson, J. L.; Fecht, K. R.; Swanson, D. A., 1987, Revisions to the areal extent and volume of the Columbia River Basalt Group [abstract]: Geological Society of America Abstracts with programs, v. 19, no. 6, p. 458.

Vance, J. A.; Clayton, G. A.; Mattinson, J. M.; Naeser, C. W., 1987, Early and Middle Cenozoic stratigraphy of the Mount Rainier-Tieton River area, southern Washington Cascades: in Schuster, J. E., editor, Selected papers on the Geology of Washington: Washington Division of Geology and Earth Resources, Bulletin 77, p. 269-290.

Walsh, T. J.; Korosec, M. A.; Phillips, W. M.; Logan, R. L.; Schasse, H. W., 1987, Geologic Map of Washington - Southwest Quadrant: Washington Division of Geology and Earth Resources Geologic Map GM-34, scale 1:250,000.

Waters, A. C., 1961, Stratigraphy and lithologic variations in the Columbia River basalt: American Journal of Science, V. 259, p. 583-611.

List of Workshop Participants

Carl Allen
Westinghouse-Hanford Co.
P.O. Box 1970
Richland, WA 99352

Jayne Aubele
Department of Geological Sciences
Brown University
Box 1846
Providence, RI 02912

Andrea Borgia
Mail Stop 183-501
Jet Propulsion Laboratory
4800 Oak Grove Drive
Pasadena, CA 91106

Paul Butterworth
Code 633
NASA Goddard Space Flight Center
Greenbelt, MD 20771

David Chadwick
Center for Earth and Planetary Studies
National Air and Space Museum
Smithsonian Institution
Washington, DC 20560

Mary Chapman
U.S. Geological Survey
2255 N. Gemini Drive
Flagstaff, AZ 86001

Bob Craddock
Center for Earth and Planetary Studies
National Air and Space Museum
Smithsonian Institution
Washington, DC 20560

Steven K. Croft
Lunar and Planetary Laboratory
University of Arizona
Tucson, AZ 85721

Larry Crumpler
Department of Geological Sciences
Brown University
Box 1846
Providence, RI 02912

Karl Fecht
Westinghouse-Hanford Co.
P.O. Box 1970
Richland, WA 99352

Randall Forsythe
Department of Geography and Earth Science
University of North Carolina
Charlotte, NC 28223

Sharon Frank
Department of Geological Sciences
Brown University
Box 1846
Providence, RI 02912

Matthew Golombek
Mail Stop 183-501
Jet Propulsion Laboratory
4800 Oak Grove Drive
Pasadena, CA 91109

Jim Head
Department of Geological Sciences
Brown University
Box 1846
Providence, RI 02912

Floyd N. Hodges
8130 W. Falls Place
Kennewick, WA 99336

Arvid Johnson
Department of Earth and Atmospheric Sciences
Purdue University
West Lafayette, LA 47907

Ted A. Maxwell
Center for Earth and Planetary Studies
National Air and Space Museum
Smithsonian Institution
Washington, DC 20560

George E. McGill
Department of Geology and Geography
University of Massachusetts
Amherst, MA 01003

Bob Peterson
Westinghouse-Hanford Co.
P.O. Box 1970
Richland, WA 99352

Virginia Pfaff
Department of Geology
Portland State University
Portland, OR 97207-0751

Stephen Reidel
Westinghouse-Hanford Co.
P.O. Box 1970
Richland, WA 99352

Richard A. Schultz
Code 621
NASA Goddard Space Flight Center
Greenbelt, MD 20771

Sean C. Solomon
54-522
Massachusetts Institute of Technology
Cambridge, MA 02139

John Suppe
Department of Geological and Geophysical Sciences
Princeton University
Princeton, NJ 08544

Kenneth L. Tanaka
U. S. Geological Survey
2255 N. Gemini Drive
Flagstaff, AZ 86001

Paul J. Thomas
Center for Radiophysics
Cornell University
Ithaca, NY 14853

Terry Tolan
Portland State University
P.O. Box 751
Portland, OR 97207

Michael J. Tuttle
Center for Earth and Planetary Studies
National Air and Space Museum
Smithsonian Institution
Washington, DC 20560

James R. Underwood, Jr.
Code EL
NASA Headquarters
Washington, DC 20546

John Watkinson
Geology Department
Washington University
Pullman, WA 99164

Tom Watters
Center for Earth and Planetary Studies
National Air and Space Museum
Smithsonian Institution
Washington, DC 20560

Jim Zimbelman
Center for Earth and Planetary Studies
National Air and Space Museum
Smithsonian Institution
Washington, DC 20560